eman ta zabal zazu

Universidad del País Vasco

Euskal Herriko Unibertsitatea

Facultad de Medicina y Enfermería

Departamento de Neurociencias

Characterizing the role of integrin β1 in early synaptic changes and gliosis triggered by amyloid β oligomers: Implications for Alzheimer's disease progression

Tesis doctoral para optar al grado de Doctor, presentada por:

Carolina Ortiz Sanz

2019

Directores de tesis:

Dra. Elena Alberdi y Dr. Jose Luis Zugaza

3xTg-AD	Triple transgenic mouse model of Alzheimer's disease
AD	Alzheimer's disease
AICD	APP intracytoplasmic domain
AIP	Autocamptide-2 Related Inhibitor Peptide
AMPA	α-amino-3-hydroxy-5-methyl-4-isoxazolepropionic acid
ANOVA	Analysis of variance
AP2	Adaptor protein 2
ApoE	Apolipoprotein E
APP	Amyloid precursor protein
ATD	Amino-terminal domain
Aβ	Amyloid β
BACE	β-site Amyloid precursor protein cleaving enzyme
BDNF	Brain-derived neurotrophic factor
BME	Eagle's Basal Medium
BSA	Bovine serum albumin
CAM	Cell adhesion molecules
CaMKII	Ca^{2+}/Calmodulin-dependent protein kinase II
Cdk5	Cyclin-dependent kinase 5
cDNA	Complementary Deoxyribonucleic acid
CERAD	Consortium to Establish a Registry for Alzheimer's Disease
CFP	Cyan fluorescent protein
CKII	Casein kinase II
CNS	Central nervous system
CREB	cAMP response element-binding
CSF	Cerebrospinal fluid
CTD	Carboxyl-terminal domain
Cx	Frontal cortex

DAB	N, N-dimethyl-4-aminoazobenzene
DAG	Diacylglycerol
DAPI	4',6-diamino-2-fenilindol
DIV	Day *in vitro*
DG	Dentate gyrus
DMSO	Dimethyl sulfoxide
EAAT	Glutamate transporters
ECM	Extracellular matrix
ER	Endoplasmic reticulum
ERK	Extracellular signal-regulated kinase
FAK	Focal adhesion kinase
FBS	Fetal bovine serum
FPRL1	Formyl peptide receptor-like 1
FRET	Fluorescent resonance energy transfer
GAPDH	Glyceraldehyde-3-phosphate dehydrogenase
HBSS	Hank´s balanced salt solution
HEPES	4-(2-hydroxyethyl)-1 piperazineethanesulfonic acid
HRP	Horseradish peroxidase
HS	Horse serum
ILK	Integrin linked kinase
IMDM	Iscove's Modified Dulbecco's Medium
LBD	Ligand-binding domain
LTD	Long-term depression
LTP	Long-term potentiation
MAGUK	Membrane-associated guanylate kinases
MEM	Modified eagle medium
mEPSCs	Miniature excitatory postsynaptic currents
MK801	Dizocilpine

NB	Neurobasal
NFT	Neurofibrillar tangles
NGS	Normal goat serum
NMDAR	N-methyl-D-aspartate receptor
PBS	Phosphate buffered saline
pCREB	CREB phosphorylation
PDL	Poly-D-Lysine
PFA	Paraformaldehyde
PK	Protein kinase
PMSF	Phenylmethylsulfonyl fluoride
PSD	Postsynaptic densities
PSN1	Presenilin 1
PSN2	Presenilin 2
PTK	Protein tyrosine kinases
RAGE	Receptor for advanced glycosylation end-products
RGD	Arginine-glycine-aspartate
RhoA	Ras homolog gene family, member A
ROI	Region of interest
RT	Room temperature
SAP	Synapse-associated protein
S.E.M.	Standard error of the mean
SDS	Sodium dodecyl sulfate
STEP61	Striatal-Enrichedprotein tyrosine Phosphatase
TBST	Tris buffered saline with Tween 20
TMD	Transmembrane domain
WT	Wild type
YFP	Yellow fluorescent protein

Accumulation of soluble amyloid-β (Aβ) oligomeric forms in the brain is a relevant early event in Alzheimer's disease (AD) etiopathogenesis. Here, we have investigated the molecular mechanisms of early synaptic changes induced by subtoxic concentrations of Aβ oligomers in neurons. Combining pharmacological, immunocytohistochemical and calcium imaging approaches, we found that Aβ oligomers differentially increased the density of both NR2B-containing NMDA receptors (NMDAR) and postsynaptic protein 95 (PSD-95) in synaptosome fractions from primary neuronal cultures. These changes resulted in enhanced synaptic NMDAR-dependent calcium influx. Mechanistically these intracellular early events were governed by Integrin β1/classical PKCs signaling pathway. Regarding the presence of NR2B subunit and synaptic proteins *in vivo*, we have determined that these proteins are selectively altered in 6-month-aged AD transgenic mice (3xTg-AD). Going further, analyzing the synaptosomal fractions purified from prefrontal cortex of control and AD patients, our results showed that, at early stages of AD (Braak II), brain samples presented an increase in NR2B, PSD95 and synaptophysin protein expression.

On the other hand, using high resolution imaging, we investigated the effects of acute Aβ treatment on dendritic arborization and spines in a long-term *ex vivo* model from CA1 organotypic hippocampal cultures of mouse. An algorithm-based analysis revealed that Aβ induced an increase in total dendritic spine density, specifically in the number of stubby spines in an Integrin β1/classical PKC dependent manner. Additionally, analysis of dendritic complexity based on a 3D reconstruction of the whole neuron morphology pointed out to an increase in the apical dendrite length and branching points in CA1 organotypic hippocampal slices treated with Aβ.

Finally, and in order to advance in the knowledge of the signaling cascades controlled by the Aβ peptide, we have created a peptide comprising the Integrin β1 signal region, which efficiently interfere both *in vitro* and *in vivo* in the Aβ oligomers/Integrin β1 toxic signaling program.

Introduction

1. Alzheimer's disease.

Alzheimer's disease (AD) is the most common form of dementia and the most prevalent neurodegenerative disease. This pathology was first reported by the german psychiatrist Aloysius (Alois) Alzheimer (1864-1915), who observed a strange symptomatology in a patient who presented hallucinations and loss of several mental functions, as memory and language impairment. *Post-mortem* analysis of brain of this patient showed the presence of abnormal extracellular aggregates of senile plaques and intracellular tangles (**Figure I1**), being these features extensively used years later for AD diagnosis.

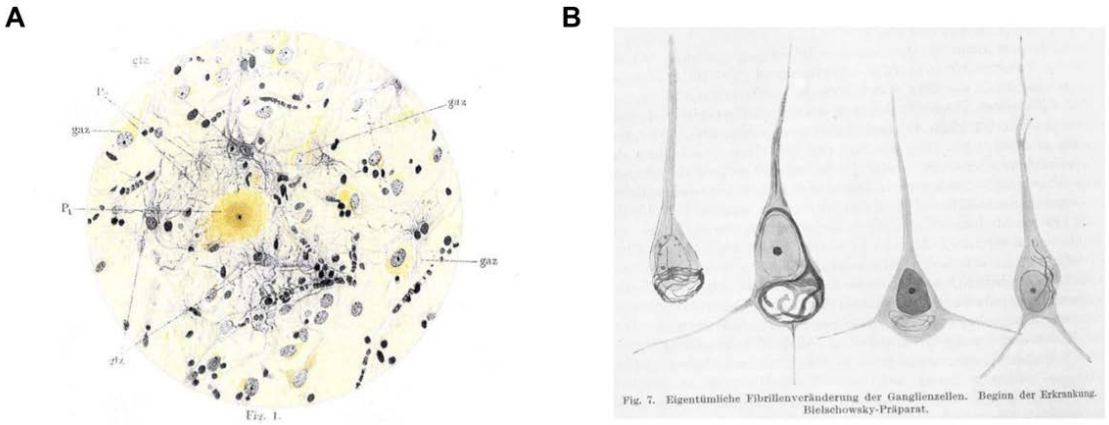

Figure I1. Pictures of original drawings of Alois Alzheimer showing pathological features of the disease. Drawings of senile plaques **(A)** and neurons with intracellular tangles **(B)** present in tissue samples from Alzheimer's disease patients.

AD is characterized by a profound cognitive decline that occurs as a consequence of a progressive and irreversible neuronal loss. The progression of the disease has been associated with a gradual damage in function and structure in the hippocampus and neocortex, the vulnerable brain areas involved in memory and cognition (Scheff *et al*., 2006). The degeneration of these specific areas produces neuronal dysfunction with the consequent synaptic loss and alterations in several cognitive functions.

1.1. Alzheimer disease subtypes.

AD has been classified mainly into two different forms, the early onset or the familial AD and the late-onset or sporadic AD.

1.1.1. Early-onset or familial Alzheimer's disease.

Familial Alzheimer's disease is a rare form of Alzheimer's that entirely passed down through a Mendelian inheritance. It represents between 2-3% of all cases of Alzheimer's and usually has much earlier onset than other types of Alzheimer's, with symptoms developing in people in their 30s-40s. Researchers believe that people with this form of AD present mutations in at least three genes: amyloid precursor protein (APP) on chromosome 21 (Goate et al., 1991), presenilin-1 (PSN1) and -2, (PSN2) on chromosomes 14 and 1, respectively (Cruts *et al*., 1996). Mutations in the APP are associated with an autosomal dominant inheritance. The Swedish mutation is one of the most well-known genetic variation that causes early onset familial AD. It produces a two-aminoacid change in the protein sequence immediately before the amyloid β (A β) peptide sequence (lysine-methionine for asparagine-leucine). The presence of these mutations implies greater amyloidogenic processing of APP or increased oligomerization of the Aβ peptide. In addition to APP, PSN1 and PSN2 may present up to 180 and 15 different mutations respectively, and all of them related to triggering the disease. However, due to the variability in the mutation penetrance, the appearance of the disease is variable.

1.1.2. Late-onset or sporadic Alzheimer's disease.

The late-onset or sporadic AD starts before 65 years old and encompasses the majority of clinical cases, around 90-95%. In these cases, AD etiology is much more complex and diffuse than familial AD. Multiple risk factors, including ageing, have being described to affect the predisposition to this subtype of the disease. In addition to ageing, the best characterized risk factor is apolipoprotein E (ApoE), which is the main cholesterol transporter in the brain and it has been related to the transport and release of Aβ peptide (Bu, 2009). The gene encoding ApoE may present three different

allelic variants, ApoEε2, ApoEε3 and ApoEε4, having this last variant, the potential to triple the probability of suffering AD in the case of heterozygous individuals (Huang, 2006). In addition, by using genetic association studies such as those carried out by Bertram and colleagues, a database has been generated gathering information of those genes which mutations could be related to the predisposition to develop AD (http://www.alzgene.org) (Bertram *et al*., 2007).

1.2. Alzheimer's disease pathology. Amyloid β peptide.

Given that the first description made by Alois Alzheimer about pre-senile dementia refers to the formation of senile plaques and neurofibrillar tangles (NFT), these elements have been traditionally considered as the key pathological hallmarks of AD. The formation of NFT follows well-established patterns while senile plaques appear and distribute in a random manner. In addition to plaques distribution, the detection of Aβ as a main constituent of the plaques (Glenner & Wong, 1984b) and the identification of gene mutations related to Aβ synthesis in familial AD has led to formulate the amyloid cascade hypothesis (J. A. Hardy & Higgins, 1992; Selkoe, 1991).

The amyloid cascade hypothesis postulates that the deposition of Aβ, which is due to the unbalance between its generation and elimination, leads to neurodegeneration and subsequent dementia (Glenner & Wong, 1984; Hardy & Allsop, 1991; Hardy & Selkoe, 2002). This hypothesis proposes Aβ peptide as a candidate for initiating the disease, appearing NFTs after Aβ-induced damage. Aβ peptide is generated as a 4.5 kDa monomer from the proteolytic processing of the amyloid precursor protein (APP). APP is a transmembrane glycoprotein with a large extracellular domain that carries out a wide range of biological functions in the central nervous system (CNS). Interestingly, it is implicated in the regulation of neurites growth during development (Herms *et al*., 2004). However, in the adult brain its role is more related to cell adhesion, neuroprotection, synapse formation, and transcription modulation of several genes (reviewed in Raychaudhuri & Mukhopadhyay, 2007). In addition, several proteins have been shown to interact with APP, regulating their processing and intracellular

signaling, which may be related to a role of APP as a cell surface receptor (Zheng & Koo, 2011).

The proteolytic sequential processing of APP mainly occurs by two different manners: I) non-amyloidogenic cascade and II) amyloidogenic cascade (**Figure I2**). The non-amyloidogenic cascade consists in that the protease, α-secretase, cleavages the APP, generating the soluble long fragment αAPPs (N-terminus) and a smaller called αAPP-CTF (C-terminus), which remains anchored to the cell membrane. Then, αAPP-CTF fragment is cleaved by other secretase, γ-secretase, producing two soluble peptides, p3 which biological function is still unknown, and AICD (APP intracytoplasmic domain), that can function as a transcriptional regulator of several genes such as glycogen synthase kinase 3β or p53 (Kimberly *et al.*, 2001; Von Rotz *et al.*, 2004). In contrast, in the amyloidogenic cascade the first cleavage is performed by the protease, β-secretase, generating βAPPs and βAPP-CTF. Further processing of βAPP-CTF by γ-secretase produces AICD and Aβ peptide, being now Aβ peptide released to the extracellular medium. Remarkably, while the non-amyloidogenic cascade is predominant in physiological conditions, avoiding excessive production of Aβ peptide, the equilibrium between the two pathways is lost in AD patients. In addition, there are several non-canonical pathways through which APP can be processed, some of them also contributing to Aβ peptide generation (Müller *et al.*, 2017).

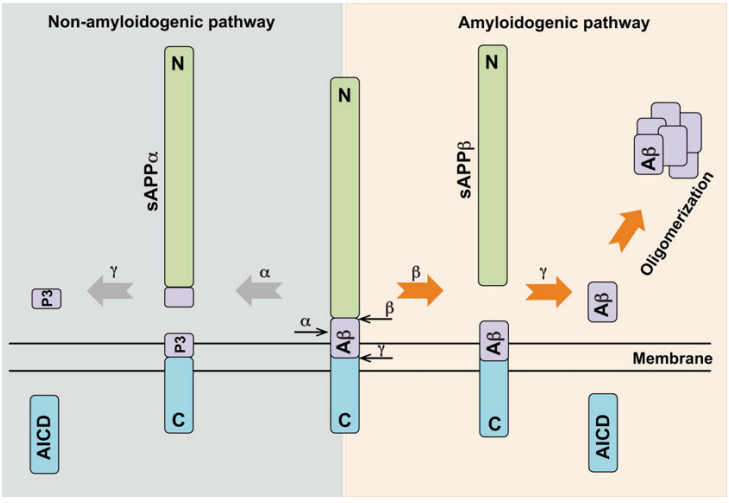

Figure I2. Schematic representation of canonical amyloid precursor protein (APP) processing. The non-amyloidogenic (blue background) and amyloidogenic (red background) pathways are shown. The

proteolytic cleavage of APP by α- or β-secretase, and subsequently by γ-secretase, generates APP intracellular domain (AICD), and p3 or amyloid β (Aβ) peptides, respectively (adapted from Maya et al., 2014).

Since γ-secretases exhibit lack of specificity of the proteolytic cleavage of APP, Aβ peptide length may vary between 37 and 49 aminoacids (Weidemann *et al*., 2002). Most of the circulating Aβ peptide consists of 40-aminoacid-long peptides, being also present in a great extent those formed by 42 or 43 aminoacids ($A\beta_{1-40}$, $A\beta_{1-42}$ and $A\beta_{1-43}$, respectively). In addition, shorter (38- or 39-aminoacid-long) and longer (46 to 49-aminoacid-long) peptides can also be found (Takami *et al*., 2009). After APP processing, Aβ monomers, especially $A\beta_{1-42}$, tend to aggregate due to their structure, forming oligomers that will lead to protofibers and fibers, and eventually generating senile plaques. In this sense, *in vitro* and *in vivo* experiments have shown that the Aβ peptide monomer aggregation into high molecular weight species makes them toxic oligomers, representing the predominant neurotoxic Aβ peptide species (Glabe, 2005; Klein, 2002).

In addition to this, Aβ peptide oligomers have been isolated from animal models of AD (Oddo *et al*., 2006; Tomiyama *et al.*, 2010) and cerebrospinal fluid (CSF) and brains from AD patients (Bao *et al*., 2012), in whom the presence of this peptide seems to correlate with the progression of the disease (Santos *et al*., 2012). In fact, nanomolar concentrations of Aβ oligomers are able to induce neuronal death in hippocampal organotypic slices (Alberdi *et al*., 2010; Lambert *et al*., 1998), but also to inhibit long-term potentiation (LTP) (Lambert *et al*., 1998; Wang *et al.*, 2004), and to promote Ca^{2+} fluxes dysregulation as well as cell membrane disruption (Alberdi *et al*., 2010; Demuro *et al*., 2005). Due to the biochemical complexity of Aβ peptides (oligomerization, varying length, etc.), they are very promiscuous molecules able to signal through a repertoire of receptors and consequently promoting a wide range of effects both in neurons and other cell types (Viola & Klein, 2015) (**Figure I3**).

Apart from the canonical receptors, a subset of membrane proteins binds Aβ peptide such as FPRL1 (formyl peptide receptor-like 1), RAGE (receptor for advanced glycosylation end-products) or integrins (Verdier *et al.*, 2004).

2. Integrins.

2.1. Integrin heterodimers and molecular mechanisms for integrin activation.

Integrins are a large family of extracellular matrix (ECM) receptors ubiquitously expressed and distributed. These glycoproteins participate in the cell–cell or cell–matrix interactions in order to instigate vital cellular events such as cell adhesion, differentiation or migration (Cheah & Andrews, 2018). These integrin-mediated adhesions are regulated by diverse factors, including the conformation-specific affinities of integrin receptors for their extracellular ligands, the clustering of integrins and their intracellular binding partners into discrete adhesive structures, mechanical forces exerted on the adhesion, and the intracellular trafficking of integrins themselves (Chanpimol *et al.*, 2017).

Regarding their structural composition, integrins are heterodimers constituted by alpha (α) and beta (β) subunits. In mammals, there are 18 different α and 8 different β subunits, and their combinations generate 24 different heterodimers (Cheah & Andrews, 2018). Each subunit is divided into three domains: a large extracellular domain, a transmembrane domain and a cytoplasmic domain (Yan et al., 2016, Van Dyke & Maddow, 2011) (**Figure I3A**). The α-subunits determine integrin ligand specificity while the β-subunits are connected to intracellular molecules, thereby involving multiple signaling pathways (Wu & Reddy, 2012). Subunit-specific differences in activation sensitivity of integrins has been recently reported (Pagani & Gohlke, 2018). During integrin activation, these glycoproteins change its configuration from an inactive form (bent low-affinity) into an active form (stable extended high-affinity conformation) (Vazquez-Sanchez *et al.,* 2018) (Van Dyke & Maddow, 2011) (**Figure I3B**).

Integrins are bidirectional signaling molecules. On the one hand, they modulate signal transduction from the cytoplasm to the cell (“inside-out”), leading to cell adhesion and migration, and ECM assembly. On the other hand, they transduce relying information from the extracellular environment to the inside of the cell (“outside-in”)

(Raab-Westphal *et al.,* 2017). This intracellular signaling is related to clustering between integrin and focal adhesions, leading to the assembly of numerous integrin associated molecules such as talin, vinculin, paxillin, focal adhesion kinase (FAK), Src and integrin linked kinase (ILK), that initiate canonical signaling pathways involving small GTPases of the Ras superfamily, ERK, JNK or AKT. Indeed, they modulate responses including adhesion, spreading, migration, growth signaling, survival signaling, secretion of proteases and invasion (Moser *et al.,* 2009; Wehrle-Haller, 2012).

Different types of integrins are categorized according to which cell surface, ECM component or inflammatory ligand they bind. Vertebrates have four receptor subgroups: laminin receptors, leukocyte-specific integrins, collagen receptors and arginine-glycine-aspartate (RGD) receptors which recognize the triplet motif found in many ECM proteins such as fibronectin, collagen, vitronectin, osteopontin and thrombospondin (Ahmedah *et al.,* 2017). However, integrins also have functional relationships with other membrane receptors such as ion channels and growth factor receptors (Morini & Becchetti, 2010)

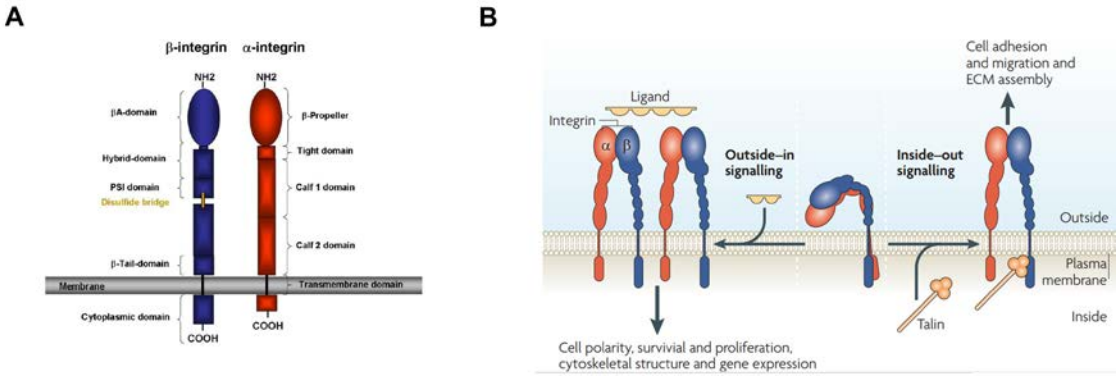

Figure I3. Schematic illustration of the integrin structure and bidirectional signaling. (A) The basis of integrins are two subunits—α and β—that are non-covalently bonded. The integrin structure is composed of three main domains: extracellular domain, transmembrane domain, and a cytoplasmic tail (adapted from Alexander and Bendas, 2011). **(B)** Integrin in its bent form is presumed to be inactive. Activation can occur either by ligand binding (outside-in signaling) or by effects on the cytoplasmic domains (inside-in signaling) leading to straightening and separation of the cytoplasmic domains, accompanied by conformational changes in them and allowing binding of cytoplasmic proteins and

signaling. All changes are reversible and can operate in either direction (adapted from Shattil *et al*., 2010).

2.2. Integrins in central nervous system.

Integrins are expressed by neurons, astrocytes, microglia, oligodendorcytes and endothelial cells in the CNS (Nieuwenhuis *et al.,* 2018). These glycoproteins represent an important group of signaling molecules that control many fundamental processes within CNS, both during development and adult stages. In neurons, they are involved in neuronal adhesion, migration, neurite outgrowth and axon regeneration, neuronal maturation and post-injury expression, and learning and memory (Cheah & Andrews, 2018; Nieuwenhuis *et al*., 2018). Different integrin subtypes participate in instincts forms of synaptic plasticity, which reflect the differences in their biophysical properties, molecular interactors and signaling systems (Park & Goda, 2016).

At synapses, cell adhesion molecules (CAMs) provide the molecular framework for coordinating signaling events across the synaptic cleft (Cingolani *et al*., 2009). Significant increases in intracellular Ca^{2+} levels have been reported to occur in response to exposure of neurons to natural ligands of integrins via activation of NMDA receptors (Sheng *et al.,* 2013). By electrophysiological approaches, it has been demonstrated that integrin β1 mutants upset synaptic transmission through ácido α-amino-3-hidroxi-5-metilo-4-isoxazolpropiónico (AMPA) receptors and diminished N-metil-D-aspartato (NMDA) receptor-dependent LTP (Chan et al., 2008). Therefore, integrin-mediated signaling is seemingly essential for maturation of CNS synapses. Thus, integrin mutated forms are likely to contribute to imbalanced synaptic function in pathological conditions in the brain such as Alzheimer's disease

At molecular level, synaptic integrins activate local protein tyrosine kinases (FAK, Pyk2 and Src kinases) which modulate NR2A and NR2B subunits tyrosine phosphorylation, together with enhanced NMDA receptor-mediated function in mature hippocampal synapses (Bernard-Trifilo *et al*., 2005).

3. NMDA receptors.

N-Methyl-D-Aspartate receptors (NMDARs) belong to the family of ionotropic glutamate receptors, which mediate most excitatory synaptic transmission in mammalian brains. NMDARs are the primary glutamate-gated cation channels that mediate Ca^{2+} signals in neurons, and contribute to the expression of long-term potentiation (LTP) and long-term depression (LTD). Therefore, NMDARs mediate key physiological functions under normal conditions such as neurodevelopment, synaptic transmission and plasticity (Iacobucci & Popescu, 2017; Zorumski & Izumi, 2012) or learning and memory (Baez *et al.,* 2018; Kono *et al.,* 2018). Conversely, aberrant NMDAR functions and/or abnormal expression levels of these receptors have been linked to numerous neurological disorders and pathological conditions such as neurodegenerative diseases, schizophrenia, depression, chronic and neuropathic pain as well as neuronal loss following ischemia or stroke (Bading, 2017; Paoletti *et al.,* 2013; Yao & Zhou, 2017).

3.1. The NMDA receptor complex.

3.1.1. NMDAR subunit composition.

NMDA receptors are heteromultimeric complexes constituted by different subunits which confer specific sensitivity both to endogenous and exogenous ligands, permeation and blockage by divalent cations, characteristic kinetic properties, and intracellular protein-protein interactions (Glasgow *et al.,* 2015; Gmel, 2010; Cull-Candy, 2001). Molecular methods have identified various NMDAR subunits: the ubiquitously expressed NR1 subunit; a family of four distinct NR2 subunits (A, B, C and D); and two NR3 subunits (A and B) (**Figure I4A**) (Kumar *et al.,* 2015). Although NMDARs are widely expressed throughout the CNS, their number, localization, and subunit composition are strictly regulated and differ in a cell- and synapse-specific manner (Sanz-Clemente *et al.,* 2013).

All NMDARs are structurally constituted of multiple NR1 subunits with at least one NR2 subunit. The majority of native NMDARs are considered tetramers, and are

constituted by two NR1 and two NR2 subunits of the same or different subunits (Glasgow *et al*., 2015) (**Figure I4B**). The basic functional structure in each receptor is considered to the NR1–NR2 dimer, being the NR2 subunits responsible for the high affinity binding to glutamate, while NR1 subunits bind glycine. Moreover, NR1 and NR2 subunits confer Ca^{2+} permeability and Mg^{2+} sensitivity (Cull-Candy & Leszkiewicz, 2004; Paoletti & Neyton, 2007). On the other hand, the NR3 subunits may co-assemble with NR1/NR2 complexes acting as a molecular brake to limit the plasticity and maturation of excitatory synapses and may have a profound impact on several functional/behavioral activities in adult animals (Henson *et al*., 2008; Mohamad *et al.,* 2013).

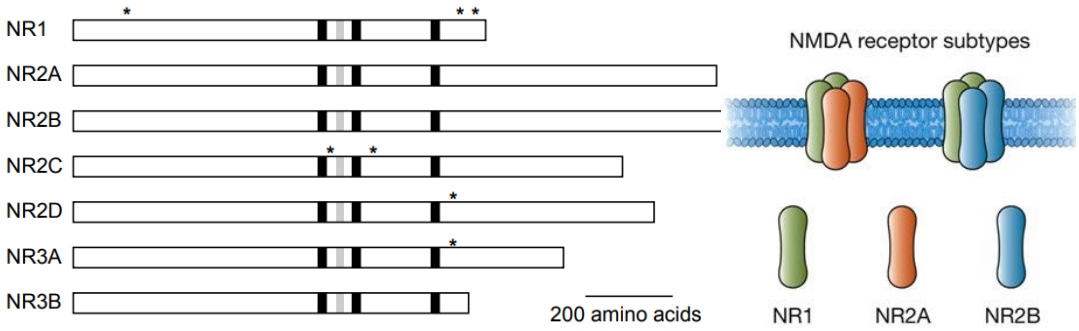

Figure I4. NMDAR subunits diversity. (A) Representation of NMDAR subunit polypeptides. Black boxes indicate transmembrane domains, and grey boxes show the transmembrane M2 re-entrant loop. NR1 is the best characterized, which has three regions of alternative splicing: the amino-terminal N1 cassette (exon 5); and the carboxy-terminal C1 (exon 21) and C2 (exon 22) cassettes. **(B)** Schematic illustration of the conventional NMDAR containing NR1 and NR2 subunits (adapted from Cull-Candy, 2001).

Over the past few decades NR2A and NR2B subunits have been the subject of intense investigation. NR2B subunit is expressed prenatally and is required for normal neuronal pattern formation and viability of the individual, but during the development these are supplemented with, or replaced by NR2A subunit, which progressively increases its expression and synaptic incorporation (Burgess *et al.,* 2016). It has been described that the switch between NR2A and NR2B subunits occurs during synaptic maturation and in response to the activity and experience, being important to mediate

the synaptic plasticity lifelong (McKay *et al*., 2018). Getting to know the roles played by different NMDAR subunits is essential to understand the normal transmission in the CNS, and should provide information about how the multiplicity of NMDAR subunits can be used in order to obtain a therapeutic advantage.

Individually, all those subunits share a common membrane topology constituted by four discrete semiautonomous domains: the extracellular amino-terminal domain (ATD), the extracellular ligand-binding domain (LBD), where glutamate and glycine bind to and which is created by two regions (S1 and S2), the transmembrane domain (TMD), which contains three transmembrane segments (M1, M3 and M4) and a re-entrant pore loop (M2), which contains a Mg^{2+} binding site as well as a critical asparagine residue that determines Ca^{2+} permeability properties of the channel, and finally an intracellular carboxyl-terminal domain (CTD), which interacts with multiple cytosolic proteins and its length varies according to the subunit (Gibb *et al*., 2018; Hansen *et al*., 2018; Zhang *et al.,* 2016) (**Figure I5**).

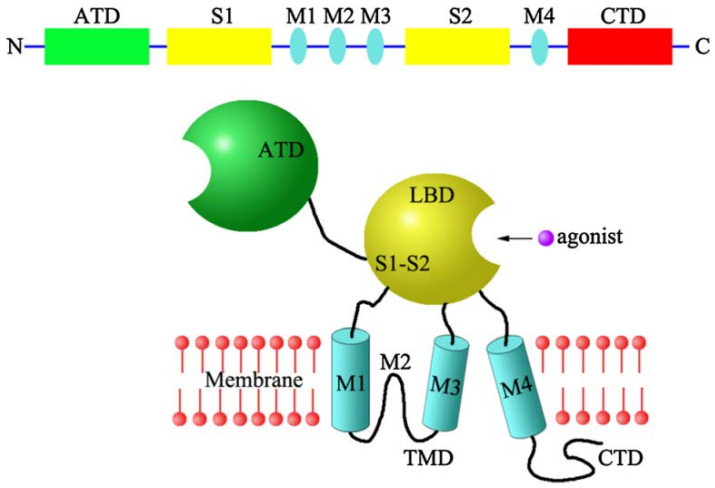

Figure I5. Structure and domain organization of NMDA receptors. Linear representation of the subunit polypeptide chain and schematic illustration of the subunit topology. NMDARs subunits have a modular structure composed of two extracellular domains: the ATD (green) and the LBD (yellow); a TMD (cyan), which forms part of the ion channel pore; and an intracellular CTD. The LBD is defined by two segments of amino acids termed S1 and S2. The TMD contains three membrane-spanning helices (M1, M3, and M4) and a membrane re-entrant loop (M2) (adapted from Zhang *et al*., 2016)

3.1.2. NMDA receptor activation mechanism.

At resting membrane potential, the pore of the NMDAR channel is blocked by physiological levels of extracellular Mg^{2+} in a highly voltage-dependent manner. NMDAR activation requires postsynaptic depolarization (to relieve Mg^{2+} blockage) which matches with the presynaptic glutamate release, thus allowing glutamate to bind to the NMDARs. Moreover, a third element is required for NMDAR activation, the presence of glycine or D-serine occupying a binding site located at the LBD. Upon NMDAR activation, the opened channel pore leads to Ca^{2+}, Na^{+} and K^{+} permeability (Burgess *et al*., 2016; Galais & Lorenzini, 2017; Labrie & Roder, 2010) (**Figure I6**).

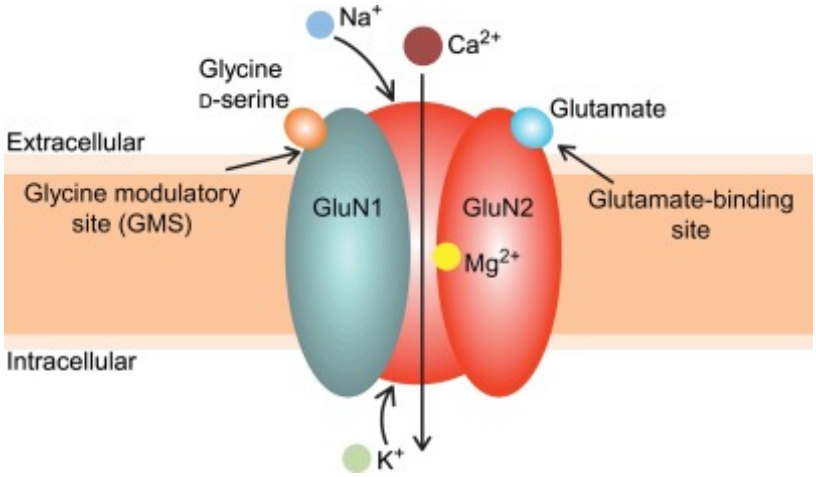

Figure I6. Schematic representation of NMDA receptor complex and its binding sites. This ionotropic channel mediates the flow of Na^{+} and Ca^{2+} cations into the cell, and K^{+} cations out of the cell. At resting state, NMDAR is blocked by the presence of extracellular Mg^{2+} cations in the channel pore. The activation and opening of NMDARs is both voltage-dependent and ligand-gated, and requires the binding of two ligands, glutamate and either D-serine or glycine (adapted from Balu, 2016).

The intracellular Ca^{2+} fluxes are required for LTP and LTD (Fetterolf & Foster, 2011; Hardingham & Bading, 2010) and also for synaptic plasticity (Sanz-Clemente *et al*., 2013). Moreover, Ca^{2+} influxes trigger various intracellular signaling cascades by activating calcium-sensitive NMDAR-interacting proteins in the multiprotein complex (Lai, *et al*., 2011; Martin & Wellman, 2011). There is increasing evidence suggesting that these interacting proteins confer versatile functions to NMDARs (Fan *et al*., 2014).

3.2. Locations of NMDARs: synaptic *vs* extrasynaptic processes.

NMDAR subunits differ not only in temporal pattern of expression, but also in cellular localization. NMDARs have been found on both synaptic and extrasynaptic locations in neurons (Duguid, 2013; Ferreira *et al*., 2017; Petralia *et al*., 2010). Synaptic NMDA receptors are localized into postsynaptic densities (PSDs) where they are structurally organized (and spatially restricted) in a large macromolecular signaling complex, comprising scaffolding and adaptor proteins, which physically link the receptors to the cytoskeleton (Scannevin & Huganir, 2000). On the other hand, extrasynaptic NMDARs are localized on dendrites or the sides of spines, many of them concentrated at contact points with adjacent processes including axons, axon terminals, or glia (Ferreira *et al*., 2017), where many proteins can associate with the NMDARs.

Synaptic NMDARs composition is highly dynamic; it changes quickly after synapse formation. The proportion of synaptically located NMDARs increases with the development, however, significant population of NMDARs remain extrasynaptic in adulthood (Petralia *et al*., 2010). Thus, synapses containing predominantly NR1/NR2B complex represent immature sites, whereas mature sites are more predominantly composed by NR1/NR2A subunits. Moreover, extrasynaptic NMDARs are usually composed by NR1/NR2B heteromers (Lopez de Armentia & Sah, 2003; Paoletti *et al*., 2013). In any case, the segregated subcellular localization is not absolute, since it has been reported the presence of NR2A in the extrasynaptic membranes of primary cultures of neurons (Thomas, 2006) and NR2B at the postsynaptic density (Sanz-Clemente *et al*., 2013).

The physiological function of extrasynaptic NMDARs is not fully understood. It was initially believed that only synaptic NMDARs were implicated in the synaptic transmission process; however, there is growing evidence regarding the involvement of extrasynaptic NMDARs in the transmission of information from the presynaptic terminal (Harris & Pettit, 2008). A number of studies suggest that extrasynaptic NMDARs function may depend on the receptor type as well as the associated proteins (Newpher & Ehlers, 2009). It has been described that activation of extrasynaptic

NMDARs by glutamate spillover may contribute, as well as synaptic NMDAR, to LTD and can reduce the miniature excitatory postsynaptic currents (mEPSCs), which may reflect early synaptic injury (Talantova *et al*., 2013). On the contrary, extrasynaptic NMDARs do not play an important role in LTP, but synaptic NMDARs do (Parsons & Raymond, 2014).

The location of the NMDARs may also profoundly affect the signals that emanate from these receptors. It has been reported that selective synaptic NMDAR stimulation increases extracellular signal-regulated kinase 1/2 (ERK) activation, cAMP response element-binding protein (CREB) phosphorylation and brain-derived neurotrophic factor (BDNF) expression, enhances antioxidant defense, and provides neuroprotection (Hardingham & Bading, 2010). On the contrary, the extrasynaptic pool of NMDARs triggers mitochondrial membrane potential breakdown, as well as cell body and dendritic damage (Leveille *et al*., 2008), inducing a signaling pathway that inactivates ERK (Ivanov *et al*., 2006). Moreover, activation of extrasynaptic NMDARs activates a general and dominant CREB shut-off pathway (Hardingham *et al*., 2002; Kaufman *et al*., 2012), suggesting that extrasynaptic NMDARs activation contributes to excitotoxicity. Therefore, research over the past decade has suggested that over activation of NMDARs located outside of the synapse plays a major role in NMDAR toxicity, whereas physiological activation of those inside the synapse can contribute to cell survival (**Figure I7**), raising the possibility of therapeutic intervention based on NMDAR subcellular localization (Parsons & Raymond, 2014). Conversely, other investigations have reported that activation of extrasynaptic NMDARs alone did not trigger cell death, but activation of both extrasynaptic and synaptic NMDARs switched on the neuronal death program, being this excitotoxic effect dependent on the magnitude and duration of the co-activation (Zhou & Sheng, 2013).

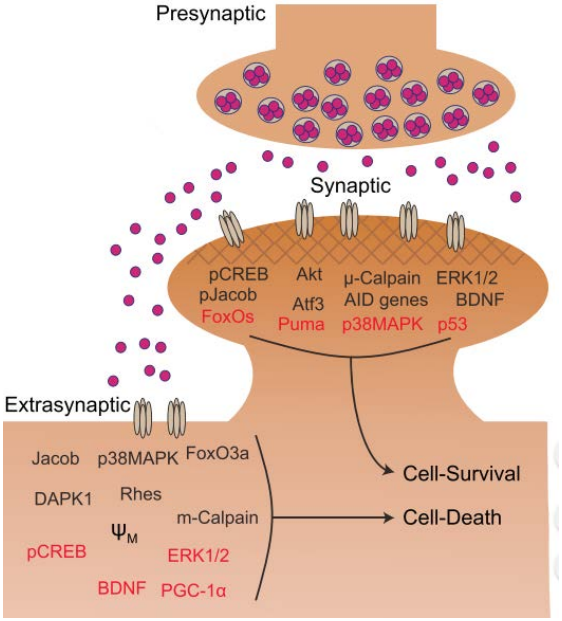

Figure I7. Scheme illustrating the main pro-survival and pro-death signals triggered by NMDAR activity. Stimulation of synaptic NMDARs activates prosurvival and inhibits prodeath intracellular signaling, whereas extrasynaptic NMDAR activation does the opposite (adapted from Parsons and Raymond, 2010).

3.3. NMDA receptor trafficking and synaptic plasticity.

NMDARs are synthesized and assembled in the endoplasmic reticulum (ER) to form functional channels with differing physiological and pharmacological properties and distinct patterns of synaptic targeting. Nascent NMDARs are processed in the Golgi apparatus and transported, in form of packets, along microtubule tracks to the neuronal surface, where they deliver their contents by membrane fusion with the plasma membrane (Pérez-Otaño & Ehlers, 2005). It seems that the NR1 receptor might play an active role in controlling the delivery of NMDA receptors to synapses *(Scott et al*., 2001; Xia *et al*., 2001). Additionally, studies involving genetically altered mice support a role for the intracellular C-terminal regions of the NR2A and NR2B subunits in synaptic localization and clustering of NMDARs. Increased insertion of NR2B-containing receptors at the synapse is independent of both glutamatergic synaptic activity and its greater density. In contrast, synaptic insertion of NR2A-containing receptors requires synaptic activity and is promoted by increased levels of NR2A

expression (Jacobs *et al*., 2015; Standley *et al*., 2012; Von Engelhardt, 2009; Yan *et al*., 2014).

Different investigations suggest that synaptic NMDAR number and subunit composition are not static, but change dynamically in a cell- and synapse-specific manner during development and in response to neuronal activity or sensory experience (Lau & Zukin, 2007). Within the plasma membrane, NMDAR laterally diffuse between synaptic and extrasynaptic sites (Tovar & Westbrook, 2002) in a NR2 subunit-dependent manner (Bard *et al*., 2010; Groc *et al*., 2006; Tovar & Westbrook, 2002). Dynamic regulation of synaptic efficacy is thought to play a crucial role in formation of neuronal connections and in experience-dependent modification of neural circuitry (Carroll & Zukin, 2002).

The number and subunit composition of synaptic NMDARs is also regulated by activity-dependent protein degradation. One of the main mechanisms underlying this process is the ubiquitin-proteasome degradation system. The regulated ubiquitin-proteasome degradation system preserves cell homeostasis by acting as the primary mechanism of protein quality control, membrane protein trafficking, receptor internalization, and degradation (Ciechanover & Iwai, 2004; Hicke & Dunn, 2003). This mechanism is crucial to the homeostatic control of synaptic NMDAR strength and provides a proper development and function of synapse growth and development, synaptic transmission and plasticity at mammalian synapses, and can mediate remodeling of protein composition of synaptic structures (Ehlers, 2003).

On the other hand, endocytosis is a fundamental mechanism by which neurons regulate intercellular signaling, synapse maturation and synaptic strength, and it occurs by the assembly of clathrin coats and the budding of clathrin-coated vesicles from the neuronal plasma membrane. NR2A and NR2B subunits contain distinct internalization motifs in their distal C-terminal region, which regulate endocytosis at somewhat different areas. Whereas NR2B is sorted to recycling endosomes and re-inserted into the plasma membrane, NR2A-containing receptors form early endosomes and are preferentially leaded to lysosomal degradation (**Figure I8**) (Tang *et al.,* 2010).

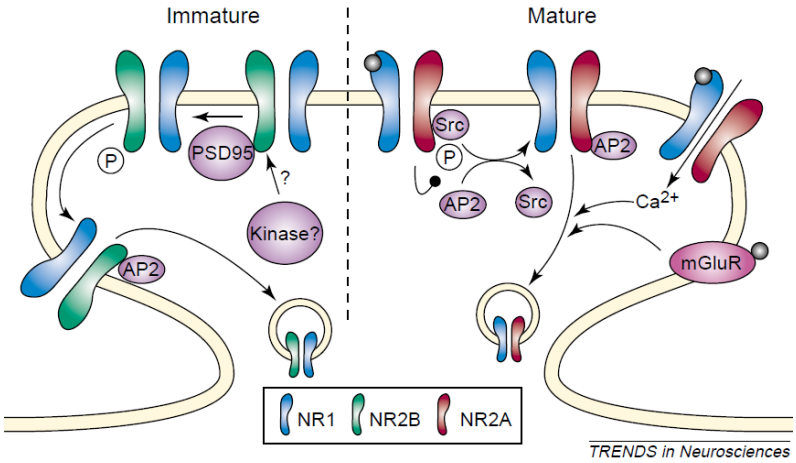

Figure I8. Regulatory mechanisms of NMDA-receptor internalization. Both, NR2A and NR2B subunits, contain motifs that bind the endocytic adaptor protein AP2 involved in the clathrin-dependent endocytosis machinery. Whereas the internalization of NR1-NR2B (highly predominated at immature synapses) is regulated by its association with PSD95, the ability of NR1-NR2A (localized at mature synapses) to associate with AP2 is modulated by dephosphorylation of tyrosine residues in its C-terminal tail. Following endocytosis, NR2A-containing NMDARs are preferentially targeted for degradation, whereas NR2B receptors are targeted for recycling (adapted from Carroll & Zukin, 2002).

Insertion and removal of NMDARs are expected to play crucial roles in the regulation of synaptic strength in the developing and mature CNS. Regulation of NMDAR trafficking and gating provides a potentially important way to modulate efficacy of synaptic transmission and to alter the LTP and LTD modification thresholds. Since NMDAR-dependent neurotransmission is affected by changes in receptor expression, trafficking and gating may be relevant in disorders characterized by NMDAR deregulation and cognitive impairments (Carroll & Zukin, 2002).

3.4. Molecular mechanism underlying synaptic localization and functional regulation of NMDA receptors.

3.4.1. NMDA receptors interact with PDZ domains-containing proteins.

The versatility of NMDAR functions may be partially attributed to its organization at the synapse, where NMDAR is linked to the plasma membrane by binding to more than 70 adhesion proteins (Grant & O'Dell, 2001; Husi *et al.*, 2000). This adhesion

protein complexes contain a group of proteins called MAGUKs (membrane-associated guanylate kinases), which include PSD-95, synapse-associated protein-90 (SAP-90) and the closely related PSD-93/chapsyn-110, SAP-97/hdlg, a.d SAP-102, all of which are found at synapses in brain (Ye *et al*, 2018). The characteristic of all these proteins is that contain several PDZ domains, which directly can bind to the distal end of the C-terminal tail of the NR2 subunits through its PDZ recognition motifs (Wang *et al*., 2008). It has been demonstrated that the NR2 subunits PDZ recognition motifs play critical roles in driving the trafficking to and stabilizing at synaptic sites. In fact, mice expressing C-terminal truncated NR2A and NR2B subunits exhibit improper localization of synaptic NMDARs (Steigerwald *et al*., 2000). Moreover, electrophysiological and confocal imaging approaches demonstrates that the disruption of the NR2B-PDZ binding domain results in a loss of synaptic NR2B (Chung, 2004).

3.4.2. NMDAR regulation by phosphorylation.

NMDAR subunits are also subject to differential regulation by several post-translational modifications, including phosphorylation. It is well established that protein phosphorylation requires many cellular processes including protein activation/deactivation, localization, mobility and many protein-protein interactions in order to transduce the physico-chemical intracellular signals (Chen & Roche, 2007). In particular, NMDAR phosphorylation is a key mechanism that regulates its function and location in the synapses.

The function and subcellular distribution of NMDARs are differentially regulated by specific phosphorylation on serine/threonine and/or tyrosine amino acid residues in the intracellular C-terminal regions (**Figure I9)**. On one hand, protein kinases catalyze protein phosphorylation while phosphoprotein phosphatases catalyze protein dephosphorylation, but both are recruited to NMDARs through interactions with postsynaptic density proteins, such as PSD-95.

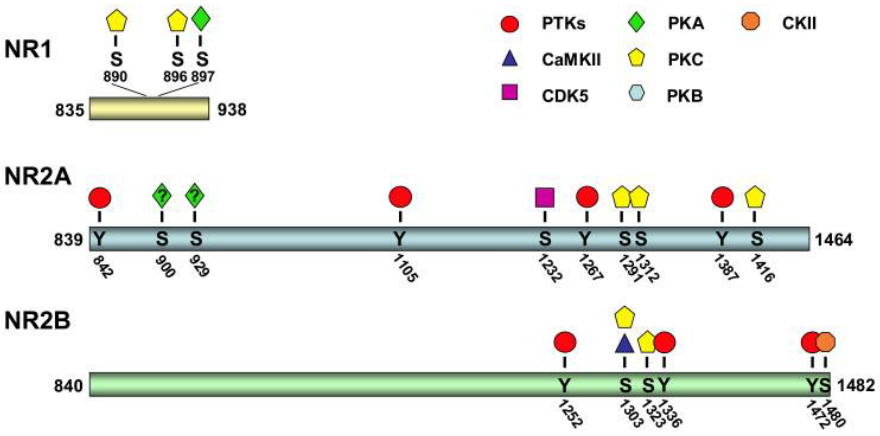

Figure I9. Phosphorylation sites in the cytosolic tails of NMDA receptor subunits. The cytosolic tails of NMDA receptor subunits NR1, NR2A and NR2B contain about 100, 630 and 640 amino acids, respectively. Each tail is phosphorylated on serine/threonine and/or tyrosine residues by a variety of kinases (adapted from Chen and Roche, 2007).

3.4.2.1. Tyrosine phosphorylation of NMDA receptors.

Several tyrosine residues susceptible to be phosphorylated by protein tyrosine kinases (PTKs) have been identified in NR2A and NR2B (see **Figure I9**). In addition, Ali and Salter reported that NMDAR tyrosine phosphorylated subunits increased Ca^{2+} currents (Ali & Salter, 2001) and this NMDA tyrosine phosphorylated receptor was also involved in the control of its internalization. Two members of the Src family protein tyrosine kinases, Src and Fyn, are able to phosphorylate NR2B at the Y^{1472} and this phosphorylation serves to control its presence into the NMDAR complex at the surface of the plasma membrane (Sinai *et al*., 2010). This membrane stabilization enhances NMDAR activity and plays an important role in LTP of CA1 neurons (Goebel-Goody, Davies *et al*., 2009).

3.4.2.2. Functional regulation of NMDA receptors by serine/threonine phosphorylation.

Many serine/threonine phosphorylation sites have been identified in NMDAR subunits, which are substrates for cAMP-dependent protein kinase A (PKA), protein kinase C (PKC), protein kinase B (PKB), CaMKII, cyclin-dependent kinase 5 (Cdk5), and casein kinase II (CKII) (see **Figure I9**). These kinases can regulate NMDARs intracellular

trafficking or functional properties resulting in changes in synaptic strength underlying many forms of synaptic plasticity (Lee, 2006).

Importantly, it has been suggested that the effect of PKC on NMDAR regulation is the result of an increase in the opening rate of NMDAR channels and up regulation of receptor surface presence (Lan *et al*., 2001). However, there are also some evidences that suggest that PKC activation can suppress NMDAR-mediated ion currents. These findings are supported due to PKC activation induces a rapid dispersal of NMDARs from synaptic sites (Fong *et al*., 2002). As wells as PKC, PKA also regulates NMDAR function, increasing the amplitude of NMDAR-mediated excitatory postsynaptic currents and regulating Ca^{2+} permeability of NMDARs (Skeberdis *et al*., 2001).

In the C-terminal of NR1, PKC and PKA phosphorylate different serine residues, which regulate cell surface expression and clustering of NMDARs and they may affect channel function by modulating the inhibitory interaction between NR1 and other proteins such as calmodulin (Yan *et al*., 2014).

Both PKC and PKA can also potentiate NR2A-containing receptor currents via the NR2A phosphorylation. S^{1416} phophorylation of the NR2A subunit mediated by PKC decreases the binding affinity between CaMKII and NR2A subunit, providing a molecular mechanism for a direct cross talk between CaMKII and PKC signaling pathways. In addition, Cdk5 also phosphorylates NR2A, which enhances NMDA receptor activity (Chen & Roche, 2007).

As well as NR2A, NR2B-containing receptors are also regulated by PKC. Studies in oocytes show that S^{1303}/S^{1323} phosphorylation of the NR2B mediated by PKC is required to potentiate NR1/NR2B receptor currents (Liao *et al.,* 2001). Intriguingly, Omkumar and collaborators demonstrated that S^{1303} of the NR2B subunit is also phosphorylated both *in vitro* and in hippocampal neurons by CaMKII (Omkumar *et al*., 1996). This S^{1303} phosphorylation is inhibitory since promote slow dissociation of the preformed CaMKII-NR2B complexes (Strack *et al.,* 2000). The presence of CaMKII bound to NR2B at synaptic sites is believed to be an important requirement for the maintenance of LTP, since disrupting this interaction reverses the LTP (Sanhueza *et al*., 2011). Nevertheless, it appears that S^{1303} phosphorylation of the NR2B mediated by CaMKII

regulates NMDA receptors in a different way than for the same residue. NR2B is also phosphorylated by CaMKII on S^{1480} which disrupts the interaction between NR2B and PSD-95 (Chung, 2004).

3.4.2.3. Role of Protein Kinase Cs (PKCs) in NMDAR regulation.

Protein kinase Cs were originally identified in 1979 in rat brain extract as a serin threonin protein kinase that requires Ca^{2+} and phospholipids to be activated (Takai *et al*., 1979). Later, diacylglycerol (DAG), one of the compounds transiently generated by receptor-mediated turnover of membrane phospholipid, was found to be able to activate PKC in a Ca^{2+}-independent manner, suggesting that diacylglycerol acts as a second messenger transducing the input through the PKCs (Kishimoto *et al*., 1980). Now, PKCs are considered a widely distributed brain-specific kinase that have important roles in many cellular processes as they are a common mechanism for transducing various extracellular signals into the cell (Chico *et al*., 2009). PKCs comprise a multigene family of phospholipid dependent serine/threonine protein kinases. In mammals, 12 PKC isozymes have currently been identified, with various PKC isozymes being usually coexpressed in the same neurons. Based on their molecular structures and sensitivity to activator molecules, PKC isozymes are divided into three subfamilies: classical PKCs (cPKCs): PKCα, PKCβ and PKCγ; novel PKCs (nPKCs): PKCδ, PKCε, PKCη and PKCθ; and atypical PKCs (aPKCs): PKCζ and PKCι/λ (**Figure I10**). The cPKC isozymes require to be activated both Ca^{2+} and phosphatidylserine, diacylglycerol or other activators. They contain four homologous domains: two regulatory (the activator-binding C1 domain and the cofactor Ca^{2+}-binding C2 domain) and two catalytic (the C3 domain, containing the ATP-binding site, and the C4 domain, containing the substrate-binding site), interspaced with the isozyme-unique (variable, or V) regions. The nPKC isozymes lack the C2 domain and are Ca^{2+}-independent. The cPKC and nPKC isozymes can thus be activated by diacylglycerol, phorbol esters and bryostatins, with cPKCs requiring Ca^{2+} as the cofactor for its activation. The aPKC isozymes are peculiar PKCs, lack both the C2 domain and half of the C1 homologous domains and are insensitive to Ca^{2+}, diacylglycerol, phorbol esters or other PKC activators.

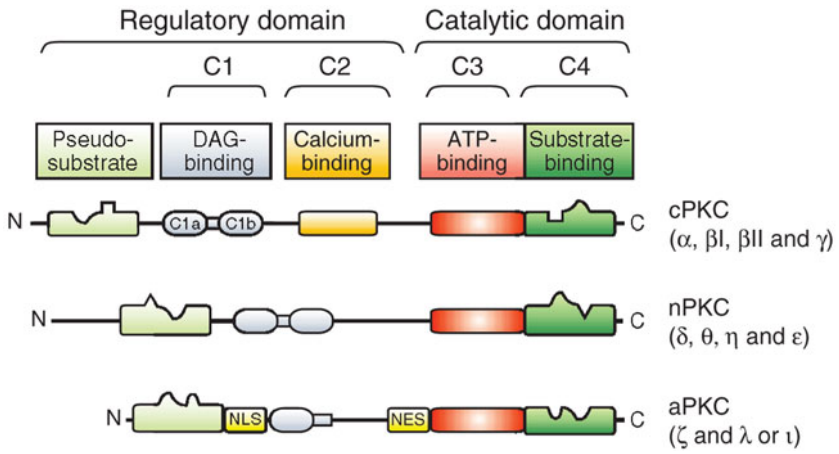

Figure I10. Structural domains of PKC isozymes. Schematic representation showing the different domains of the classical (cPKCs; α, β, γ), novel (nPKCs; ε, δ, θ, η) and atypical (aPKCs; ζ, λ/ι) PKC family members. The pseudosubstrate, C1, C2, and kinase domains in all PKC isozymes and the phosphotyrosine binding motif in aPKCs are indicated (adapted from Spitaler and Cantrell, 2014).

All of them contain, near the C1 domain, a N-terminal pseudo-substrate motif, which binds to the catalytic domain in the inactive state, functioning as an autoinhibitory domain, which allows PKCs to remain in a "closed" conformation. PKC isozymes are activated in response to many different stimuli, including high levels of Ca^{2+}, caused by open NMDA channels. Upon activation, PKCs rapidly translocate from the cytoplasm to the plasma membrane and interacts with phospholipids, leading to release the pseudo-inhibitory substrate from the catalytic domain resulting in an "open" and active configuration. In this active conformation, these kinases produce a myriad of downstream effects, which are translate at the end in a variety of cellular functions including proliferation, apoptosis, differentiation, motility, or inflammation. Moreover, PKC activation is necessary for maintenance but not for induction of LTP (Antal & Newton, 2014).

Finally, interaction of PKC isozymes with compartment and signal-organizing scaffolds display specific and distinct abilities to interact and promote membrane targeting of different PKC isozymes. For example, annexins modulate the localization and activity of PKC family members and participate in the regulation of PKC signaling in health and disease, creating microenvironments to support PKC signal complex formation. Therefore, annexins are scaffolds for PKC isozymes to regulate spatiotemporal PKC signaling (Hoque *et al.*, 2014).

4. Synapses and its structures.

4.1. Dendritic spines.

Synapses are the sites where neurons connect and communicate with each other's in order to constitute functional neuronal circuits (Lu & Zuo, 2017). The majority of excitatory synapses are presented at dendritic spines, tiny protrusions emanating from dendrites. Santiago Ramón y Cajal discovered the dendritic spines in 1888, and he subsequently reported that the processes were present not only in numerous human neuronal subtypes and human brain regions but also are conserved in other animal species. Based on these observations, Cajal hypothesized that these structures could serve to increase the surface area of dendrites to accommodate the vast complexity and number of neural connections in the brain (see review Yuste, 2015b). Technological evolution such as the high resolution microscopy techniques has revolutionized the study of the dendritic spines and synapses, revealing substantial heterogeneity in dendritic spine morphology and associated metrics. Now, it is well described that dendritic spines contain the postsynaptic molecular machinery for synaptic transmission and plasticity (Bourne *et al*., 2008; Sheng & Hoogenraad, 2007; Sheng & Kim, 2011), and act as an intracellular signal transduction functional compartment (Paulin *et al*., 2016). These structures could be related to the locus of memory storage in the brain since it has been reported that neurological diseases leading to impairment in memory and cognitive capabilities are often associated with structural alteration of dendritic spines (Parajuli *et al*., 2017).

4.2. Spine morphology and classification.

More than 100,000 dendritic spines can be present into the dendritic arbor of a single neuron. In general, dendritic spines consist of a rounded "head" (diameter ~1 µm), which receives primarily excitatory synaptic input and a thinner "neck" (diameter ~0.1 µm) in the top (Yuste, 2015a) (**Figure I11A**). However, neurons exhibit many variations of dendritic spine subtypes based on their morphological and physiological properties, each with unique putative functions. Over the years, investigators have

developed various criteria for classifying spines into specific categories based on their overall morphology: stubby, mushroom and thin (**Figure I11B**).

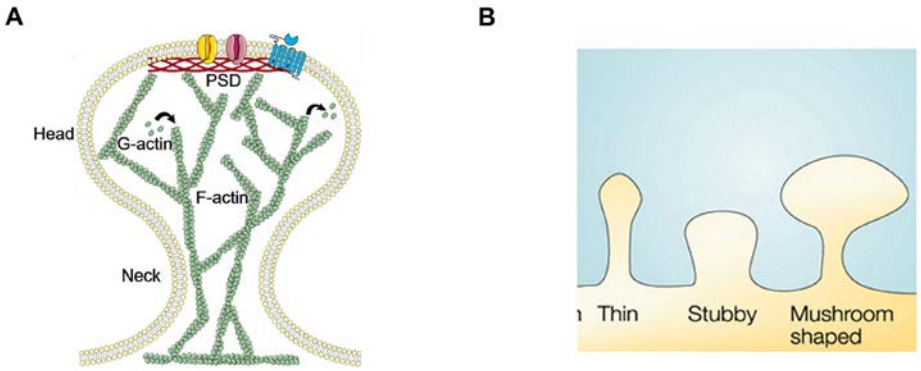

Figure I11. Dendritic spines are multifunctional integrative units of neuronal connectivity and signaling in the nervous system. (A) Spines typically have neck and head compartments, whose structure is largely built on an actin cytoskeleton. G-actin polymerizes into F-actin to build the primary cytoskeletal structure, and thus remodels the spine during synaptic plasticity. This process continually reshapes brain circuitry and synaptic connections. At the PSD, membrane-bound proteins are continually inserted or retracted from the membrane, including ionotropic and metabotropic receptors (adapted from Gipson and Olive, 2017). **(B)** Morphological classification of dendritic spines. Spine morphology and density change throughout life, reflecting the maturation and reorganization of excitatory circuits (adapted from Hering and Sheng, 2001).

Since dendritic spine head diameter and volume have been positively correlated with synaptic strength (Sala & Segal, 2014), it would seem reasonable to conclude that these morphological changes in dendritic spines are anatomical substrates of increased synaptic efficacy.

4.3. Short term morphological and functional plasticity of spines.

Dendritic spines are highly plastic and dynamic in nature, having the capacity to change their morphology, size, number, density, and motility within relatively short timeframes (Gipson & Olive, 2017; Segal, 2017). They are constantly remodeled both morphologically and functionally in response to experience. New dendritic spines are

formed upon learning (Fu *et al*., 2012)and the retention of the learned skill correlates well with their survival (Yang *et al*., 2014), suggesting that the nascent dendritic spines are the structural substrate for novel information storage in the brain. The density of spines along dendrites varies among different types of neurons; it is not even uniform across all dendritic branches of the same neuron (Grifoni *et al*., 2002).

As mentioned above, Cajal postulated that dendritic spines served to increase the surface area of dendrites, thereby increasing their capacity to receive synaptic inputs. This hypothesis continues to be today supported, recent advances in electrophysiology, microscopy, and biochemical techniques have allowed formulating additional postulated regarding the function of dendritic spines. These functions include (1) the efficient regulation of single synapses at the pre- and post-synaptic levels; (2) expanding the computational capacity of neurons; and (3) compartmentalization of postsynaptic biochemical signaling and gene expression (Yuste & Majewska, 2001).

The combination of two-photon microscopy techniques with fluorescent and light-regulated proteins has enabled us to longitudinally monitor spine structural plasticity in living tissue *in vivo* or *ex vivo* and thus study its molecular mechanisms. These approaches have revealed that NMDAR-dependent LTP is associated with the long-term increase of the volume of dendritic spines in hippocampal neurons (Matsuzaki *et al*., 2004). This knowledge also advances our understanding of the pathophysiology of neuropsychiatric disorders.

5. Synaptic dysfunction in Alzheimer's disease.

It is fully accepted that glutamatergic neurotransmission is an important process in learning and memory. However, this system is severely disrupted in patients with AD due to the increase in oxidative stress associated with the amyloid β-peptide accumulation in the brains (Cheignon *et al*., 2018). Therefore, therapeutic strategies directed at the glutamatergic system may hold promise.

Under normal conditions, when a neuron is depolarized, glutamate is released into the synaptic cleft where it binds to glutamate receptors triggering the proper glutamatergic signaling. The concentration of glutamate into the extracellular space is regulated by specific transporters, localized in both nerve endings and surrounding glial cells. This transport system prevents cell damage generated by excessive glutamate concentration and activation of glutamate receptors (Omote *et al*., 2011).

However, in AD, soluble Aβ peptide promotes the reduction of synaptic glutamatergic transmission, which has been severely affected by neurons in the cerebral cortex and hippocampus. Several studies demonstrated that Aβ oligomers bind to synapses and promotes NMDAR endocytosis (Snyder *et al.*, 2005), triggering a decrease in the surface density of NR2 subunits. Herring et al. postulate that this modulation could be explained due to a decrease in reelin levels. Reelin is a protein that mediates NMDAR activity, and which is depleted in AD brains (Herring *et al*., 2012). Even though, the decrease in NMDAR subunits may also be due to an increase in STEP61 (Striatal-Enrichedprotein tyrosine Phosphatase 61), which has been reported to contribute to the NR1/NR2B and NR1/NR2A receptors endocytosis (Kurup *et al*., 2010; Snyder *et al*., 2005). Additionally, Aβ can also partially relieve the voltage-dependent Mg^{2+} block of NMDA receptors, which allows the continuous entry of calcium into neurons by altering the homeostasis and thus causing cell death.

On the other hand, Aβ enhances the activation of extrasynaptic NMDARs by decreasing neuronal glutamate uptake and consequently inducing glutamate spillover which is responsible of the neurotoxicity. Moreover, Aβ also has a direct effect on glial glutamate release, further increasing the probability of extrasynaptic NMDAR activation (Talantova *et al*., 2013). In AD, extrasynaptic NMDAR-mediated signaling pathway inactivates CREB and activates FOXO transcription factors, promoting the related pro-death and oxidative stress signaling (Hardingham & Bading, 2010).

Extrasynaptic NMDAR activation raises Aβ production by increasing a shift from α- to β-secretases activity. This extrasynaptic NMDAR-mediated production of Aβ thus generates a toxic positive feedback in which Aβ promotes extrasynaptic NMDAR activity, which stimulates further Aβ production and secretion. Interfering with this

positive feedback could provide therapeutic benefit to AD patients (Ferreira *et al.*, 2015).

Accordingly, the balance between the regionalized NMDAR signaling in synaptic and extrasynaptic regions is tilted towards the downstream signaling pathways that eventually leads to the neuronal death in AD (as illustrated in **Figure I12)**.

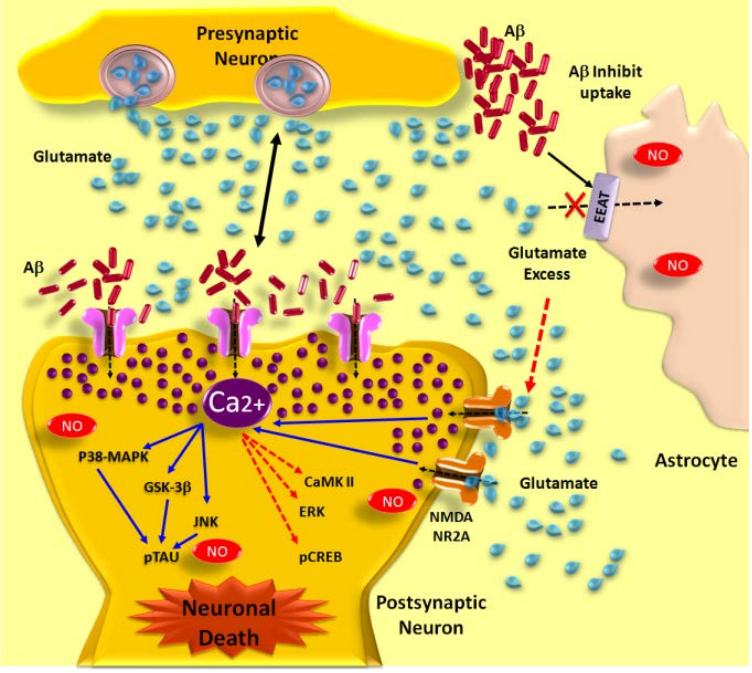

Figure I12. Glutamatergic transmission in Alzheimer's disease. Aβ oligomers enhance the pre-synaptic release of glutamate together with the simultaneous blockade of glutamate uptake by astrocytes through glutamate transporters (EAAT), due to this, glutamate concentration in synaptic cleft increases. Activation of NMDA receptors increases the influx of $Ca^{2+}$and activates signaling pathways responsible for neuronal shrinkage and synaptic loss (p38-MbAPK, GSK-3b, JNK), leading to Tau phosphorylation and neuronal death (adapted from Campos-Peña and Meraz-Rios, 2013).

5.1. Dendritic spines in Alzheimer's disease.

There is a wealth of evidence that maladaptive spine dynamics may contribute to, and/or be a target of, brain disease processes. Some experimental evidences in AD suggest that the loss of dendritic spines is one of the first structural changes that occur into the neurons of AD patients (Penzes *et al.*, 2011; Frankfurt and Luine, 2015). This dendritic spine loss is directly correlated with the loss of synaptic function, and is likely a result of Aβ accumulation, tau hyperphosphorylation, excitotoxicity,

neuroinflammation, dysfunction of intracellular cytoskeletal regulators, or a combination of these factors (Fiala *et al*., 2002; Knobloch & Mansuy, 2008).

Abnormal levels of Aβ in dendritic spines can have detrimental effects on synaptic function such as decreasing dendritic spine density. This decrease affects the NMDAR-mediated Ca^{2+}influx into active spines in rat organotypic slices containing pyramidal neurons (Shankar *et al*., 2007). Most research efforts on slowing the progress of AD have focused on Aβ clearance, neuroprotection, and delay of cognitive decline. However, new observations suggest that the induction of synaptogenesis and/or spinogenesis by epigenetic mechanisms may have potential benefits (Gipson *et al*., 2017). Thus, both intrinsic and extrinsic factors affecting spine dynamics may open unsuspected avenues for treating age-related neurodegenerative diseases.

5.2. Signaling Pathways Associated with NMDARs and AD Pathogenesis.

The best-characterized neuronal survival pathway described is the PI3K/AKT cascade (Brunet *et al*., 2001) and it has been suggested that in some neurodegenerative diseases, including AD, this signaling pathway is altered. Recently, it has also been reported that Aβ oligomers block PDK1-mediated AKT phosphorylation by preventing a direct interaction between them. The effect of rendering this antiapoptotic pathway non-functional leads to an increase in neuronal cell death (Lee et al., 2009). Additionally, PDK1 can also phosphorylate and activate other key intracellular signaling molecules, such as p70- S6K, PKA (Vanhaesebroeck *et al*., 2000) and some PKC family members (Le Good *et al.,* 1998; Gao *et al*., 2001). PKCs are critical components in the signal-transduction pathways that control not only cell survival (Cordey *et al*., 2006; Weinreb *et al*., 2004), but also proapoptotic pathways in neurons (Maher *et al*., 2001; Choi *et al.,* 2006). It is still unknown how PKCs maintain proper balance between cell survival and apoptosis in neurons. Probably this equilibrium depends on the different stimuli reaching cells. As several studies have demonstrated, the novel PKCs are involved in programmed cell death signaling acting through proapoptotic signals, and the PKC inhibitor Rottlerin is able to protect cells from apoptosis induced by H_2O_2, ultraviolet radiation, taxol and other toxins (Konishi *et al*.,

1997; Denning *et al*., 1998; Majumder *et al.,* 2000; Reyland *et al*., 2000; Matassa *et al*., 2001). In addition, it has been reported that the novel PKCδ is activated in response to oxidative stress stimulated by glutamate (Maher, 2001; Choi *et al*., 2006) and that PKCδ activation in retinal neurons contributes to apoptosis (Kim *et al*., 2008).

PKCs signaling pathways have been pointed to regulate important molecular events in the neurodegenerative pathophysiology of AD. The relationship between PKC and AD was first suggested because examining the presence PKC isozymes in postmortem samples from AD patients, researchers realized that these kinases were deficient (Battaini *et al*., 1999). Abnormal PKC activation could lead not only to a loss of memory, but also to increased levels of Aβ. Consequently, the accumulation of amyloid plaques increases the levels of tau protein hyperphosphorylated form, resulting in neurofibrillary tangles, and activation the inflammation program (Serrano-Pozo *et al*., 2011). Several lines of evidence suggest that classic and novel PKCs can activate direct or indirectly the alpha-secretase-mediated APP processing through ERK1/2 (Lanni *et al*., 2004). At the initial stages of AD, PKC-mediated irregular ERK1/2 phosphorylation, perhaps as part of an early inflammatory process. PKC also phosphorylates molecular substrates that are directly involved in regulation of synaptic connections such as adducin (Matsuoka *et al*., 2000). Thus, PKC dysfunction in AD could directly alter synaptic function within presynaptic and postsynaptic compartments.

Hypothesis and Objectives

Accumulation in the brain of soluble oligomers of Aβ peptide is a relevant early event in Alzheimer's disease pathogenesis. Several studies have reported that Aβ peptide presents a complex molecular behavior given, that it is able to interact with many types of receptors, and consequently to trigger intracellular mechanisms that cause synaptic loss and neurotoxicity. Considering the pivotal role of Aβ peptides in the pathobiology of AD, we hypothesize that oligomers of Aβ directly bind to integrin receptors to alter NMDARs density, localization and function in synaptic terminals of neurons. In order to investigate this hypothesis, we plan to examine and to characterize the molecular mechanisms of early synaptic changes induced by subtoxic levels of amyloid β oligomers in neurons.

To that aim, the following specific objectives were addressed:

Aim 1. To analyze alterations in membrane localization of NR2A- and NR2B-containing NMDARs induced by oligomeric amyloid β peptides in primary neuronal cultures.

Aim 2. To define the effects of Aβ peptides on the Ca^{2+} permeability properties of NR2A- and NR2B-containing NMDARs in neurons.

Aim 3. To decipher the molecular mechanisms of Aβ/integrin receptor signaling underlying changes in NMDARs localization and function led by Aβ oligomers in neurons.

Aim 4. To study dynamics of synaptic protein and receptor expression of human AD cortex synaptosomes during the progression of the disease.

Aim 5. To examine the effects of Aβ oligomers in spine density and dendritic arborization in an *ex vivo* model from organotypic cultures of mouse hippocampus.

Aim 6. To develop an efficient molecular tool based on integrin β1 sequence to interfere with the Aβ oligomer- triggered pathology in mouse brain.

Experimental procedures

1. Animals.

All experimental procedures followed the European Directive 2010/63/EU, and were approved by the Ethic Committees of the University of the Basque Country UPV/EHU.

Animals were housed in standard conditions with 12 h light cycle and with *ad libitum* access to food and water. All possible efforts were made to minimize animal suffering and the number of animals used. Experiments were performed in Sprague Dawley rats and in the triple transgenic mouse model of Alzheimer´s disease (3xTg-AD), which harbours the Swedish mutation in the human amyloid precursor protein (APP^{Swe}), presenilin knock-in mutation ($PS1^{M146V}$), and Tau^{P301L} mutant transgene (Tau^{P301L}) (Oddo et al., 2003).

2. Cell cultures.

2.1. Primary cortical neuron culture.

Cortical neurons were isolated from E18 Sprague-Dawley rat embryos according to previously described procedures (Ruiz *et al*., 2009). Brain hemispheres were separated, meninges and basal nucleus were removed and cortical lobes were extracted.

Selected cortical tissue was enzymatically digested with 0.25% trypsin and 0.004% deoxyribonuclease in Hank´s balanced salt solution (HBSS, Sigma-Aldrich) for 5 min at 37°C. Afterwards, the enzymatic reaction was stopped by adding Neurobasal® medium (Invitrogen) supplemented with 10 % FBS, B27 (Invitrogen), 2 mM glutamine and antibiotic-antimycotic mixture, centrifuged at 1,000 rpm for 5 min and the cell pellet was resuspended in 1 ml of the same solution. Mechanical dissociation was performed by using 23-, 25-, and 27G- gauge cutting needles, and the resulting cell suspension was filtered through a 40 µm nylon mesh (Millipore). 10 µl of filtrate was collected to determine by tripan blue staining (Sigma-Aldrich) the cell number and

viability, and all the rest was seeded onto poly-L-ornithine-coated 6/24/48 well plates or glass coverslips (12 mm ø) at 10^4 or 10^5 cells per well, depending on the experiment. For confocal single cell imaging experiments, cells were seeded onto glass-bottom μ-dishes (Ibidi GmbH, Germany). Prior to the cell culture, the plates and/or glass coverslip were coated by treating with 30 μg/ml Poly-L-ornithine (Sigma-Aldrich) for 1h at RT and washed three times in sterile distilled water.

24 h after seeding cells, culture medium was replaced by supplemented Neurobasal® medium w/o FBS in order to avoid astroglial growth. Cell cultures were essentially free of astrocytes and microglia and were maintained at 37°C and 5% CO_2. Cortical neuron cultures were used at 8–10 days (DIV).

For cell transfection, 2×10^6 cortical rat neurons were transfected in suspension with 3 μg of cDNA using Rat Neuron Nucleofector Kit (Lonza, Switzerland) according to the manufacturer's instructions and seeded and maintained as described above.

2.2. Organotypic hippocampal slice culture.

Hippocampal slice cultures were prepared from 6-7 days old mouse pups and processed as described previously (Sündermann *et al*., 2012). Brain was separated into two hemispheres and hippocampi were cut out and placed on ice, in a small petri dish with MEM supplemented with 1% glutamine and 1% Pen-Strep. Hippocampi were sliced using a tissue McIllwain chopper (400 μm of thickness) and intact individual slices were selected under microscope and transferred onto membrane inserts with fresh culture medium (MEM, pH 7.2 supplemented with 25% HS, 25% BME, 3% glucose, 1% glutamine, 0.5% Pen-Strep and 0.5% fungizone).

Cell cultures were maintained at 37°C and 5% CO_2 and culture medium was changed every 2 days. On day 11, culture medium was changed to NB medium supplemented with 0.5% HS 1% N1, 3% glucose, 1% glutamine, 0.5% Pen-Strep and 0.5% fungizone.

2.3. Astrocyte cell culture.

Primary cultures of cerebral cortical astrocytes were prepared from P0–P2 Sprague Dawley rats as described previously (McCarthy & de Vellis, 1980). Cortical lobes were extracted and enzimatically digested with 400 µl of 2.5% trypsin and 40 µl of 0.5% deoxyribonuclease in Hank´s balanced salt solution (HBSS, Sigma-Aldrich) for 15 minutes at 37^0C. The enzymatic reaction was stopped by adding IMDM medium supplemented with 10 % FBS (Gibco) and centrifuged at 1,200 rpm for 6 min. The cell pellet was resuspended in 1 ml of the same solution and mechanical dissociation was performed by using 21- and 23G- gauge cutting needles. Resulting cell suspension was centrifuged at 1,200 rpm for 6 min and plated onto 75cm^2 flasks coated with 30 µg/ml Poly-D-Lysine (PDL).

After 8 days, cells were plated onto PDL-coated plates and maintained for 2 days. Culture medium was replaced with IMDM with 1% FBS 24 h before Aβ-treatment.

3. Human samples.

Patients gave informed consent to all clinical investigations, which were performed in accordance with the principles embodied in the Declaration of Helsinki.

Frozen samples from prefrontal cortex of 6 subject controls and 31 AD patients were obtained from the Neurological Tissue Bank Hospital Clinic-IDIBAPS Biobank (Table 3). AD samples were grouped by Braak and Braak (Braak and Braak, 1995) into AD-II, AD-III, AD-IV and AD-V-VI, and by CERAD classification (Mirra et al., 1991) into AD-A, AD-B and AD-C.

Case number	Ref. nº	Braak stage NFT	CERAD Senile plaque	Gender	Age	Age (mean±S.D.M.)	Postmortem delay*
C1	1378	-	-	M	78	78.5±3.72	6:00
C2	1491	-	-	M	83		13:00
C3	1648	-	-	M	73		6:10
C4	1733	-	-	M	76		11:30
C5	1536	-	-	M	79		4:45
C6	1423	-	A	F	82		5:00
AD1	1697	I-II	-	M	78	76.0±8.02	6:00
AD2	1468	II	-	M	64		10:00
AD3	0575	II	-	F	86		13:30
AD4	1357	II	-	F	79		10:30
AD5	1687	II	-	F	69		12:00
AD6	1405	II	-	M	80		5:30
AD7	1570	III	-	F	86	79.5±7.55	4:00
AD8	1557	III	-	M	86		10:15
AD9	1144	III	A	M	73		4:20
AD10	1759	III	-	M	74		9:00
AD11	0754	III	B	M	87		2:30
AD12	1022	III	B	M	71		10:30
AD13	0497	IV	B	M	82	80.0±7.87	2:30
AD14	0849	IV	B	M	70		5:00
AD15	0948	IV	B	M	79		5:30
AD16	1255	IV	C	M	89		7:00
AD17	1230	V	C	M	79	76.3±2.23	4:15
AD18	1286	V	C	M	79		5:00
AD19	1622	V	C	M	76		5:00
AD20	1392	VI	C	M	77		5:00
AD21	1445	VI	C	F	73		3:30
AD22	1456	VI	C	F	74		3:30

AD23	1585	VI	C	F	74	6:30
AD24	1637	VI	C	M	78	7:00
AD25	1645	VI	C	F	77	5:30

Table 1. Characteristics of controls and AD subjects, categorized as stages I to VI of Braak and Braak and A, B or C of CERAD criteria. *Time (h) elapsed between death and sample extraction.

4. Preparation of $A\beta_{1-42}$ oligomers.

$A\beta_{1-42}$ oligomers were prepared as reported previously (Dahlgren et al., 2002). Briefly, $A\beta_{1-42}$ (ABX) was initially dissolved to 1 mM in hexafluoroisopropanol (Sigma-Aldrich) and distributed into aliquots in sterile microcentrifuge tubes. Hexafluoroisopropanol was totally removed under vacuum in a speed vac system and the peptide film was stored dried at -80°C. For the aggregation protocol, the peptide was first resuspended in anhydrous DMSO (Sigma-Aldrich) to a concentration of 5 mM, to finally bring the peptide to a final concentration of 100 µM in Hams F-12 (PromoCell) and to incubate it at 4°C for 24h. The preparation was then centrifuged at 14,000 g for 10 min at 4°C to remove insoluble aggregates and the supernatants containing soluble $A\beta_{1-42}$ were transferred to clean tubes and stored at 4°C.

5. Drugs and Inhibitors.

The following drugs and inhibitors were used: Gö6983 (Tocris), PMA (Sigma-Aldrich), AIP (Anaspec), RGDS (Tocris), hamster anti- rat CD29 (BD Pharmingen), hamster IgM (BD Pharmingen), TS2-16 (St. Cruz), MK801 (Tocris), TCN-201 (Tocris), Calcyculin A (Sigma-Aldrich) and Bicuculline (Tocris).

6. Protein extracts preparation and detection by western blot.

6.1. Total neuron protein preparation.

After treatment, cultured neurons were washed twice in cold 0.1 M phosphate buffered saline (PBS). Triplicates of 2 x 10^5 cells were scraped in 200 µl sample loading buffer (62.5 mM Tris pH 6.8, 10% glycerol, 2% SDS, 0.002% bromophenol blue and 5.7% β-mercaptoethanol in dH_2O). All this process was performed on ice to enhance the lysis process and prevent protein degradation. After that, samples were boiled at 95^oC for 5 min.

6.2. Biotinylation surface assay.

To examine changes in proteins localized in cell surface, biotinylation assays were performed according to the method described previously (Arancibia-Cárcamo *et al*., 2006). Cortical neurons were grown in 100 mm ø petri dishes as described above. At DIV 9, cells were treated with Aβ and cooled on ice in order to prevent receptor endocytosis and membrane trafficking during the biotin labeling step. Neurons were washed twice in cold Mg^{2+}/Ca^{2+} 0.1 M PBS pH 7.5 (0.5 mM $MgCl_2$ and 1 mM $CaCl_2$ in 0.1 M PBS). For membrane protein biotinylation, neurons were incubated in PBS containing 1 mg/ml sulfo-NHS-LC-biotin (Pierce, Thermo Scientific) for 20 min at 4°C with continuous gentle agitation to ensure equal coverage of all neurons.

After biotinylation, cells were rinsed three times in cold Mg^{2+}/Ca^{2+} PBS supplemented with 50 mM Glycine and 0.5% BSA to remove all unreacted biotin. After quenching the reaction, neurons were washed twice with cold Mg^{2+}/Ca^{2+} PBS and lysed in 200 µl RIPA buffer (50 mM TrisHCl pH 7.5, 150 mM NaCl,0.5% Sodium deoxycholate, 0.1% SDS, 1% NP-40) with protease inhibitors cocktail (Roche). Ten percent of the lysate was used for protein quantization, while the remainder was left to solubilize with rotation on a wheel at 4^oC for 2 hr. After solubilization, cell and nuclear debris were removed by centrifugation at 14,000 x g for 15 min. The supernatant was incubated with NeutrAvidin agarose (using 3:1 of cell lysate and avidin beads) to purify

biotinylated proteins. The suspension was then washed twice with RIPA buffer supplemented with 500 mM NaCl followed by a further wash in standard RIPA buffer. Biotinylated proteins were eluted with sample loading buffer by heating at 95^{o}C for 5 min prior to separate by SDS-PAGE followed by Western blotting. The ratio between biotinylated receptor and total receptor was measured.

6.3. Synaptosomes isolation from neuron culture

In order to isolate synaptosomes, Thermo Scientific Syn-PER Synaptic Protein Extraction Reagent® was used. The method was performed according to the manufacturer's instructions (Thermo-Fischer) with some modification to advance the technique.

After treatment, cultured neurons were washed in cold 0.1 M PBS twice and 1x10^{6} were scraped in 200 μl of Thermo Scientific Syn-PER Synaptic Protein Extraction Reagent® with protease inhibitors cocktail (synaptosome buffer) and centrifuged at 1,200 x g for 10 minutes at 4^{o}C. Pellet was resuspended in 40 μl of synaptosome buffer and saved as nuclear fraction, and the supernatant was centrifugated at 15,000 x g for 20 minutes at 4^{o}C. Supernatant was saved as the cytosolic fraction and pellet was resuspended in 40 μl of synaptosome buffer. After that, sample loading buffer was added and samples were boiled at 95^{o}C for 5 min or at 37^{o}C for 30 min, depending on the primary antibody.

To verify synaptosomes isolation, Western blot of the nuclear and cytosolic proteins were also probed with specific antibodies.

6.4. Subcellular fractionation from animal tissue and human samples.

Subcellular fractionation was performed following a previously method (Chuanzhou *et al*., 2017). Brain tissues from both animal and human samples were, first, homogenized on ice sucrose buffer (10 mM HEPES pH 7.4, 0.32 M sucrose), and centrifuged at 1,000 x g for 10 min at 4^{o}C. An aliquot of supernatant was collected for

further analysis as the total protein (TP) fraction, with the remainder being centrifuged at 14,000 x g for 20 min at 4°C to obtain the crude synaptosomal fraction (P2) and the cytosolic protein (Cyt) enriched supernatant. The P2 pellet was washed twice with wash buffer (4 mM HEPES, 1 mM EDTA, pH 7.4) by resuspension and centrifugation at 12,000 x g for 20 min at 4°C and then resuspended in buffer A (20 mM HEPES pH 7.2, 100 mM NaCl, 0.5% Triton X-100). After rotation for 1 h at 4°C, the suspension was centrifuged at 12,000 x g for 20 min at 4°C to yield the non-PSD fraction containing extrasynaptic proteins. The resultant pellet was washed twice in the wash buffer and resuspended in buffer B (20 mM HEPES pH 7.5, 0.15 mM NaCl, 1% Triton X-100, 1% SDS, 1mM dithiothreitol, 1% deoxycholate) for 1 h at 4°C, followed by centrifugation at 10,000 x g for 20 min at 4°C to obtain the PSD fraction containing synaptic proteins. All buffers were freshly supplemented with protease inhibitors cocktail (Roche), 100 mM Na_3VO_4 and 100 mM phenylmethylsulfonyl fluoride (PMSF) prior to use, and fractions were stored as aliquots at -80°C.

Samples were quantified with a detergent-compatible assay reagent (Pierce™ BCA Protein Assay Kit) according to the manufacturer's instructions (ThermoFisher Scientific). Samples were boiled at 95°C for 5 min and analyzed by western blot.

6.5. Western Blotting.

Protein lysates were separated by SDS-PAGE using Criterion™ TGX™ Precast 4-20% and 7.5% Tris-Glycine polyacrylamide gels (Bio-Rad). Electrophoresis was conducted in a Tris-Glycine buffer (25 mM Tris, pH 8.3, 192 mM glycine, 0.1% SDS in dH_2O) by using the Criterion cell system (Bio-Rad). Gels were transferred to Trans-Blot® Turbo™ Midi Nitrocellulose Transfer Packs (Bio Rad, Hercules, CA, USA).

For immunoblotting, membranes were blocked in TBST buffer (20 mM Tris, 137 mM NaCl, 0.1% Tween-20 in sH_2O, pH 7.6) in the presence of 4% BSA (Sigma-Aldrich), or 5% Phosphoblocker Blocking Reagent (Cell Biolabs) during 1h at RT. Then, membranes were incubated overnight with the specific primary antibodies in the same solution at 4°C with gentle shaking. Afterwards, membranes were washed three times

with TBST and incubated with secondary antibodies in the blocking solution for 1 h at RT.

Immunoreactive bands were detected by using enhanced electrochemical luminescence (Super Signal West Dura or Femto, Pierce) and ChemiDoc XRS Imaging System (Bio-Rad). Signals were quantified using Image Lab software (Bio-Rad) and values were normalized to β-actin or tubulin signal and provided as the mean ± SEM of at least three independent experiments.

When needed, membranes were stripped of antibodies using Restore Western Blot Stripping Buffer® (Thermo Fisher Scintific) for 8 min at RT. Membranes were then washed in TBST for three times, blocked and incubated again with other primary antibodies.

6.6. Antibodies for Western Blot.

The following antibodies were used for protein detection: rabbit anti-NR2B (1:1000, Millipore), rabbit anti-pSer^{1303}NR2B (1:1000, Millipore), rabbit anti-NMDAR2A (1:1000, Millipore), rabbit anti-NR1 (1:1000, Millipore), rabbit anti-PSD95 (1:500, abcam), mouse anti-Synaptophysin (1:500, Millipore), rabbit anti-Ezh2 (1:1000, Cell Signaling), rabbit anti-phosho PKC (1:1000, Cell Signaling), rabbit anti-phospho SRC (1:1000, Life technologies), mouse anti-SRC (1:1000, Cell Signaling), rabbit anti-Integrin β1 (1:1000; Cell Signaling), mouse anti-GAPDH (1:2000; Millipore), mouse anti-tubulin (1:5000, abcam), rabbit anti-β-actin (1:5000; Sigma-Aldrich), mouse anti-6E10 (1:1000, Biolegends) and rabbit anti-GST (1:5000, Sigma). Secondary antibodies conjugated with horseradish peroxidase were purchased from Sigma (1:5000).

7. Measurement of intracellular Ca^{2+} concentration.

Neurons were preincubated with fura-2 AM (Invitrogen) at 5 μM in culture medium for 30 min at 37 ◦C and washed as previously described (Alberdi et al., 2013).

Experiments were performed in a coverslip chamber, mounted on the stage of a inverted epifluorescence microscope (Zeiss Axiovert 35) equipped with a 150 W xenon lamp Polychrome IV (T.I.L.L. Photonics) and a Plan Neofluar 40X oil-immersion objective (Zeiss). Cells were visualized with a high-resolution digital black/white CCD camera (ORCA C4742-80-12 AG; Hamamatsu Photonics Iberica). Calcium levels were estimated by the 340/380 ratio method and data were analyzed with Excel (Microsoft) and Prism software (GraphPad Software).

8. Binding assay.

Binding experiments with *E.coli*-derived proteins were done as follows (Zugaza *et al*., 2002). Gluthation beads coated with fusion proteins (500 ng GST_0, GST-R_T, GST-R_W, GST-R_D or GST-R_S) were incubated with 100 pmol Aβ in binding buffer (50 mM Tris-HCl pH7.5, 5 mM $MgCl_2$, 20 mM KCl, 500 μg/ml BSA) for 1 h at RT. Immobilized GST beads were washed twice with binding buffer and five times with 50 mM Tris-HCl pH 7.5, 150 mM NaCl. Proteins were eluted adding sample buffer and separated by SDS-PAGE followed and analyzed by immunoblots with anti-6E10 and anti-GST antibodies.

9. Intrahippocampal injection in adult mice.

10-week-old males mice (C57BL6/J) were subjected to intrahippocampal injections in the right dentate gyrus (DG). For the surgery, animals were anesthetized with 0.3 ml of Avertin, with addition of 0.1 ml if needed. Mice were immobilized with a stereotaxic apparatus and injected with the corresponding preparations: the first group (Aβ) was injected with 3 μl of Aβ oligomers at 10 μM, the second group (Aβ + GST_o) with 3 μl of 10 μM Aβ plus 0.45 μg/μl of GST_o, and the third group (Aβ + R_S) with 3 μl of 10 μM Aβ plus 0.45 μg/μl of R_S peptide. Coordinates for the injection were Bregma -2.2 mm, lateral 1.5 mm and DV 2 mm. After injection and before removal, the needle was left on site for 5 min to avoid reflux.

Mice were anesthetized with chloral hydrate and perfused with 30 ml of phosphate buffer followed by 30 ml of 4% PFA in 0.4 M PB. The brains were extracted and postfixed with the same fixative solution for 4 h at RT, placed in 30% sucrose in 0.1 M PBS pH 7.5 at 4°C and then kept in cryoprotectant solution (30% ethylene glycol, 30% glycerol and 10% 0.4 M PB in dH_2O) at -20°C.

10. Measurement of ROS generation

For the quantification of generated ROS in stimulated *in vitro* cells, fluorescent dye 5-(and6)-chloromethyl-2'7dichlorodihydrofluorescein diacetate acetyl ester (CM-H2 DCFDA) was used. Astrocytes ($1x10^4$) were exposed to 5 μM Aβ-oligomers alone or together with fusion proteins and loaded with 10 μM CM-H2DCFDA for 30 min immediately after the excitotoxic stimulus. After three washes with PBS, fluorescence was measured with an excitation and emission wavelengths of 485 nm and 520 nm respectively.

11. Immunochemistry

11.1. Immunofluorescence.

11.1.1. Cultured neurons.

To analyze NR2B expression, cortical neurons were transfected with 3 μg pEGFP (Clontech) or 3 μg pEGFP-NR2B (Addgene). At DIV 9, living neurons were incubated with EGFP antibody in culture medium at 37°C for 20 min and fixed in 4% paraformaldehyde (w/v) in PBS for 5 min. Cells were incubated for 30 min in blocking solution (PBS pH 7.5, 4% normal goat serum (NGS, Palex), 0.05% Triton X-100 (Sigma-Aldrich)) and incubated with PSD-95 antibody in blocking solution overnight at 4°C. After three washing steps with PBS, cells were incubated with secondary

fluorochrome-conjugated antibody in blocking solution for 1 h at RT. Then, cells were washed and incubated with DAPI (4 μg/ml, Sigma-Aldrich) for 10 min. Finally, cells were washed again twice and coverslips were mounted on glass slides with Fluoromount-G mounting medium (SouthernBiotech).

Double-immunofluorescence labeling was performed in cortical neurons. DIV 9 neurons were fixed in methanol for 10 min at 4°C and rinsed three times with PBS. Fixed cells were permeabilized with blocking buffer (4% normal goat serum (NGS, Palex), 0.1% Triton X-100 in PBS) for 1 hour at RT and were incubated with primary antibodies in blocking buffer overnight at 4°C. Then, cells were rinsed with washing buffer (0.1 M PBS pH 7.5, 0.1% Triton X-100) and incubated with the fluorochrome conjugated secondary antibodies in blocking solution for 1 h at RT. Cells were washed and incubated with DAPI (4 μg/ml, Sigma-Aldrich) for 10 min. Finally, cells were washed again twice and coverslips were mounted on glass slides with Fluoromount-G mounting medium (SouthernBiotech). Preparations were kept at 4°C until examination.

11.1.2. Animal tissue.

Mouse tissue was cut using a Leica VT 1200S vibrating blade microtome (Leica microsystems) to obtain coronal 40 μm-thick sections. Slices were kept in PBS at 4°C and permeabilized and blocked with 0.1 M PBS pH 7.5, 10% NGS, 0.1% Triton X-100 for 1 h at RT. Then, slices were incubated with primary antibodies overnight at 4°C with gently shaken. Slices were then washed three times with 0.1 M PBS pH 7.5, 0.1% Triton X-100 (washing buffer) and incubated with blocking solution containing fluorochrome conjugated secondary antibodies for 1 h at RT. After that, slices were washed three times with washing buffer, incubated with DAPI (4 μg/ml, Sigma-Aldrich), washed again twice and mounted on glass slides with Fluoromount-G mounting medium (SouthernBiotech).

11.2. DAB staining.

Slices were washed in PBS and incubated with light stirring in 0.1 M PBS containing 3% H_2O_2 for 10 minutes at RT. Then, slices where rinsed three times with PBS and incubated with light stirring in blocking solution (PBS pH 7.5, 4% HS, 0.1% Triton X-100) for 30 min at RT. Next, slices were incubated with the corresponding specific primary antibodies, in the same blocking solution, overnight at 4^{o}C with gentle shaking. Afterwards, slices were washed three times with PBS and incubated with secondary antibodies in the blocking solution for 1 h at RT. Slices were incubated with the ABC complex following the manufacturer's instructions (Vector Laboratories) for 1h at RT, and then washed three times with PBS. Slices were treated with DAB (Vector Laboratories) according to the manufacturer's instructions and washed three times with PBS. Finally, slices were mounted on glass slides with DPX.

11.3. Antibodies.

The following antibodies were used for immunofluorescence: rabbit anti-NMDAR2B (1:1000, Millipore), rabbit anti-NMDAR2B extracellular (1:500, Alomone), rabbit anti-PSD95 (1:500, Millipore), mouse anti-Synaptophysin (1:500, Millipore), rabbit anti-HOMER (1:500, SYSY), mouse anti-MAP2 (1:1000, Sigma), rabbit GFAP (1:1000, Sigma), rabbit S100β (1:500, Dako) and mouse GRP78 (1:500, Enzo Life Sciences). Secondary antibodies coupled to Alexa 488 or Alexa 594, were purchased from Invitrogen (1:500). For DAB immunostaining, mouse anti-GFAP (1:1000, Millipore) and rabbit anti-S100β (1:500, Dako) antibodies were used. Secondary anti-rabbit or anti-mouse biotinylated antibodies were purchased from Vector Laboratories (1:500).

11.4. Image acquisition and analysis.

Fluorescence immunostaining for cultured neurons was taken with Leica TCS SP8 microscope using 63x oil-immersion objective to generate z-stack projections. For fluorescence intensity analysis, images were taken with the same setting for all

experiment and mean value along the stack profile was quantified with LAS AF Lite software (Leica).

For colocalization quantization, neuronal dendrites of several cells were selected as ROIs and Overlap coefficient was calculated using Leica AF software.

To analyze reactive astrogliosis, DAB stained area was measured with the intensity threshold, and a coefficient between stained area and total area selected was obtained to perform statistical analysis.

12. Fluorescence Resonance Energy Transfer (FRET) assays.

12.1. Neuron transfection and FRET assay.

Neurons were transfected with Myr-Palm-CKAR, a reporter for PKC-mediated phosphorylation. CKAR is composed of monomeric CFP and monomeric YFP, next to a PKC sequence which is bound by a flexible linker to an FHA2 phosphotreonine-binding domain. When the PKC substrate is phosphorylated, it binds FHA2, causing a conformational change that results in alterations in FRET. Therefore, thanks to this genetically encoded fluorescent reporter, FRET changes can be monitored and PKC activity measured in a continuous manner (Violin et al., 2003).

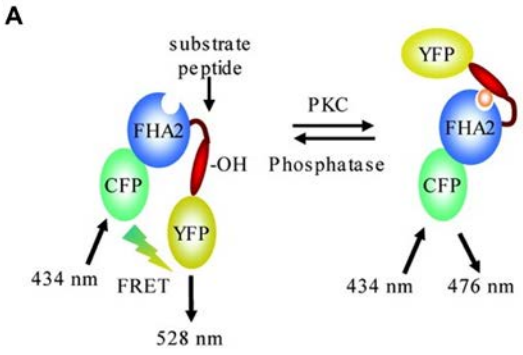

Figure EP1. Myr-Palm-CKAR reporter is comprised of mCFP, the FHA2 domain, a PKC substrate sequence and mYFP. (adapted from Violin *et al*., 2003).

In DIV 8, transfected neurons were transferred to incubation buffer Hank's balanced salt solution (HBSS w/o Ca^{2+}/Mg^{2+}). To quantify the PKC activity, neurons were imaged by a TCS SP8X confocal microscope (Leica, Germany) as described (Hill et al., 2014). Cells were excited at 458 nm (argon laser line), and CFP and YFP emission were acquired by HyDTM detectors for FRET ratio quantification at an acquisition rate of 1 frame/15 s during 8 min. Pinhole was set at 300 μm and images were taken with a 63 x oil objective (1.4 NA).

12.2. Recording graph analysis.

For data analysis, a homogeneous population of 3–5 cells was selected in the field of view and neuronal somata membrane selected as Region of Interest (ROI). Background values were always subtracted and data are expressed as $R/R_0 \pm$ SEM (%) in which R represents the CFP/YFP fluorescence ratio for a given time point and R_0 represents the mean of the resting FRET ratio.

13. Dendritic and spine complexity.

13.1. Sindbis virus infection.

Virus infection was performed as described previously (Sündermann *et al*., 2012). On DIV 12, slice cultures were infected with pSinRep5 EGFP virus following the droplet method. Low infection rate was performed, which permitted imaging of single neurons by high resolution cLSM with minimal overlap of dendritic arbors and imaging of single dendritic fragments. Cultured hippocampal slices were visually examined on DIV 14 to ensure the expression of the fluorescent protein. On DIV 15, slices were treated with inhibitors and Aβ and fixed with cold fixing solution and mounted with confocal matrix.

13.2. Confocal microscopy, image processing and analysis.

13.2.1. Dendritic spine analysis.

Analysis of dendritic spine density was performed using Leica SP2 CLSM quipped with 63x objective (NA: 1.2) and 488 nm Argon laser. Dendritic branches of individual CA1 pyramidal neurons on the apical side were imaged with voxel size of 0.08 x 0.08 x 0.25 µm in the x-y-z directions. Images were deconvolutioned with Autodeblur 9.3 software and spine analysis was performed with 3DMA Version 0204 software.

13.2.2. Neuronal morphology analysis.

Confocal high resolution microscopy of complete CA1 hippocampal neurons was performed as described previously (Golovyashkina *et al*., 2015). Each single neuron was imaged in 8 to 12 overlapping image stacks with voxel size 0.30 x 0.30 x 0.45 in x-y-z directions. 3D reconstruction of whole neurons was performed using Neuromantic software (University of Reading, Reading, UK) in semiautomated mode. Sholl analysis was performed separately for basal and apical parts of dendritic trees.

14. Statistical analysis.

All data were expressed as mean ± S.E.M. Statistical analysis were performed using absolute values. GraphPad Prism sowtware was used applying one-way analysis of variance (ANOVA) with the pos hoc Fisher's least significant difference (LSD) test for multiple comparisons and one-tailed, paired Student's t test for comparison of the two genotypes at control conditions.

Results

1. Aβ oligomers regulate NMDA receptor function and its membrane location in neurons

1.1 Aβ oligomers increase the incorporation of the NR2B subunit into NMDA receptor in cell surface of primary cortical neurons.

Previous studies have reported that Aβ oligomers involve NMDA receptors in order to lead to synaptic dysfunction and neurodegeneration (Mota et al., 2014; Parameshwaran et al., 2008). In the present study, we have investigated the role of Aβ oligomers on the ratio between NR2A and NR2B subunits present in the NMDA receptors located in the cell membrane. For that purpose, we have used primary cultures of cortical neurons which have been treated with 1 μM Aβ oligomers at two different time points: 30 min (acute treatment) and 24h (chronic treatment), and cell surface receptors have been determined by cleavable biotinylation assay followed by SDS-PAGE and Western blot analysis. As shown in **Figure R1A**, acute Aβ treatment potentiated the presence of NR2B at surface level, whereas chronic treatment did the opposite, reduced its presence. Regarding NR2A subunit, only chronic treatment produced an effect, reducing its presence.

In fact, acute Aβ treatment increased NR2B membrane incorporation (129.8 ± 7.61% compared to control levels, 100%) without affecting NR2A surface levels (**Figure R1B**). Nevertheless, chronic Aβ treatment dramatically reduced the presence of both, NR2A and NR2B subunits (46.92 ± 16.62% and 53.24 ± 9.79% respectively, compared to the control levels, 100%) (**Figure R1B**). Regarding total cell lysate, neither acute nor chronic Aβ treatments exerted significant effect on the total expression of NR2A or NR2B (**Figure R1C**). These results suggest that Aβ modulates the membrane location of NR2A and NR2B subunits in NMDA receptors of primary cortical neurons.

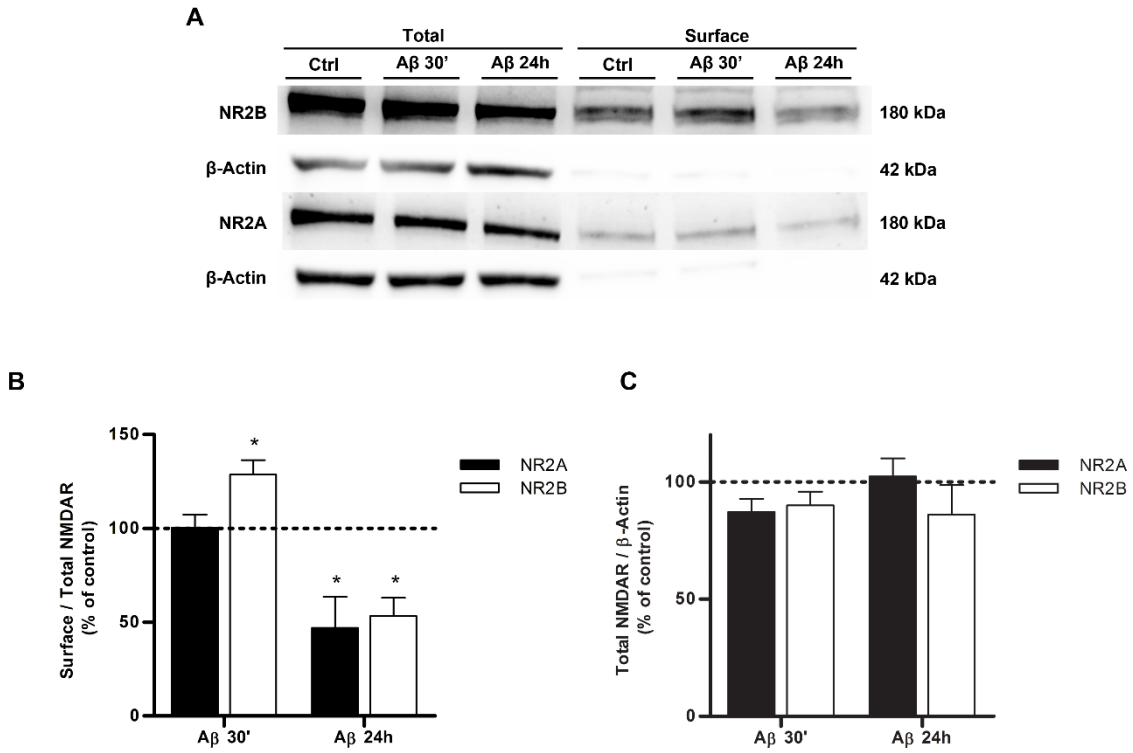

Figure R1. Aβ promotes alterations of NR2A and NR2B distribution on neuronal membrane surface. (A) Cultured cortical neurons were incubated in the absence (Ctrl) or in the presence of 1 μM Aβ for 30 min or 24h, and surface expression of NR2A and NR2B was measured by biotinylation assays. β-Actin (only expressed in the total fraction) was used as loading control. **(B** and **C)** Quantification of immunoblots for NMDA receptor subunits labeled with cleavable biotin and total NMDA receptor are shown (n=4). Graph bars (means ± S.E.M.) represent the volume band intensities of surface NMDA receptor subunits normalized to total NMDA receptor loading (B) and total NMDA receptors normalized to β-Actin (C) and expressed as a percentage of untreated cells. *p<0.05, compared to non-treated (Control) cells; paired two-way ANOVA.

1.2 Aβ oligomers deregulate NMDA-dependent Ca^{2+} homeostasis in cortical neurons.

Since it is well known that the overactivation of NMDA receptor causes aberrant $[Ca^{2+}]_i$ increase (Choi *et al*., 1995), we postulated that the Aβ could modified NMDA receptor location, and this alteration could correlate with changes in Ca^{2+} homeostasis. For that, we measured NMDA receptor-mediated Ca^{2+} influx in primary cortical neurons pretreated with 1 μM Aβ oligomers for 30 min and 24h. By using microfluorimetry, it was observed that acute Aβ pretreatment enhanced the Ca^{2+} influx

induced by NMDA 30 µM, while the chronic Aβ oligomers pretreatment reduced the Ca^{2+} response by NMDA receptor activation (**Figure R2A** and **B**). These results point out that Aβ oligomers modify the Ca^{2+} permeability of NMDA receptor by modulating the function of NMDA receptor complex on neuronal cell surface.

To examine the subunit specificity of Aβ oligomer-mediated NMDA receptor potentiation, we recorded NMDA-dependent Ca^{2+} influx in the presence of 10 µM TCN-201, a NR2A- specific inhibitor, in control and in Aβ-treated cells. The percentage of Ca^{2+} influx response of TCN201-insensitive recorders, largely NR2B-mediated NMDA receptor, were different at both culture conditions being more prominent in Aβ-treated than in control cells, 75% versus 55% respectively. (**Figure R2C**). Altogether, these data indicate that NR2B containing NMDA receptor is the target of Aβ oligomer modulation.

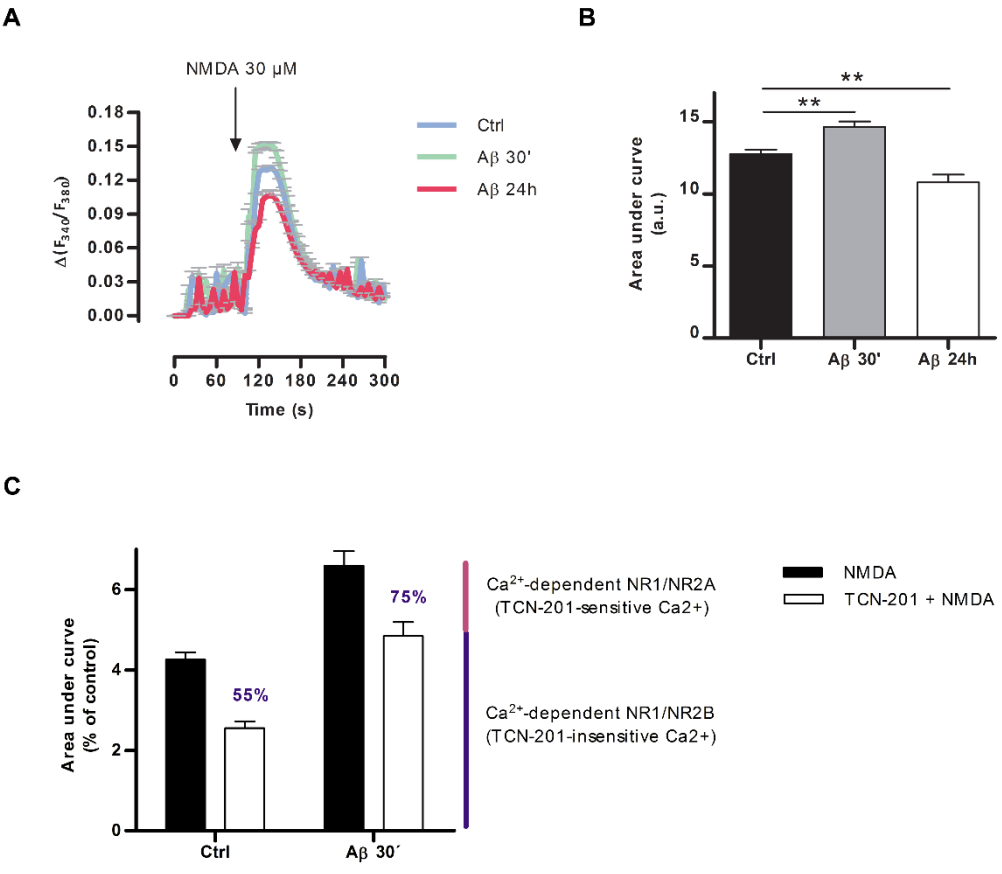

Figure R2. Effect of Aβ on NMDA-induced intracellular Ca^{2+} overload. (A) Neurons were exposed to 1 µM Aβ for 30 minutes or 24 h, and loaded with Fura-2AM for 30 minutes. NMDA-dependent intracellular Ca^{2+} levels were measured by microfluorimetry and representative fluorescence ratio was obtained with NMDA in control neurons (Ctrl) and in Aβ-pretreated neurons at different times, as

indicated. Arrows indicate the application of NMDA. Recordings represent the time course of the intracellular Ca^{2+} levels of 52 cells from 3 independent experiments. **(B)** Histogram represents the mean ± S.E.M. of area under Ca^{2+} curve for each condition. **p<0.01, compared to non-treated cells; paired one-way ANOVA. **(C)** 10 μM TCN-201 was used as a NR2A inhibitor in control and treated-cells with 1 μM Aβ for 30 min. Histogram shows average ± S.E.M. of area under Ca^{2+} curve for each condition.

2. Aβ oligomers induce changes in NR2B subunit localization in neuron synaptosomal preparations.

2.1. Characterization of synaptosomes from primary cortical neuron cultures.

NMDA receptors are crucial in activity-dependent synaptic regulation. They control synaptic plasticity and memory function (Cull-Candy, 2001). Since the vast majority of NMDA receptors are located post-synaptically on dendrites and dendritic spines, we examined whether Aβ oligomers modified NR2B incorporation at the synaptic sites. Synaptosomes are commonly used to study synaptic function because they contain functional ion channels, receptors, enzymes and proteins, as well as the intact molecular machinery for the releasing, uptake and storage of neurotransmitters (**Figure R3A**). Thus, we used an efficient protocol for isolating synaptosomes, as we describe in Material and Methods section.

To verify specificity of the extraction procedure, we separated proteins by SDS-PAGE followed by Western blot analysis from the total, synaptic and cytosolic fractions and we tested the presence of PSD-95 in the synaptic fraction, histone methyltransferase Ezh2 in the nuclear fraction and β-Actin, a ubiquitous protein. As expected. PSD-95 was enriched in synaptosome fraction, and β-Actin was present in all fractions (**Figure R3B**). Therefore, we observed that this protocol was effective for isolating synaptosomes containing synaptic proteins from primary neuronal cultures.

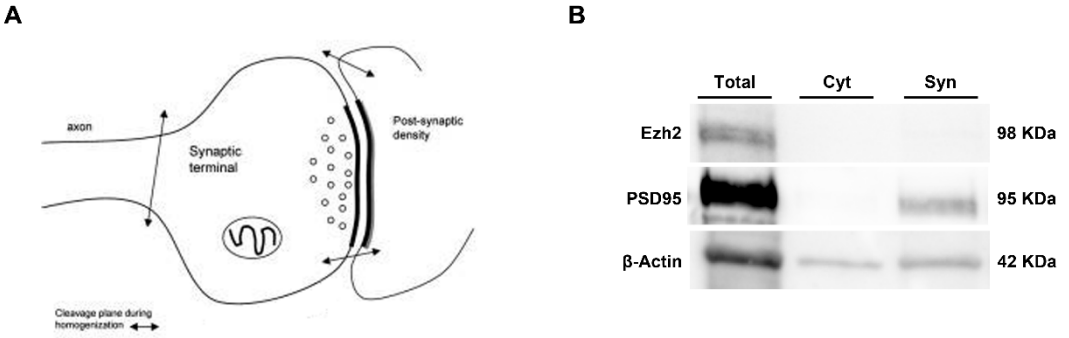

Figure R3. Enriched synaptic protein fractions from cortical neurons. (A) Schematic of a synaptosome formed from the detached nerve terminal and part of the postsynaptic membrane during mechanical homogenization (Adapted from Sokolow *et al*., 2013). **(B)** Western blot analysis showing enrichment of hallmark proteins in total lysates (Total), cytosol fraction (Cyt) and synaptosome suspension (Syn).

2.2. Aβ oligomers change the abundance of synaptosomal NR2B subunit and PSD-95 of cortical neurons to the synaptosome.

Next, we analyzed the presence of NR2B in the synaptosome fraction from primary cortical neurons after Aβ treatments at different time points. As shown in **Figure R4A**, in the presence of 1 μM Aβ oligomers for 30 min, the density of the NR2B subunit in synaptosomes increased (0.58 ± 0.19) compared to the control conditions, (0.37 ± 0.17), while no significant changes were observed in Aβ oligomer- treated cells for longer time (3h or 24h) (**Figure R4B**). Similar results were obtained when PSD-95 protein was analyzed in the synaptosomes of Aβ-treated cells (4.67 ± 1.18) compared to the control (3.16 ± 1.14) (**Figure R4C**).

To consolidate our observation that relates Aβ oligomers to higher density of NR2B subunit, we compared the increment of this NR2B subunit by the two different techniques developed in this work, protein surface biotinylation and synaptosome extraction. As shown in **Figure R4D**, both methodologies had the same sensitivity to detect the NR2B increase on cell surface, 145.1% ± 13.23% for biotinylation and 153.8% ± 8.3% for synaptosome extraction, compared to control levels, 100%.

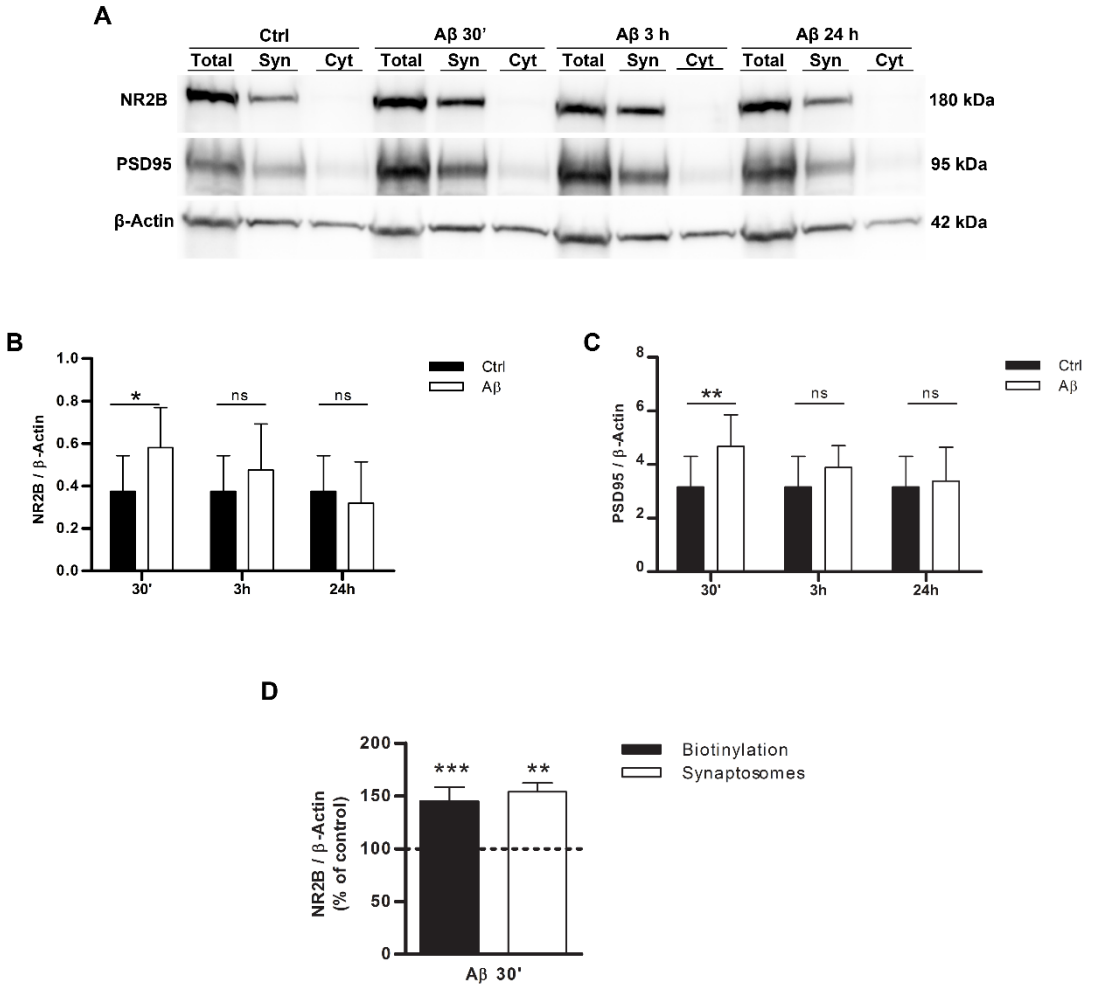

Figure R4. Effects of Aβ on the presence of NR2B subunit and PSD-95 protein in synaptosomes. (A, B, C) Primary cortical neurons were exposed to 1 μM Aβ for 30 min, 3h and 24h. Total, cytosolic and synaptic protein samples were extracted and NR2B and PSD95 levels were detected by immunoblot with specific antibodies **(A)**. **(B-C)** Histograms show NR2B subunit and PSD95 levels and data are represented as means ± S.E.M of three independent experiments. **(D)** Histogram compares the NR2B subunit presence by two techniques protein surface biotinylation and synaptosome extraction. Data are represented as means ± S.E.M. of band volume intensities normalized to corresponding β-Actin. *p<0.05, **p<0.01, ***p<0.001 compared to non-treated cells; paired two-way ANOVA (B, C); paired Student`s t test (D).

3. Aβ oligomers modulate synaptic function in primary cortical neurons.

3.1. Aβ oligomers promote NR2B/PSD95 co-localization in dendrites.

Schaffold proteins within the postsynaptic density are major regulators of NR2B trafficking and location (Bard & Groc, 2011). The C-terminal of NR2B subunit is a well-known hub for interactions with several intracellular partners, especially PDZ schaffold proteins such as PSD-95. Since our results point to a robust Aβ induced- increment of NR2B and PSD-95 at synaptic sites, we hypothesized that these two proteins could co-localize leading to a relevant increment of the synaptic function. To test this, we overexpressed NR2B subunit in primary cortical neurons and performed immunocytochemistry experiments on living cells, in order to label extracellular NR2B subunit and subsequently staining with the post-synaptic marker PSD-95 (**Figure R5A**). Then, NR2B subunit levels and the number of co-assembled EGFP-NR2B with PSD-95 were quantified in dendrites by measuring EGFP fluorescence intensity and compared among the different conditions (**Figure R5B**).

First, the fluorescence intensity of EFGP revealed a strong increase of NR2B subunit in the membrane after the treatment with Aβ oligomers for 30 min (12.43 ± 0.71 compared to control levels, 9.59 ± 0.96) (**Figure R5C**). Second, as shown in **Figure R5D**, acute Aβ oligomer treatment mediated the colocalization of NR2B and PSD-95 proteins increased to 0.010 ± 0.002 from 0.007 ± 0.001 (control levels). Overall, these results suggest that the Aβ increased the presence of NR2B subunit and PSD-95 protein in neuron surface and both proteins co-localize in the same processes and consequently could lead to the functional alterations in neuron synapses.

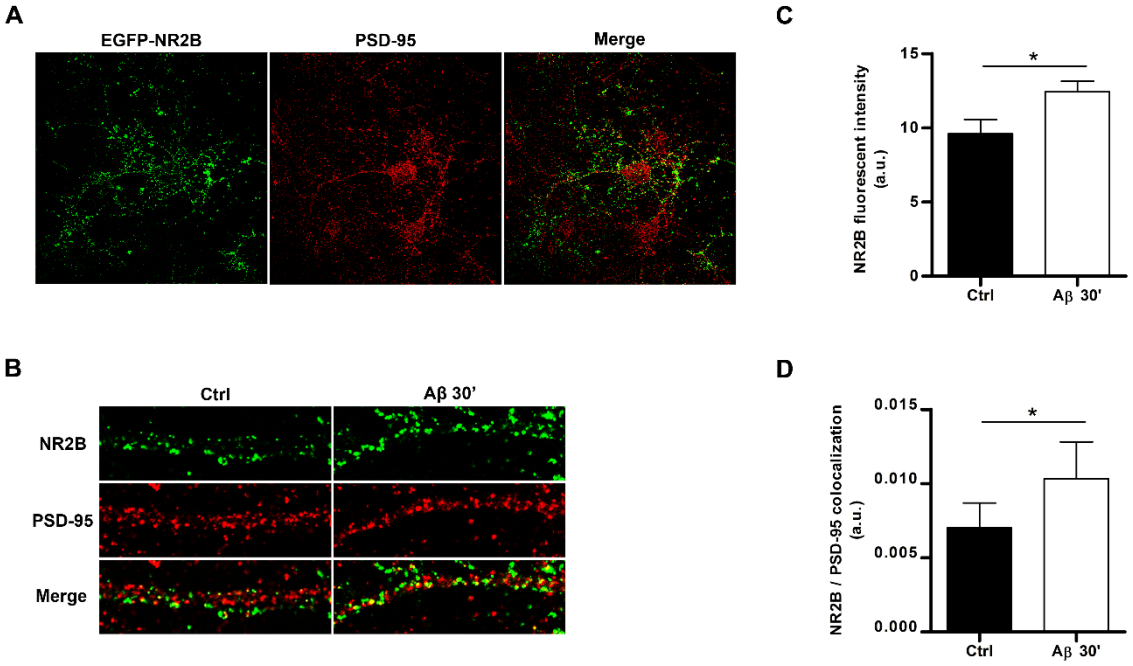

Figure R5. Aβ treatment increases the presence in the membrane surface of NR2B subunit and PSD-95 and facilitates their co-localization. (A) Primary cortical neurons were transfected with pEGFP-NR2B. After incubation with 1 μM Aβ, surface NR2B subunits were labeled *in vivo* using an antibody against EGFP (green). Neurons were fixed in methanol and stained with PSD-95 (red). **(B)** Immunodetection of extracellular NR2B and co-localization with the postsynaptic marker PSD-95 was performed in dendrites from neurons treated or not with Aβ oligomers. **(C)** Quantification of extracellular EGFP-NR2B intensity in control and Aβ conditions were expressed as arbitrary units. **(D)** Co-assembled EGFP-NR2B with PSD-95 was calculated with the Pearson correlation coefficient. Data are represented as means ± S.E.M. of 52 ROIs from at least 3 independent experiments *p<0.05, compared to non-treated cells; paired Student`s t test.

3.2. Aβ oligomers preferably enhance synaptic NMDAR-dependent calcium influx.

As an additional manner to analyze the effects of Aβ oligomers on functional NMDA receptors, we applied a pharmacological protocol which specifically activates the different NMDA receptor pools. This approach allowed us to measure the whole-cell Ca^{2+} mobilization to selectively activate synaptic and extrasynaptic NMDA receptors. Primary cortical neurons were bathed in magnesium- and glycine-free media containing bicuculline with 4-AP, a competitive antagonist of $GABA_A$ receptors in order to selectively activate synaptic NMDA receptors (Leveille et al., 2008). MK-801

is an open channel blocker of NMDA, which enters the channel only after its activation. Its application during bicuculline treatment provides a use-dependent blockade of synaptic NMDA receptors allowing the extrasynaptic NMDA receptor population to be subsequently activated with bath applied NMDA.

To test whether Aβ oligomers induced changes in synaptic and/or extrasynaptic NMDA-dependent ion currents, Ca^{2+} influxes from control and Aβ oligomer-treated neurons were compared using the compounds previously mentioned. Under these conditions, Aβ-oligomer treatment induced an increase in both synaptic and extrasynaptic NMDA-evoked Ca^{2+} mobilization (**Figure R6A**). However, synaptic Ca^{2+} increase is significantly higher than the extrasynaptic effect, demonstrating that Aβ oligomers modulate Ca^{2+} permeability by NMDA receptors preferably at synaptic sites (**Figure R6B**).

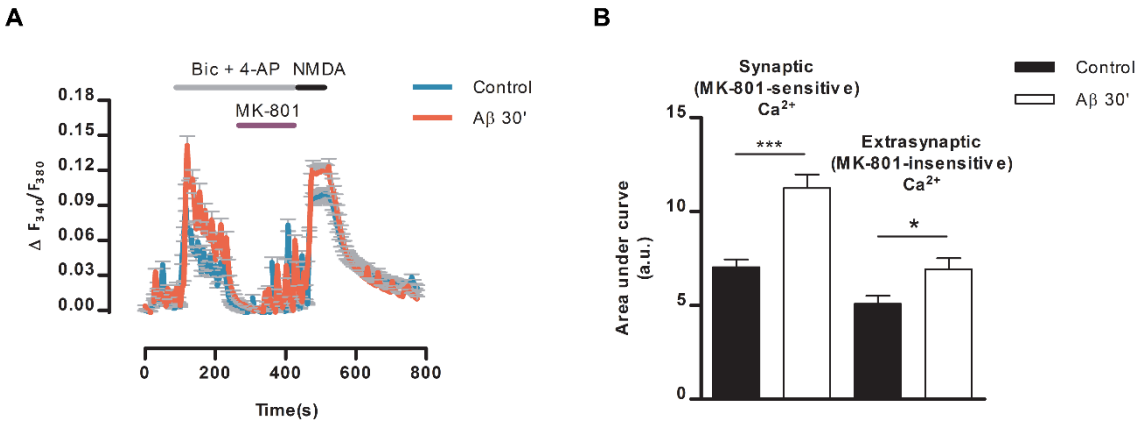

Figure R6. Effect of Aβ oligomers on synaptic and extrasynaptic NMDAR-dependent Ca^{2+} influx. (A) Recordings of Ca^{2+} responses to whole cell synaptic and extrasynaptic NMDA receptor activation in untreated (Control) and treated primary cortical neurons with 1 μM Aβ oligomers for 30 min. NMDA synaptic receptor activity was measured after the addition of 50 μM bicuculline and 2.5 mM 4-AP. Extrasynaptic NMDA receptor-mediated ion fluxes were recorded following blockade of synaptic NMDA receptors with 10 μM MK-801. NMDA receptor inhibitor was applied during treatment with bicuculline. **(B)** Quantification of synaptic and extrasynaptic NMDA receptor-mediated Ca^{2+} responses was done in 41 cells from 3 independent experiments. Histogram bars represent the mean ± S.E.M. of area under Ca^{2+} response curve for each condition. *p<0.05, ***p<0.001 compared to non-treated cells; paired one-way ANOVA.

4. Aβ oligomers promote phosphorylation and activation of PKC, which controls NR2B surface location

4.1. Aβ oligomers induce phosphorylation of PKC in primary cortical neurons.

There are many evidences that the function of the NMDA receptor is regulated by a variety of protein kinases (Mammen *et al*., 1999; Roche *et al*., 1994). The post-translational modifications of proteins by phosphorylation are key to control intracellular signal transduction pathways that lead to many important cellular processes, such as the functionality of ion channels or receptor localization at synapses. Many phosphorylation sites have been identified in NMDA receptor subunits. Considering that the Src tyrosine kinase family has been extensively related to AD (Gianni et al., 2003; Williamson et al., 2002), we first investigated whether Aβ oligomers altered phosphorylation of Src tyrosine kinase level.

The activation of Src proteins was evaluated in total cell extracts from neurons treated with 1 μM Aβ for 30 min by analysing the levels of Src (pSrc) phosphorylated at Tyr^{418}. Aβ produced a rapid decrease in the Tyr^{418} phosphorylation at 15 and 30 min (**Figure R7A**), from 0.32 ± 0.015 (control) to 0.26 ± 0.018 (15 min) and 0.19 ± 0.029 (30 min) (**Figure R7C)**.

In addition to Src, other kinases have been associated with intracellular trafficking and channel properties of NMDA receptors, such as Protein Kinase C (PKC). It has been demonstrated that PKCs protect neurons from Aβ cytotoxicity and also plays a key role in various cognitive functions including learning and memory (Chen & Roche, 2007). We, therefore, studied the effect of Aβ on PKC phosphorylation. Interestingly, Aβ treatment for 15, 30 and 60 min induced PKC phosphorylation (2.48 ± 0.4, 2.74 ± 0.47 and 2.48 ± 0.2, respectively, compared to control levels, 1.49 ± 0.1 (**Figure R7B** and **D**). These results indicated that Aβ oligomers upregulate phosphorylated PKC levels and, therefore, we focused on studying the relevance of PKC in Aβ-mediated signal transduction.

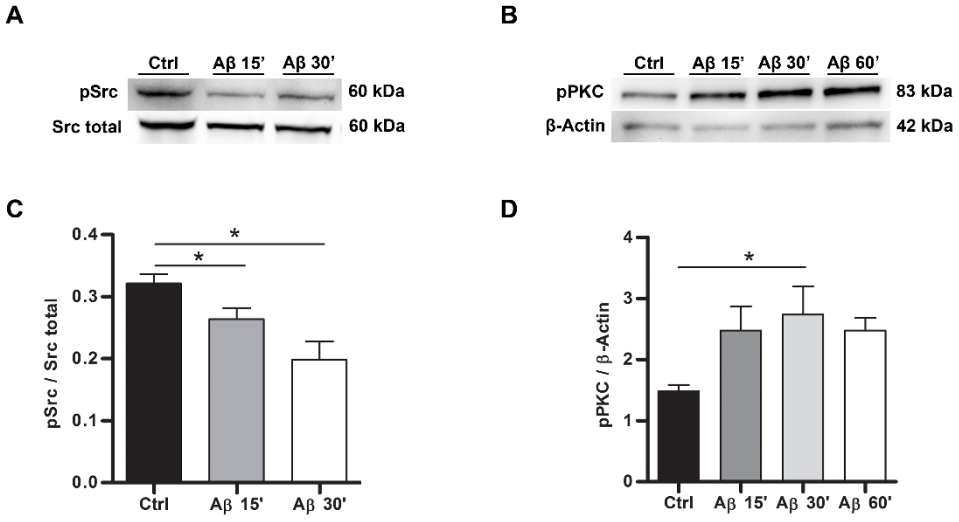

Figure R7. Aβ oligomers change tyrosine and serin-threonine protein kinase phosphorylation. (A) Primary cortical neurons were exposed to 1 μM Aβ oligomers for 15 and 30 min, and phosphorylation of Src kinase (pSrc) was examined by Western blot. **(C)** Quantification of phospho Src protein levels was obtained by analysis of immunoblot images (n=3). **(B)** Primary cortical neurons were exposed to 1 μM Aβ oligomers for 15, 30 and 60 min, and phosphorylation of PKC was examined (pPKC) by Western blot. **(D)** Quantification of phospho PKC levels was obtained by analysis of immunoblot images (n=5). Histograms represent means ± S.E.M. of band volume intensities normalized to corresponding Src-total (C) or β-Actin (D). *p<0.05, compared to non-treated cells; paired one-way ANOVA.

4.2. Study of PKC activity by FRET assays in living neurons.

Imaging approaches have been developed and used for quantifying the activity of many proteins, included PKC family members. Since changes in protein activity or protein-protein interactions are often accompanied by conformational changes, it is important to monitor these changes in living cells. In the last years, several fluorescent resonance energy transfer (FRET)-based sensors for measuring PKC activity have been designed allowing real time imaging of kinase activity. In order to examine the Aβ oligomer-mediated PKC activation, a genetically encoded fluorescent reporter was transfected in primary cortical neurons. This reporter, called myristoylated and palmitoylated C kinase activity reporter (Myr-Palm CKAR), monitors PKC-mediated activation by FRET (Violin et al, 2003).

First, we have verified that measuring FRET in Myr-Palm CKAR-expressed living neurons is a good choice to probe PKC activity in these cells. For that, primary cortical

neurons were transfected with a myristoylated form of Myr-Palm CKAR as shown in **Figure R8A**. On the other hand, primary cortical neurons were treated with specific inhibitors against classical (Gö6983) and novel PKCs (Rottlerin), and FRET signal was examined.

Results showed that FRET signal was rapidly decreased by the broad spectrum cPKC inhibitor Gö6983 (**Figure R8B**). Similarly, the application of AIP significantly reduced FRET signal (**Figure R8C**). By contrast, Rottlerin (nPKC inhibitor), did not affect FRET ratio (**Figure R8D**). Taken together, CKAR senses cPKC but not nPKC activity in living neurons. Next, we treated primary cortical neurons with PMA, a potent PKC activator. **Figure R8E** showed that this compound produced a robust increase in the FRET signal. Therefore, Myr-Palm CKAR was considered to be a useful reporter to analyse PKC-activation during time.

Finally, we examined the effect of Aβ oligomers in PKC activation on Myr-Palm CKAR-transfected neurons. Cells were pretreated with the phosphatase inhibitor calyculin A (100 nM) for 10 min, and stimulated with 1 μM Aβ oligomers. Results showed a large increase in FRET signal (**Figure R8F**), similar to that observed when cells were stimulated with PMA. These results suggest that Aβ oligomers stimulate PKC activation in neurons.

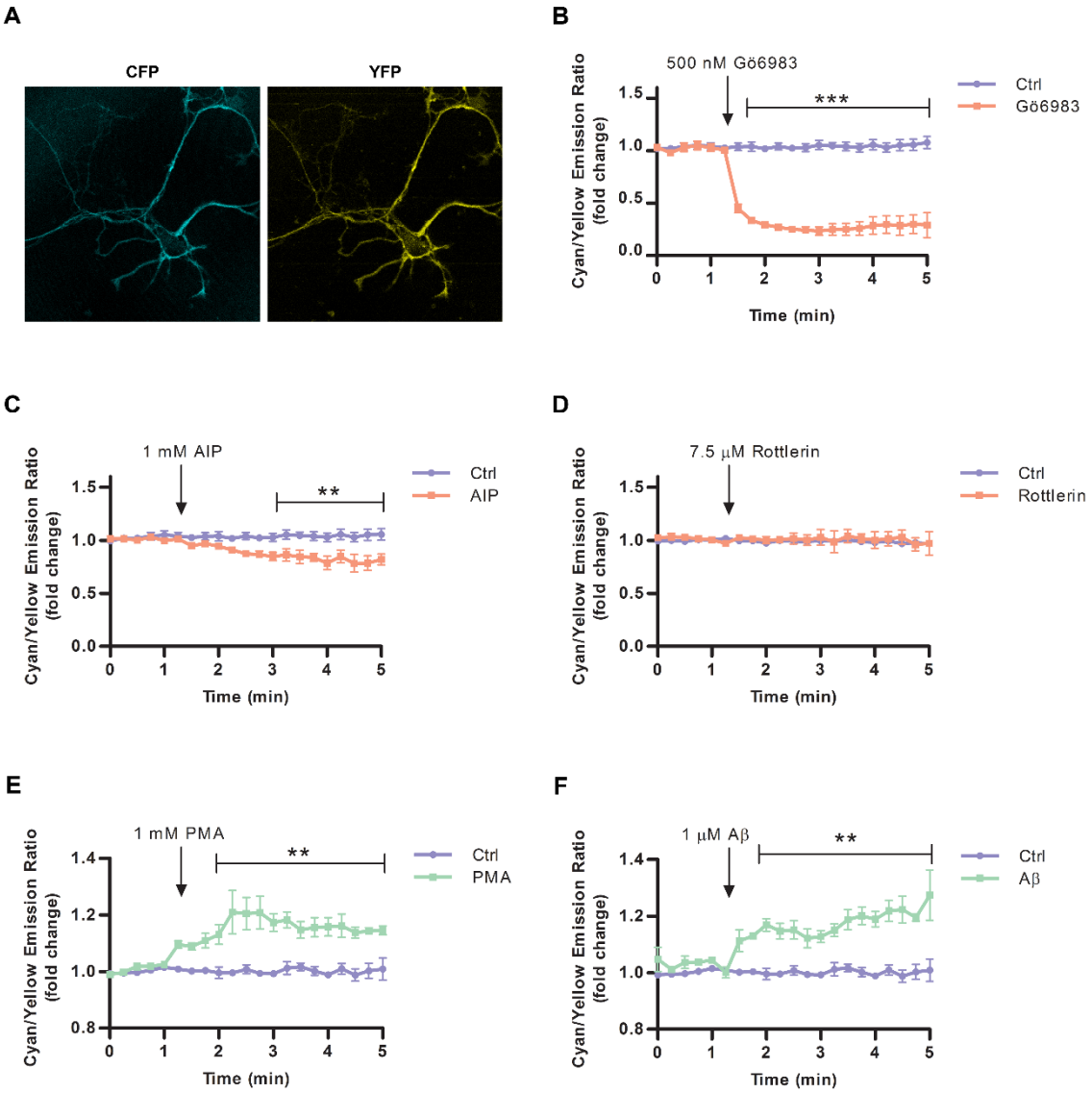

Figure R8. Analysis of PKC activity using a Myr-Palm CKAR in neurons. (A) Image shows effective targeting of CKAR into primary cortical neuron plasma membranes. **(B)** Application of 1 µM Gö6983 significantly reduces the PKC-mediated CKAR phosphorylation. **(C)** 1 mM AIP treatment also reduces PKC activation **(D)** 7.5 µM Rottlerin (nPKCs inhibitor) does not change basal FRET. **(E)** 1µM PMA stimulates CKAR activation. **(F)** 1 µM Aβ oligomers modulate CKAR activation upon PKC stimulation. Data presented in the graphs are plotted as the ratio of cyan fluorescence (which decreases when FRET increases) to yellow emission (which increases as FRET increases), being inversely proportional to FRET signal and are represented as means ± S.E.M. of three to five experiments, **p<0.01, ***p<0.001 compared to non-treated cells; paired one-way ANOVA.

4.3. Aβ oligomers control NR2B subunit location in neuronal membrane surface via PKCs.

It has been very well established that PKCs regulate NMDA receptor function. In fact, PKCs increase the opening rate of NMDA receptor channels and upregulate the presence of the receptor at the cell surface (Lan et al., 2001). Based on this, we investigated the involvement of PKC in the increase of Aβ-induced NR2B membrane surface. For that, primary cortical neurons were pretreated with 100 nM Gö6983 for 30 min, incubated with Aβ oligomers for 30 min, and levels of receptors in the cell membrane were quantified by biotinylation. As shown in **Figures R9A** and **B,** treatment of 1 μM Aβ for 30 min induced NR2B subunit upregulation from 0.42 ± 0.02 (control) to 0.66 ± 0.06 (Aβ-treated cells), which was attenuated by preincubation with Gö6983 to 0.56 ± 0.13 (compared to its respective control level, 0.59 ± 0.11).

Moreover, to assess if Gö6983 also blocked NR2B subunit level at synaptic sites, we analysed the presence of NR2B in synaptosomes. Similar to the results obtained by protein surface biotinylation, results in **Figure R9C** showed that 100 nM Gö6983 blocked the increase of Aβ-induced NR2B levels in the synaptosome fraction (1.35 ± 0.04, second bar compared to first bar, 0.98 ± 0.02) and (0.9 ± 0.23, fourth bar compared to third bar, 1.02 ± 0.07) (**Figure R9D**).

Altogether, these results indicate that Aβ oligomers control NR2B protein levels in the neuron surface through classic PKCs.

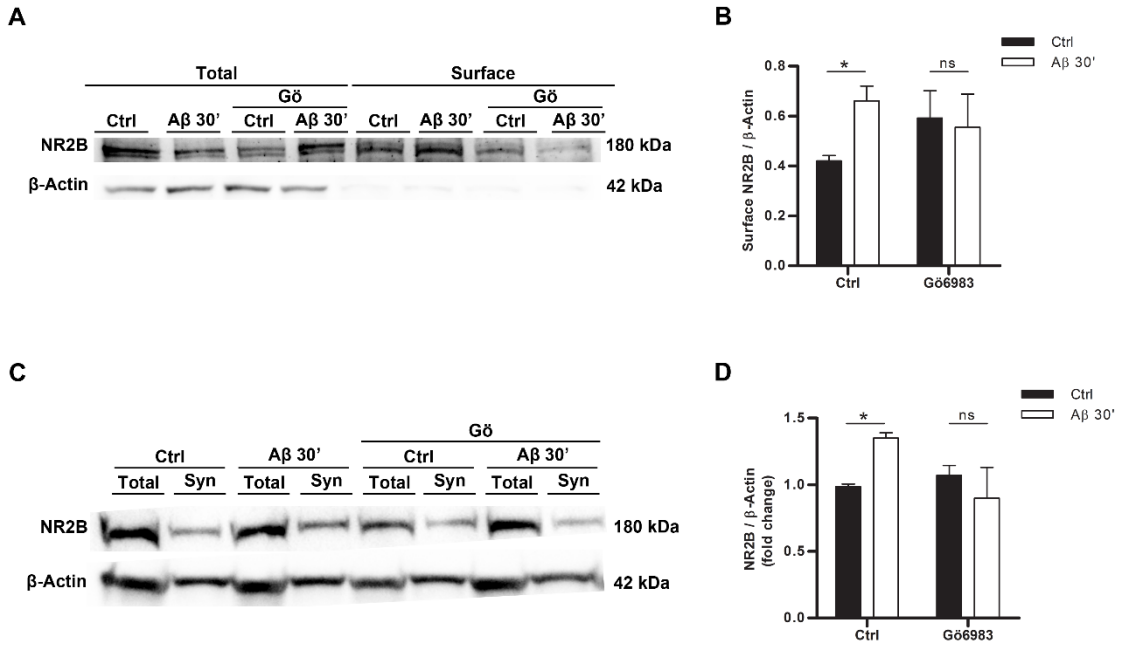

Figure R9. PKC controls Aβ-mediated NR2B location in neuronal membranes. (A) Primary cortical neurons were treated with 1 μM Aβ for 30 min in the presence or in the absence of 100 nM Gö6983 and NR2B subunit levels were examined by biotinylation assay and western blot. **(B)** Graph bar shows quantification of biotinylated NR2B in the immunoblots (n=3). **(C)** Primary cortical neurons were treated with 1 μM Aβ for 30 min in the presence or in the absence of 100 nM Gö6983 and the levels of NR2B subunit were examined by western blot in total and synaptic fractions. **(D)** Quantification of synaptic NR2B levels shows that Gö6983 blocks the Aβ-mediated NR2B upregulation (n=3). Data are represented as means ± S.E.M. of band volume intensities normalized to β-Actin. *p<0.05, compared to non-treated cells; paired two-way ANOVA.

4.4. Effect of Aβ-induced PKC activity on dendritic localization of NR2B-containing NMDA of primary cortical neurons.

Since previous results have shown that classical PKCs are involved in the NR2B subunit location in the cell membrane, we carried out immunocytochemistry of NR2B protein in neuron dendrites and we analyzed several regions of interest (R.O.I.). For this purpose, the presence of microtubule-associated protein 2 (MAP2) was used as control since MAP2 is specifically expressed in dendrites (Bernhardt et al., 1984). NR2B fluorescence intensity was measured in dendritic processes from neurons pretreated or not with 100 nM Gö6983 for 1 hour and stimulated or not with Aβ. As shown in **Figure R10A** and **B**, Aβ increased NR2B subunit level in dendritic processes while

Gö6983 treatment prevent it in an unquestioned manner. Quantification of these fluorescence signals shows that NR2B subunit level was increased from 8.9 ±0.86 (control neurons) to 10.61 ± 0.93 (Aβ-treated neurons). By contrast, Gö6983 blocked the Aβ-induced NR2B subunit increases in dendrites from 8.43 ± 0.56 (third bar) to 8.02 ± 0.87 (fourth bar) (**Figure R10C**).

Therefore, these results agreed with previous findings, supporting the idea that classic PKC may be key contributors of Aβ-induced NR2B location changes.

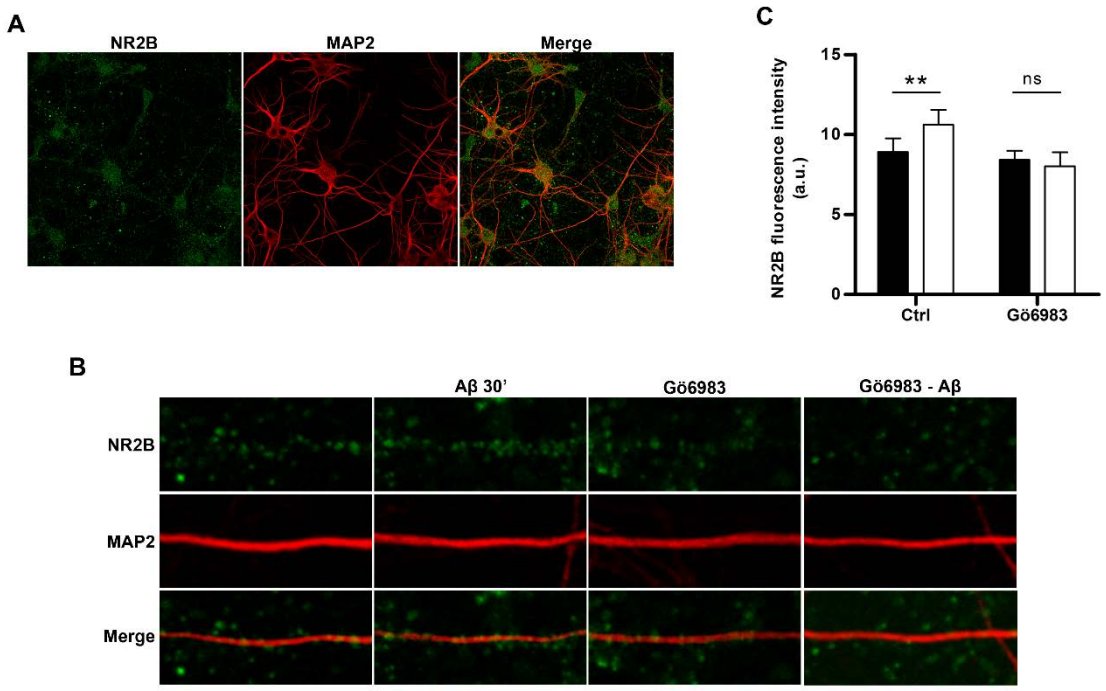

Figure R10. Aβ triggers location of NR2B subunit protein in dendrites through cPKC. (A) Immunofluorescence images of non-treated cells showing NR2B (green) and MAP2 (red) localization in cortical neurons. **(B)** Representative images of NR2B and MAP2 levels from dendrites treated with 1μM Aβ for 30 min in presence or absence of Gö6983. Constant MAP2 fluorescence signals were obtained. **(C)** Quantification of NR2B fluorescence intensity in dendrites. Data are represented as means ± S.E.M of 52 ROIs from at least 3 independent experiments. **p<0.01 compared to non-treated cells; paired two-way ANOVA.

4.5. Aβ oligomers enhance NMDA-mediated Ca^{2+} influx through a PKC-dependent mechanism.

We showed that acute treatment of Aβ oligomers enhanced the NMDA-induced Ca^{2+} response; therefore, we postulated that PKC could be involved in this dysregulation of function receptor. For that, we pretreated primary cortical neurons with 100 nM Gö6983 for 30 min and treated with 1μM Aβ oligomers. As shown in the **Figure R11A** and **R11B**, enhancement of NMDA-dependent Ca2+ influx by Aβ was blocked by Gö6983 treatment, indicating that Aβ oligomers modulated Ca^{2+} permeability of NMDA receptor in a cPKC-dependent manner (**Figure R11C**).

To further investigate the role of PKC in the Ca^{2+} signalling, we postulated that PKC stimulation with 1 μM PMA could modulate NMDA dependent Ca^{2+} influx. As shown in **Figure R11D**, PMA efficiently triggered an enhanced NMDA- Ca^{2+} response compared to control treatment.

These results suggest that cPKC modulated Ca^{2+} permeability of NMDA receptors.

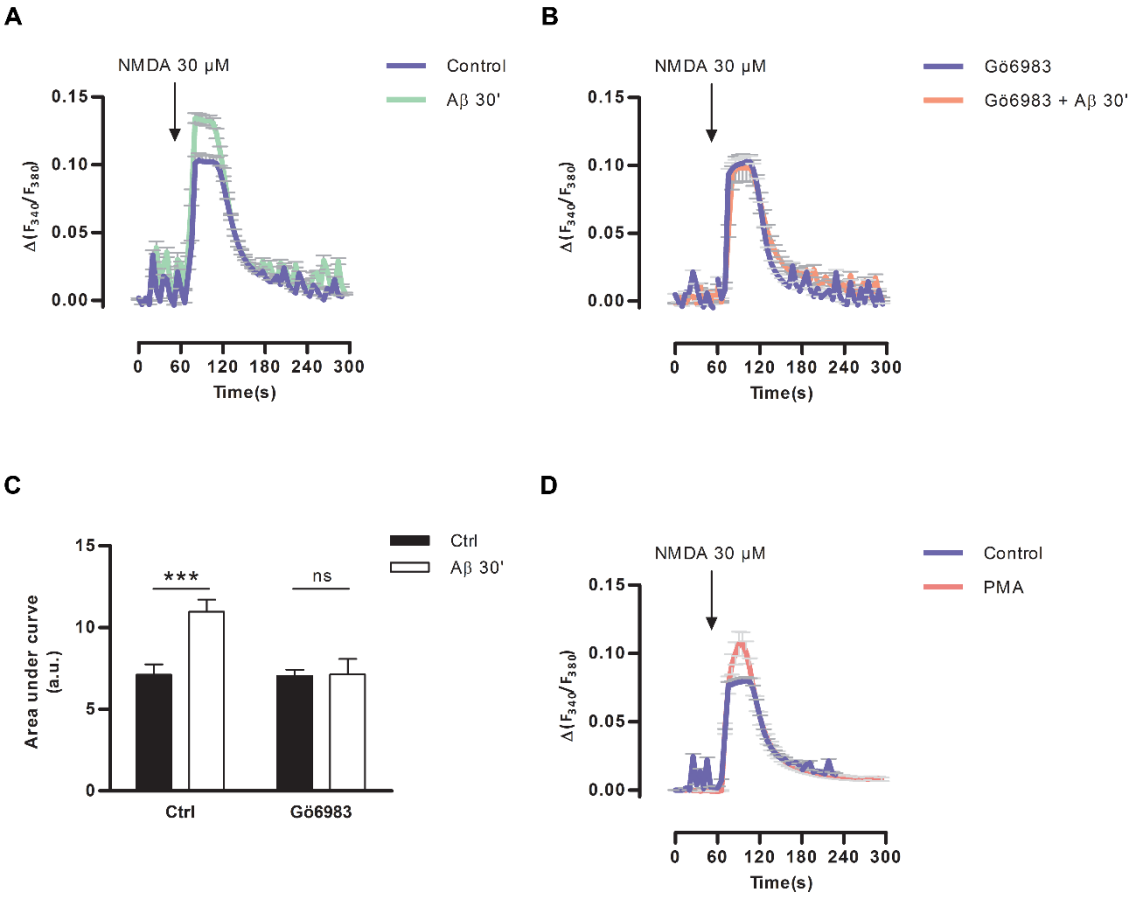

Figure R11. PKC modulates Aβ-induced $[Ca^{2+}]_i$ increase through NMDA receptors in neurons. (A-B) Addition of 1μM Aβ oligomers together with 100 nM Gö6983 for 30 min attenuated the Aβ oligomer-modulated Ca^{2+} response through NMDA receptor/cPKC pathway in neurons. **(C)** Histogram represents changes on Ca^{2+} levels in neurons treated with Gö6983. **(D)** NMDA-mediated Ca^{2+} influx in neurons after treatment with PMA. Recordings represent the time course of the intracellular Ca^{2+} levels of 61 cells from at least 3 independent experiments. ***p<0.001, compared to non-treated cells; paired one-way ANOVA.

4.6. Aβ oligomers promote phosphorylation of NR2B subunit protein at Serine^{1303} via cPKCs.

Finally, we investigated the possibility that Aβ oligomers induced NR2B subunit phosphorylation through PKC activity. Sequence alignment of NR2B showed that S^{1303} and S^{1323} are residues that are susceptible to being phosphorylated by PKCs (Chen et al., 2007), consequently we proposed to examine the effects of Aβ oligomers on the NR2B S^{1303} phosphorylation level (pSer^{1303} NR2B). Firstly, western blot analysis showed that Aβ oligomers promoted phosphorylation of this residue in primary cortical neurons (1.01 ± 0.07 compared to control levels, 0.86 ± 0.04). Secondly, cPKC inhibitor Gö6983, blocked NR2B Ser^{1303}phosphorylation (0.73 ± 0.09 compared to their correspondent control levels, 0.81 ± 0.1), suggesting that Aβ oligomers induced NR2B phosphorylation at Serine^{1303} in a cPKC-dependent manner (**Figure R12A** and **B**).

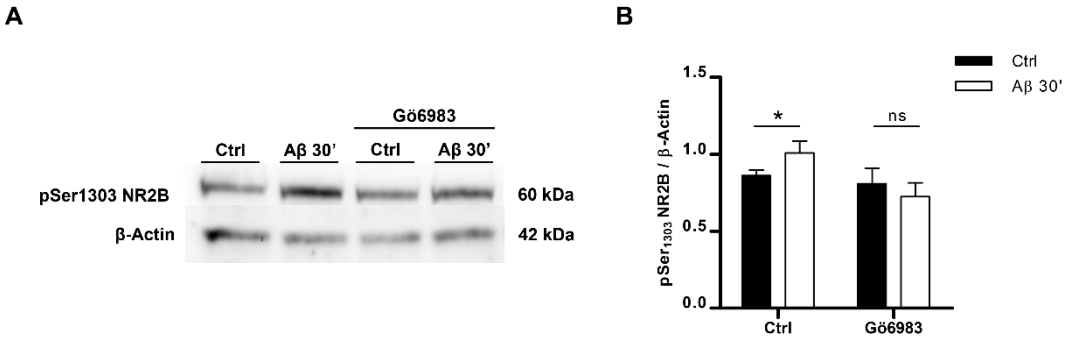

Figure R12. Aβ oligomers promote NR2B S^{1303} phosphorylation via cPKCs. (A) Primary cortical neurons were pretreated or not with 100 nM Gö6983 for 1h and stimulated or not with 1 μM Aβ for 30 min, as indicated. Immunoblots show phosphorylated NR2B (S^{1303}) levels in total cell extracts. **(B)** Graph bar represents quantification of phosphorylated NR2B (S^{1303}) normalized with β-Actin Data are represented. as means ± S.E.M. of band volume intensities normalized to corresponding β-Actin *p<0.05, compared to non-treated cells; paired two-way ANOVA.

5. Aβ oligomers upregulate NR2B subunit density via β1-integrin/PKC signalling pathway.

5.1. β1-Integrin mediates Aβ-induced PKC activation in primary cortical neurons.

In order to investigate the signalling pathway underlying Aβ-increased density of NR2B subunit through PKC activity, we first examined what receptorial system mediated Aβ-induced PKC activation. It has been described that Aβ oligomers bind among several receptors. We focused our investigation on integrin protein family, because this transmembrane receptor has been described as a partner in Aβ signalling that induces astrocyte dysfunction in AD (Wyssenbach et al., 2016).

To study the involvement of integrin receptors on Aβ-mediated PKC phosphorylation, primary cortical neurons were preincubated with 100 μM RGDS peptide (this peptide interacts with cell surface integrins, blocking intracellular signalling regulated by this receptor), and treated with 1 μM Aβ oligomers for 30 min. As shown in **Figure R13A** and **B**, Aβ induced PKC phosphorylation, as expected 0.45 ± 0.11 (compared to control levels, 0.29 ± 0.09). Nevertheless, this phosphorylation was blocked when cells were preincubated with RGDS peptide (0.36 ± 0.13, compared to control levels, 0.31 ± 0.09) (**Figure R13A**, lanes 3 and 4, and **R13B** bars 3 and 4).

Next, to confirm integrin involvement in PKC activation, we analyzed PKC phosphorylation in the presence of 0.5 μg/ml S2-16 antibody, which activates specifically β1-integrin. As shown in **Figure R13C** and **D**, TS2-16 induced PKC phosphorylation (0.54 ± 0.07 compared to control levels, 0.27 ± 0.08), this observation was also reproduced when cells were incubated with 1μM Aβ for 30 min (0.42 ± 0.07, in relation to control levels, 0.27 ± 0.08) (**Figure R13C,** and **D**). These results confirm that PKC is phophorylated by mechanisms which involve β1-integrin receptor.

To further explore the Aβ oligomer-mediated PKC activation via β1-integrin, primary cortical neurons were transfected with Myr-Palm CKAR probe, pretreated with 0.5 μg/ml CD29 antibody and stimulated with 1 μM Aβ oligomers, to finally measure FRET in Myr-Palm CKAR-expressed living neurons. CD29 is an antibody that specifically

binds β1-integrin and blocks the signalling pathways emanated from β1-integrin. Results showed that Aβ oligomers increased FRET signal even in the presence of 0.5 μg/ml IgM (internal control) (**Figure R13E**, green and orange lanes). However, this PKC activity was blocked when cells were preincubated with 0.5 μg/ml CD29 antibody (**Figure R13E,** blue lane). Taken together, these results pointed out that Aβ oligomers required β1-integrin to modulate PKC phosphorylation and activation.

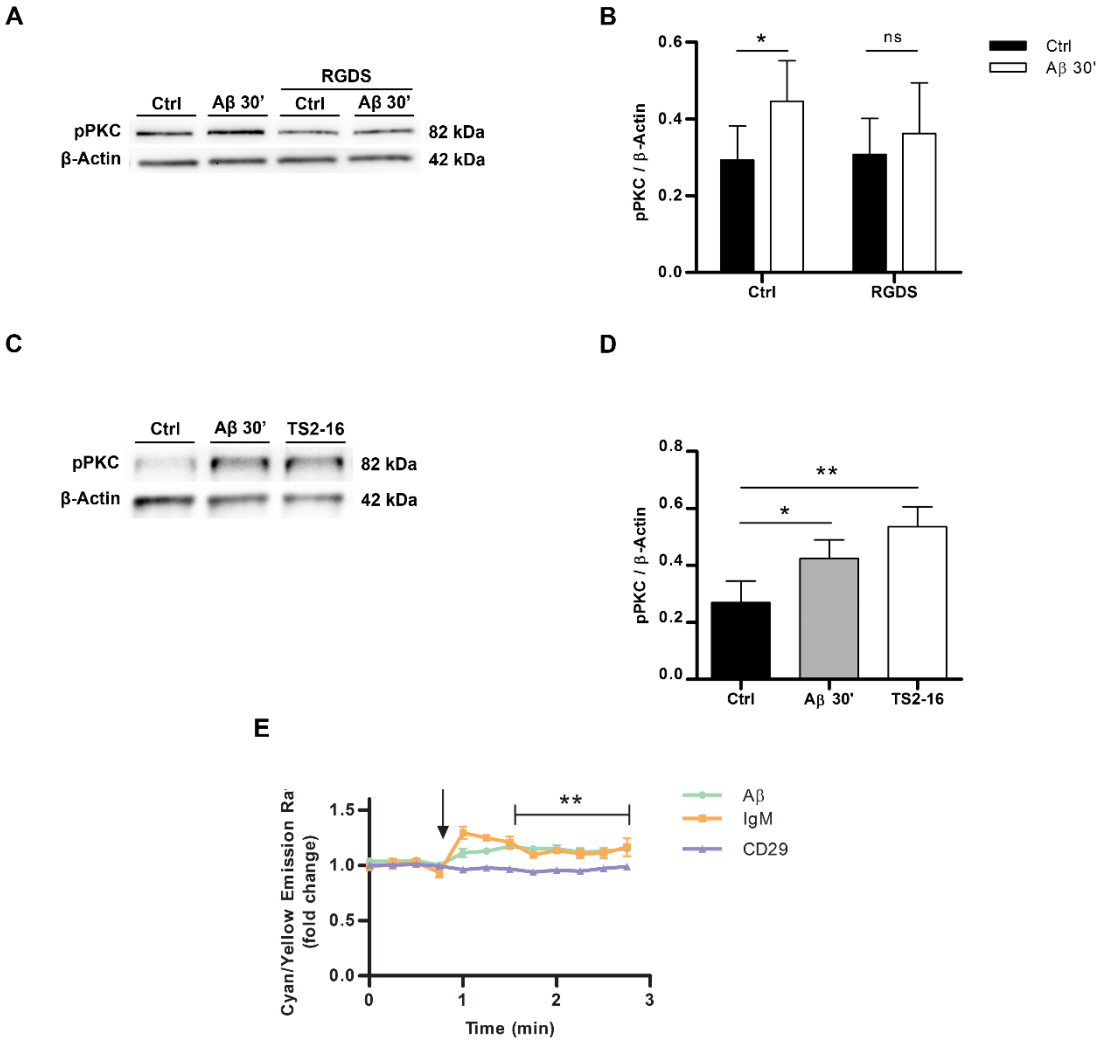

Figure R13. Aβ oligomers promote PKC activation through β1-integrin in primary cortical neurons. (A) PhosphoPKC levels in total cell extracts that previously have been preincubated with 100 μM RGDS and stimulated with 1 μM Aβ were analyzed by Western blot. **(B)** Histogram of phosphoPKC analysis is shown (n=4). **(C)** Total cell extracts were obtained after treatment with 1 μM Aβ or 0.5 μg/ml TS2-16 for 30 min and PKC phosphorylation was analysed by western blot. **(D)** Quantification of phosphoPKC levels in total protein extract (n=4) is shown. **(E)** Myr-Palm-CKAR expressed primary cortical neurons are

activated upon Aβ or Aβ+IgM stimulation, while 0.5 μg/ml CD29 inhibits PKC activation induced by Aβ oligomers. Data are represented as means ± S.E.M. of band volume intensities normalized to corresponding β-Actin (B, D). PKC activity is represented as means ± S.E.M. of three to five different experiments (E). *p<0.05, **p<0.01 compared to non-treated cells; paired two-way ANOVA (B) and one-way ANOVA (D, E).

5.2. β1-integrin receptor mediates Aβ-induced NR2B surface increase in primary cortical neurons.

Regarding previous results, we examined whether integrin receptor contributed to the Aβ oligomer-mediated increase of NR2B density in membrane surface. For that purpose, biotinylation assays were performed in the presence of 100 μM RGDS (**Figure R14A**). We observed that the application of 1μM Aβ oligomers for 30 minutes induced an increase of NR2B-subunit levels on neuronal membrane surface (0.75 ± 0.03 compared to control, 0.51 ± 0.008), while RGDS prevented it (0.411 ± 0.11 compared to control, 0.51 ± 0.034) (**Figure R14B**), suggesting that integrin receptor is involved in Aβ-modulated upregulation of NR2B subunit surface expression.

These results were strengthened by analysing NR2B density in functional synaptosomes. For that, primary cortical neurons were pretreated with 0.5 μg/ml CD29, and incubated with 1 μM Aβ for 30 min. Synaptosome fractions were extracted and NR2B subunit levels were detected by western blot. IgM was used as negative control for CD29 treatment. As shown in **Figure R14C** and **D**, while Aβ treatment induced an increase in NR2B protein level in the synaptosomes from 1.03 ± 0.07 (control cells) to 1.4 ± 0.13 (treated cells), CD29 blocked the presence of NR2B in these processes (0.8 ± 0.06, compared to control levels 1.12 ± 0.06) (**Figure R14D**). These results suggested that Aβ oligomers require β1-integrin/cPKC pathway in order to mediate actively on NR2B location to the synaptosomes.

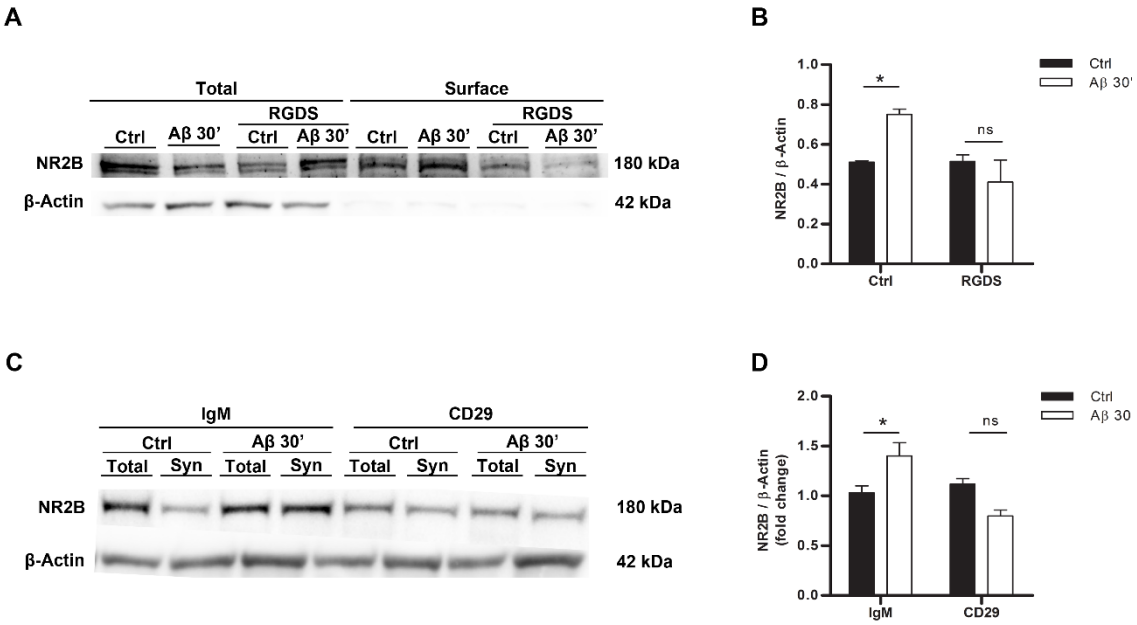

Figure R14. Aβ-oligomers favour NR2B expression on cell surface via β1-integrin. (A) Western blot analysis of total and surface NR2B density in biotinylated primary cortical neurons that previously were preincubated with 100 μM RGDS and stimulated with 1 μM Aβ . **(B)** Quantification of NR2B levels in neuron surface is shown (n=3). **(C)** Immunoblots of NR2B subunit levels and β-actin in functional synaptosomes of primary cortical neurons that previously have been preincubated with 0.5 μg/ml CD29 or 0.5 μg/ml IgM antibodies (as negative control) and stimulated with 1 μM Aβ. **(D)** Histogram shows NR2B levels after β1-integrin inhibition with CD29 (n=4). Data are represented as means ± S.E.M. of band volume intensities normalized to corresponding β-Actin. *p<0.05, compared to non-treated or IgM- treated cells; paired two-way ANOVA.

5.3. Aβ oligomers require β1-integrin to increase Ca^{2+} permeability of NMDA receptors.

Finally, we investigated whether modulation of NMDA receptor function by Aβ oligomers would be dependent of β1-integrin activity. For that, we preincubated primary cortical neurons with 0.5 μg/ml CD29 antibody or 0.5 μg/ml IgM and then treated with 1μM Aβ oligomers for 30 min, and we observed that enhancement of Ca^{2+} permeability of NMDA receptor by Aβ oligomers was prevented by CD29 (**Figure R15A** and **B**), meaning that Aβ modulated NMDA-mediated Ca^{2+} influx through β1-integrin receptor.

In addition, we used the β1-integrin activator antibody, TS2-16 (0.5 μg/ml), to verify the relationship between β1 integrin activation and modulation of NMDA receptor permeability. As shown in **Figure R15C** and **D**, TS2-16 potentiated Ca^{2+} influx through NMDA receptors, as expected. This result confirmed that β1-integrin modulates Ca^{2+} permeability of NDMA receptors.

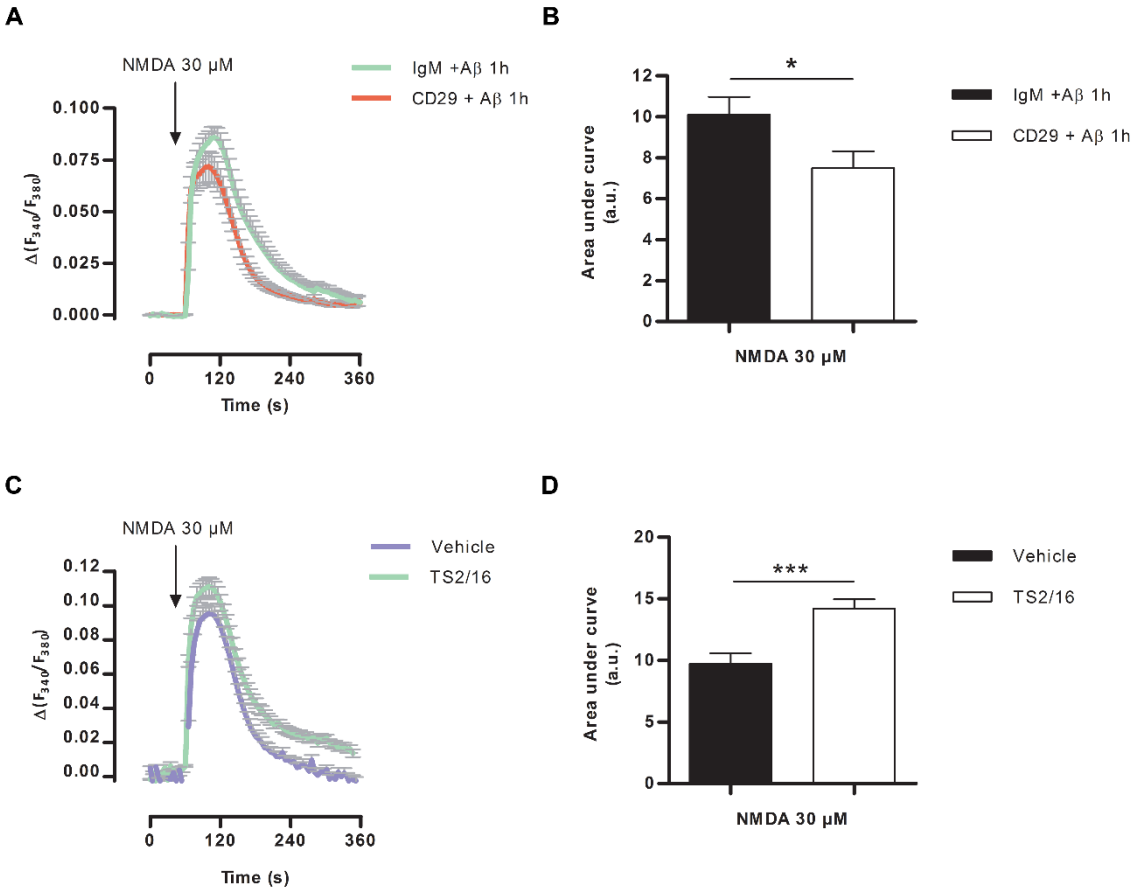

Figure R15. Aβ oligomers/β1-integrin tandem is involved in NMDA-mediated Ca^{2+} overload (A) Primary cortical neurons, loaded with Fura 2-AM, were preincubated with IgM or CD29 (0.5 μg/ml, overnight) and exposed to 1 μM Aβ. Intracellular Ca^{2+} levels after 30 μM NMDA application were measured by microfluorimetry. **(B)** Graph illustrates average of fluorescence ± SEM responses of 90 cells from at least 3 experiments. **(C)** Traces represent the time course of average of fluorescence ±SEM of NMDA-mediated Ca^{2+} permeability in 0.5 μg/ml TS2-16-stimulated neurons. **(D)** Histogram represents changes in Ca^{2+} levels in vehicle- or TS2-16-stimulated neurons of 70 cells from at least 3 independent experiments. *p<0.05, ***p<0.001, compared to IgM- or vehicle-treated cells; paired one-way ANOVA.

In summary, these results demonstrate that Aβ oligomers require β1-integrin in order to activate PKC and control Ca^{2+} permeability and membrane surface overexpression of NMDA receptor (**Figure R16**).

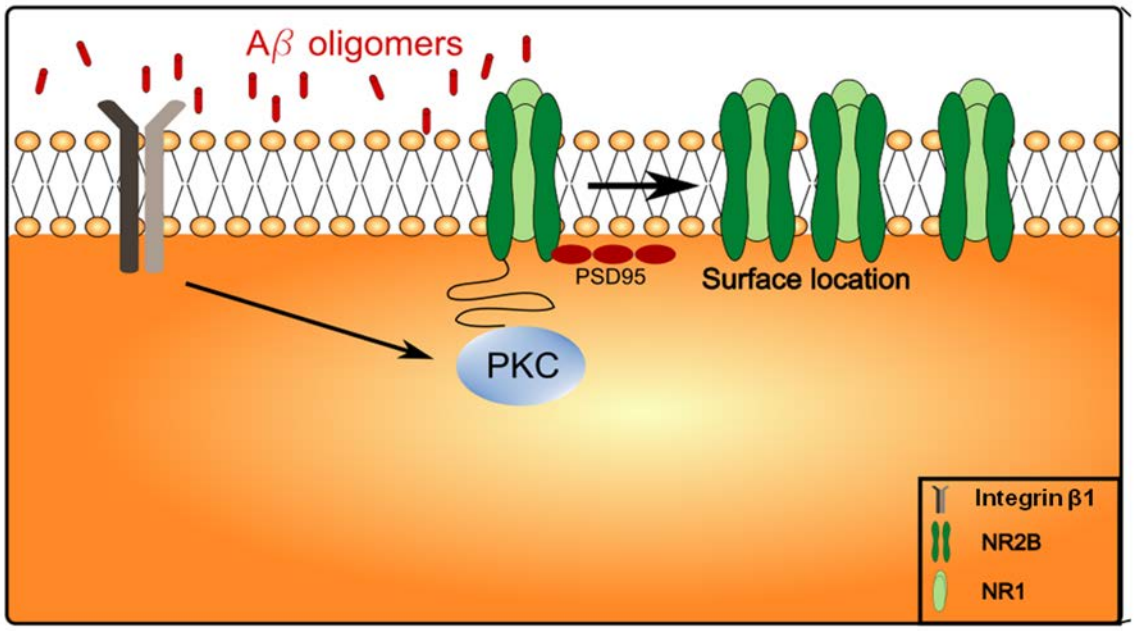

Figure R16. Aβ oligomers signaling pathway increases NR2B density in membrane. Model of the signaling cascade activated by Aβ oligomers in neurons.

6. NR2B subunit and synaptic proteins are selectively altered in AD transgenic mice.

In order to assess whether NR2B subunit and synaptic proteins (PSD-95, and synaptophysin) levels are altered in a mouse model of AD, we investigated this subject in the triple transgenic mouse (3xTg-AD), a murine model that reproduce this pathology. We planned to examine the NR2B subunit, PSD-95 and synaptophysin protein levels at different ages in isolated synaptosomes of hippocampal region. It has been very well established that 1-month-old 3xTg-AD mice are cognitively unimpaired and do not present extracellular amyloid plaques (Oddo *et al*., 2003). Based on that, we first analysed in synaptosomes from 1-month old 3xTg-AD and wild-type (WT) levels of NR2B, PSD-95 and synaptophysin by Western blot (**Figure R17A**). Immunoblot quantification showed that total protein concentration in isolated sysnaptic terminals

did not change in the 1-month-old 3xTg-AD mice group compared to control (W.T.) mice (1.09 ± 0.09 *vs* 1.09 ± 0.09) (**Figure R17B**). These results confirmed that these mice did not show synaptic deficit. Similarly, no significant differences were observed in NR2B (1.51 ± 0.24 *vs* 1.13 ± 0.08), PSD-95 (6.14 ± 0.9 *vs* 4.39 ± 0.57) and synaptophysin (2.16 ± 0.31 *vs* 2.31 ± 0.31) expression in the 1-month-old 3xTg-AD mice compared to controls (**Figure R17C** and **E**).

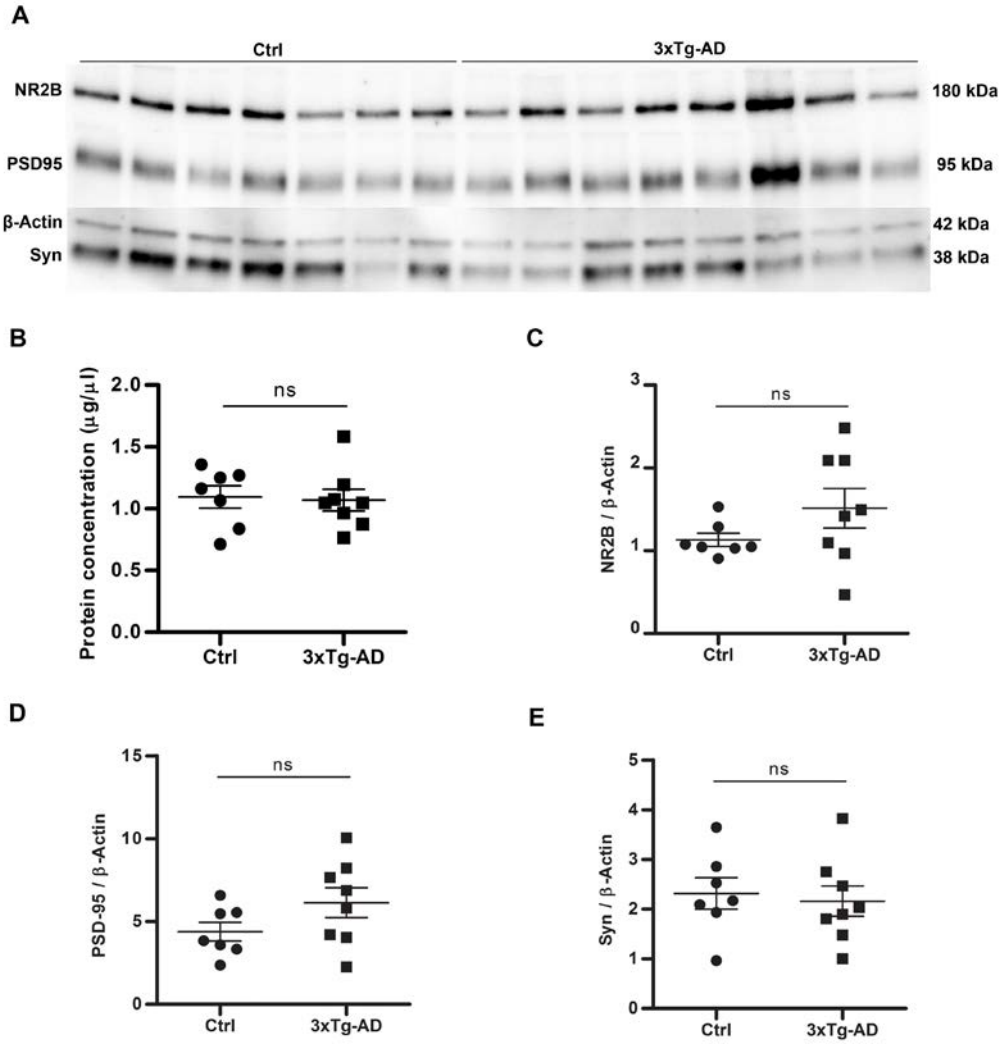

Figure R17. 1-month-old 3xTg-AD mice do not present changes in NR2B subunit and synaptic proteins. **(A)** Western blot showing NR2B, PSD-95, β- Actin and synaptophysin levels in isolated synaptic terminals of hippocampus of 1 month-old 3xTg-AD and WT mice. **(B)** Total protein concentration of control and 3xTg-AD mice. **(C-E)** Quantitative analysis of proteins (n=7-8 animals per group). Dot plots represented as means ± S.E.M. of optical density values normalized to corresponding β-Actin; paired Student's t test.

3xTg-AD mice developed extracellular amyloid plaques in the neocortex and hippocampus at 6 months old (Oddo *et al*., 2003), so we chose this age to analyse the NR2B subunit and synaptic protein levels. As shown in **Figure R18A,** synaptosomal fractions of 3xTg-AD hippocampus had a significant decrease of total protein concentration (0.74 ± 0.09) compared to the W.T. mice (1.28 ± 0.04). However, NR2B protein level clearly showed a significant increase (1.28 ± 0.29) compared to the WT group (0.52 ± 0.07) (**Figure R18C**). Moreover, both PSD-95 (from 2.39 ± 0.29 to 5.83 ± 2.81, **Figure R18D**) and synaptophysin (from 2.72 ± 0.62 to 4.83 ± 0.73, **Figure R18E**) also increased significantly their levels in 6-months-old 3xTg-AD mice compared to W.T. group.

Thereby, these results indicated that 6-month-old 3xTgAD mice showed synaptic protein deficits concomitant with enhanced expression of NR2B subunit, PSD-95 and synaptophysin proteins in isolated synaptic terminals of hippocampus.

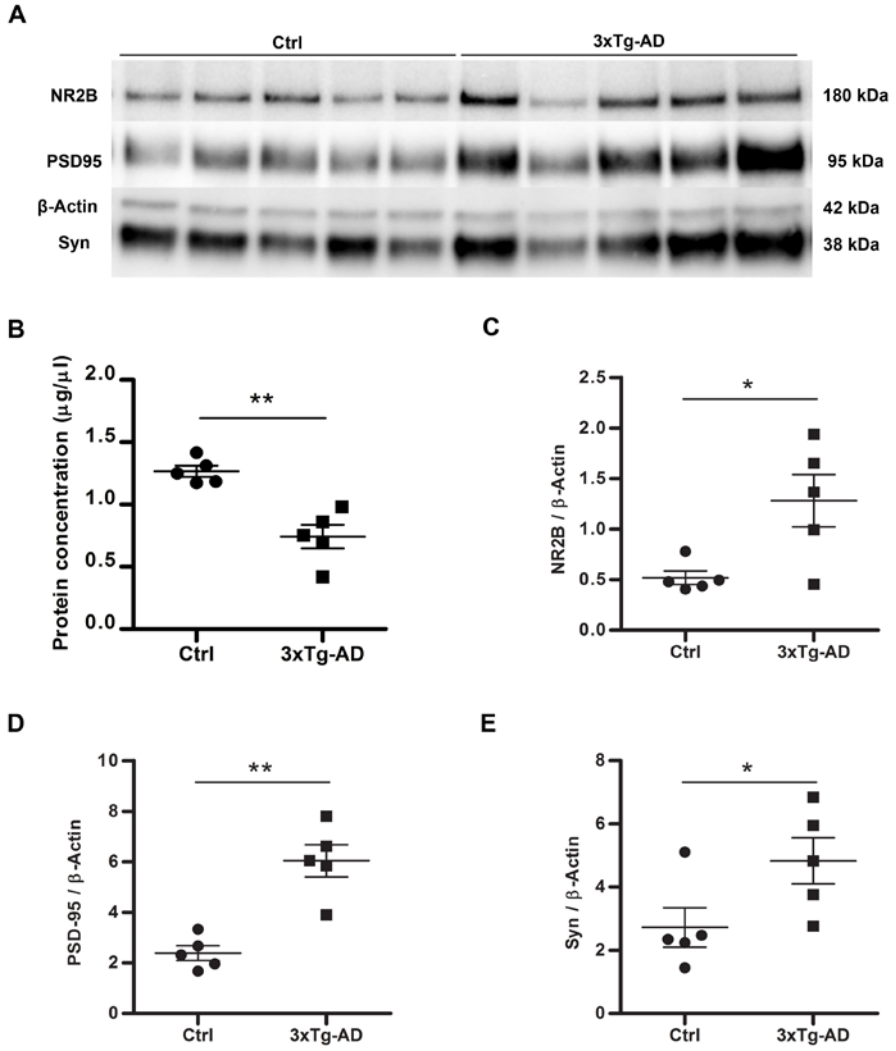

Figure R18. 6-months-old 3xTg-AD mice exhibit NR2B and synaptic proteins levels increased in hippocampus. (A) The presence of NR2B, PSD95, β- Actin and synaptophysin in hippocampus of 6 month-old 3xTg-AD and W.T. mice were analysed by Western blot. **(B)** Total protein concentration of control and 3xTg-AD mice. **(C-E)** Quantitative analysis of proteins (n=5 animals per group). Dot plots represented as means ± S.E.M. of optical density values normalized to corresponding β-Actin. *p<0.05, **p<0.01; paired Student's t test.

7. NR2B and synaptic protein levels are abnormally increased at early stages in prefrontal cortex of Alzheimer's disease patients.

Finally, we examined whether NR2B and synaptic proteins were differentially expressed in *post-mortem* prefrontal cortex from healthy subjects and AD patients.

Tissues from AD subjects were classified according to Braak stage (II, III, IV or V-VI) (Braak and Braak, 1995).

Firstly, we obtained a PSD-enriched fraction (PSD) and a synaptophysin-enriched fraction (non-PSD) from prefrontal cortex of human samples, and protein concentration for each sample was measured. As shown in **Figures R19A** and **B**, protein concentration in both fractions are decreased according to disease progression. In fact, in Braak IV and Braak V-VI stages, protein concentration in PSD fraction was reduced significantly compared to Braak II samples. However, no significant changes were observed in protein concentration of non-PSD fraction.

This observation suggests that progressive protein loss of synaptic-enriched fractions could reflect synapse deterioration across AD.

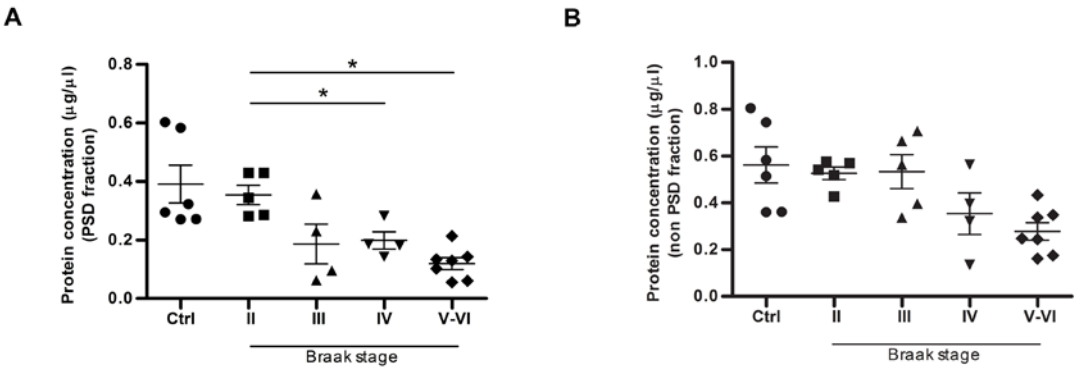

Figure R19. Protein concentration inversely correlates with AD disease stage in PSD and non-PSD fractions of prefrontal cortex in human samples. (A) Protein density in PSD fraction in relation to AD stage. **(B)** Non-PSD fraction protein concentration in relation to AD stage. Dot plots represented as protein concentration (μg/μl) obtained by fluorimetric assays. *p<0.05; paired Student's t test.

Next, we prepared samples at the same protein concentration in order to compare protein expression in synapse enriched-fraction of progressive AD brain samples. As shown in **Figure R20A**, in the PSD fraction NR2B and PSD-95 are increased in Braak II stage, while in the other stages both proteins decreased concomitantely**.** β-Actin levels did not show any variation between different samples. Low synaptophysin levels showed an effective PSD enriched fraction isolation. Quantitative analysis of

these proteins clearly showed a significant increase of the NR2B and PSD-95 protein levels in prefrontal cortex of AD patients at Braak II stage, compared to control group and Braak V-VI classified subjects (**Figure R20C** and **D**), without altering the β-Actin levels (**Figure R20B**).

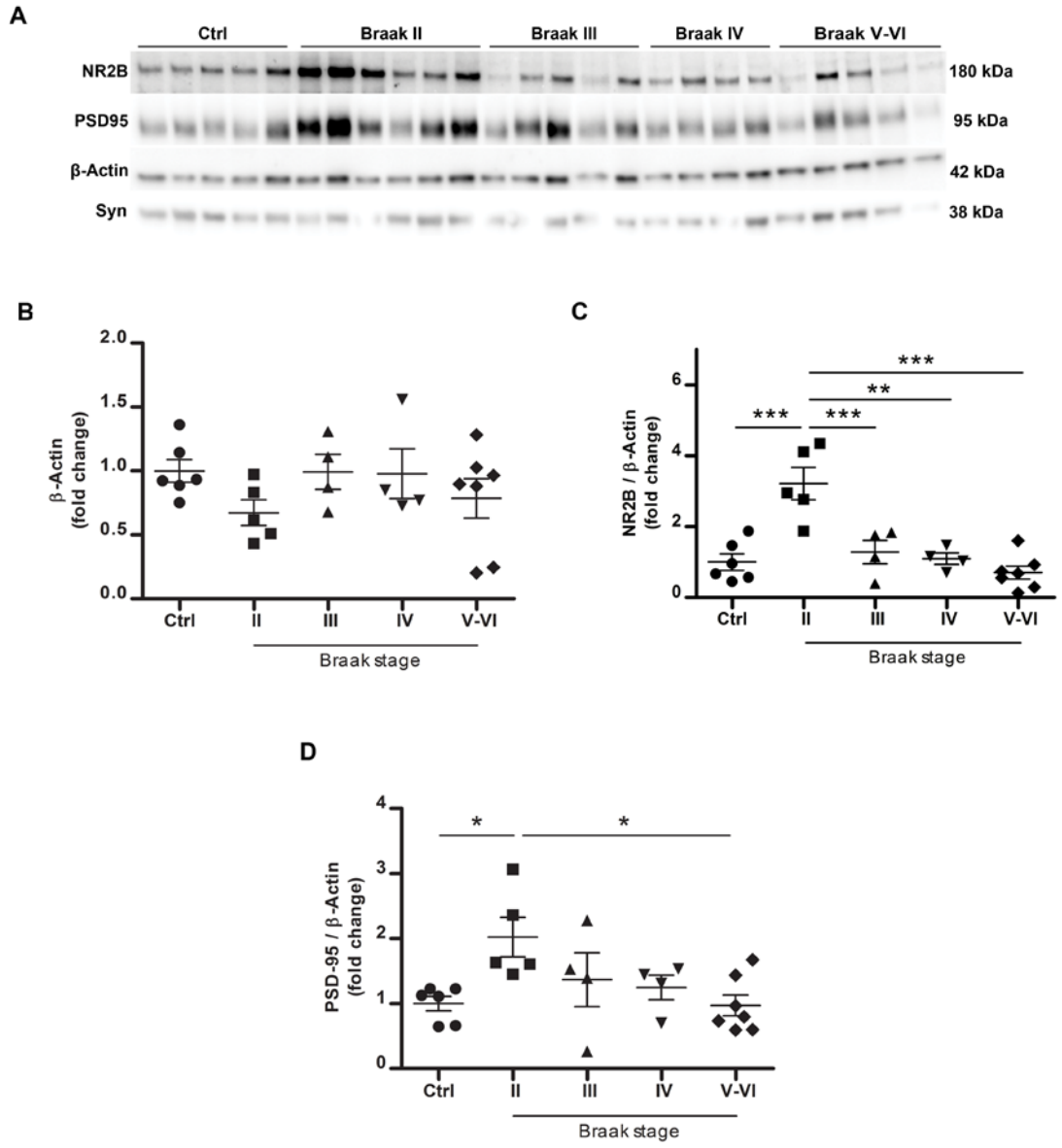

Figure R20. NR2B and PSD-95 levels are increased in prefrontal cortex from AD patients at early disease stages. (A) Western blot of NR2B, PSD-95, synaptophysin and β-Actin protein expression in *post-mortem* prefrontal cortex from controls (Ctrl) and AD patients at different Braak stages (Braak II-VI). Low synaptophysin levels showed an effective PSD enriched fraction isolation. **(B-D)** Scatter plot showing NR2B, PSD-95 and β-Actin levels in Ctrl and AD subjects (n=4-7 per group). *p<0.05, **p<0.01, ***p<0.001; paired Student's t test.

Regarding non-PSD fraction, we have observed again no changes in the β-Actin levels along of different disease stages (**Figure R21A** and **B**). However, it was observed a significant increment in synaptophysin expression of prefrontal cortex of AD patients at Braak II stage (**Figure R21A** and **C**).

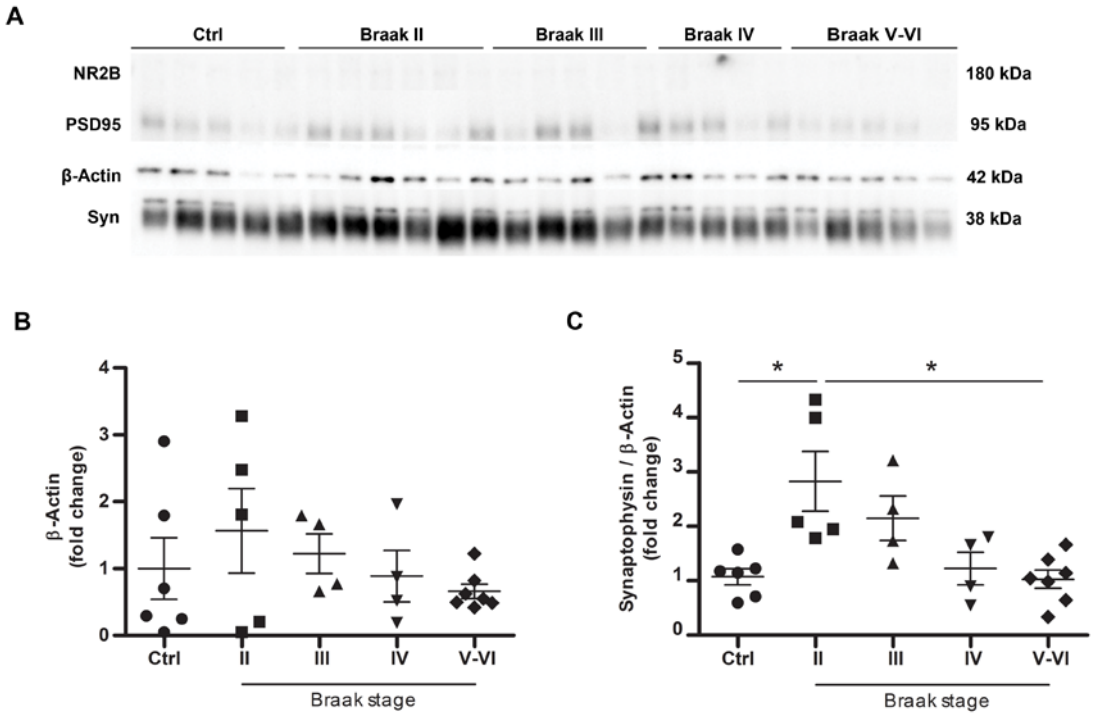

Figure R21. Prefrontal cortex from AD patients shows increased levels of synaptophysin at early stages. (A) Western blot of PSD-95, synaptophysin and β-Actin levels in control (Ctrl) and AD subjects classified according to Braak criteria. PSD-95 expression was not detected demonstrating and effective non-PSD enriched fraction isolation. **(B-C)** Scatter plot of β-Actin and synaptophysin levels in Ctrl and AD subjects (n=4-7 per group). *p<0.05; paired Student's t test.

In summary, analysis of synapse-enriched fractions of prefrontal cortex of healthy and AD individuals revealed a strong increase of NR2B, PSD-95 and synaptophysin levels at early stage (Braak II) of AD subjects compared to healthy individuals.

8. EGFP-Sindbis virus infected-CA1 neurons as a tool to evaluate spines and to analyze the dendritic complexity in organotypic hippocampal slice culture.

Synaptic failure is considered to be the first step of the cognitive decline and memory dysfunction in AD. Here, we showed that NR2B and synaptic protein levels are abnormally increased in Aβ-treated cultured neurons and at early stages in prefrontal cortex of AD patients. To complete these findings, we decided to analyze by high-resolution imaging the morphological dynamics of dendritic spines in hippocampal organotypic cultures that had been treated with Aβ. For that, we cultured hippocampal slices from wild type mice and slices were infected with the neurotropic Sindbis virus expressing EGFP (**Figure R22A**). Spines and dendrites were visualized by confocal high-resolution imaging and evaluated by 3DMA analysis (**Figure R22B**) and by an algorithm-based 3D reconstruction (**Figure R22C**), respectively.

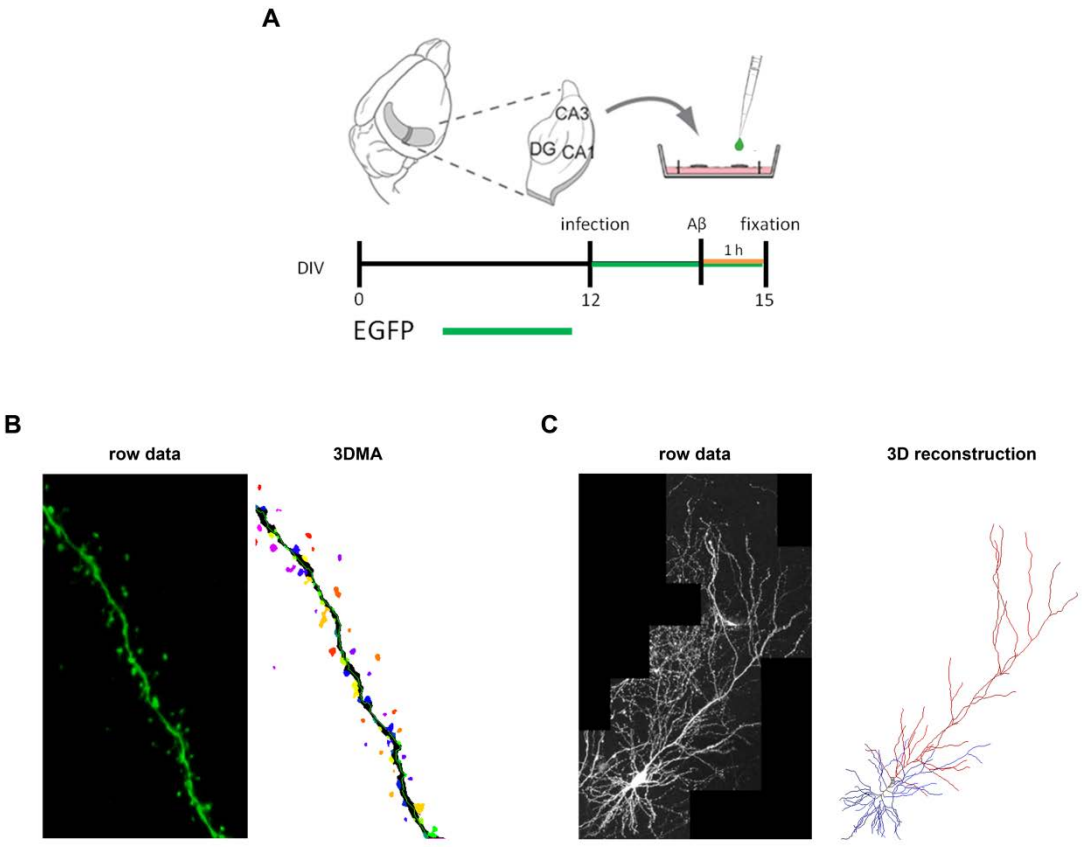

Figure R22. Analysis of spine and dendritic simplification in organotypic hippocampal slices. (A) Outline of the experimental approach. 400 μm-thick hippocampal sections were cultured using the membrane interface technique. Sindbis virus infection expressing EGFP was performed at day 12 *in*

vitro. Three days later, slices were treated with Aβ oligomers and fixed at day 15 *in vitro* as indicated on the time line. **(B)** Confocal image of dendrite from CA1 neurons (left) and 3DMA analysis (right), which permits measurement of different spine parameters are shown. **(C)** Images show a high resolution fluorescence micrograph of a CA1 pyramidal neuron after semi-automated stitching (left) and 3D reconstruction (right).

8.1. Aβ oligomers promote an increase in spine density through PKC and β1-integrin.

EGFP-expressing slices were treated with 1 μM Aβ oligomers for 1 h and spines were analysed. As shown in **Figure R23A**, quantitative analysis of cultures treated with Aβ oligomers clearly showed a significant increase in synaptic density compared to untreated neurons **Figure R23B** (1.24 ± 0.04 *vs* 1.03 ± 0.03). However, no significant differences were observed in the spine mean length (**Figure R23C**, 451.1 ± 11.2 *vs* 442.3 ± 12.56).

In this work, we have described that both cPKCs and β1-integrin actively participated in the signal transduction pathways emanated from Aβ in primary cortical neurons. Based on this, we analyzed the role of PKC and β1-integrin in spine alteration from Aβ-treated organotypic hippocampal cultures.

EGFP-expressing slices were pretreated with AIP (PKC inhibitor), IgM and CD29 antibodies (β1-integrin inhibitor) for 1h, treated with 1 μM Aβ oligomers for 1 hour and spines were analysed. As is shown in photographs (**Figure R23A)** and in quantitative analysis of the spine density (**Figure R23B**), pharmacological inhibition of PKC activity with AIP blocked the effect of Aβ on spine density of CA1 neurons (1.03 ± 0.03 *vs* 1.24 ± 0.04). Similar inhibition occurred when the β1-integrin activity was blocked by CD29 antibody, while no inhibition was observed with control antibody IgM (1.11 ±0.02 *vs* 1.28 ± 0.05). These results show that Aβ oligomers increased significantly the spine density of CA1 neurons in organotypic slices after 1 hour of peptide treatment. According to our previous findings, spine density increment induced by Aβ oligomers was prevented by AIP and CD29 inhibitors, confirming that PKC and β1-integrin participated in formation of new spines.

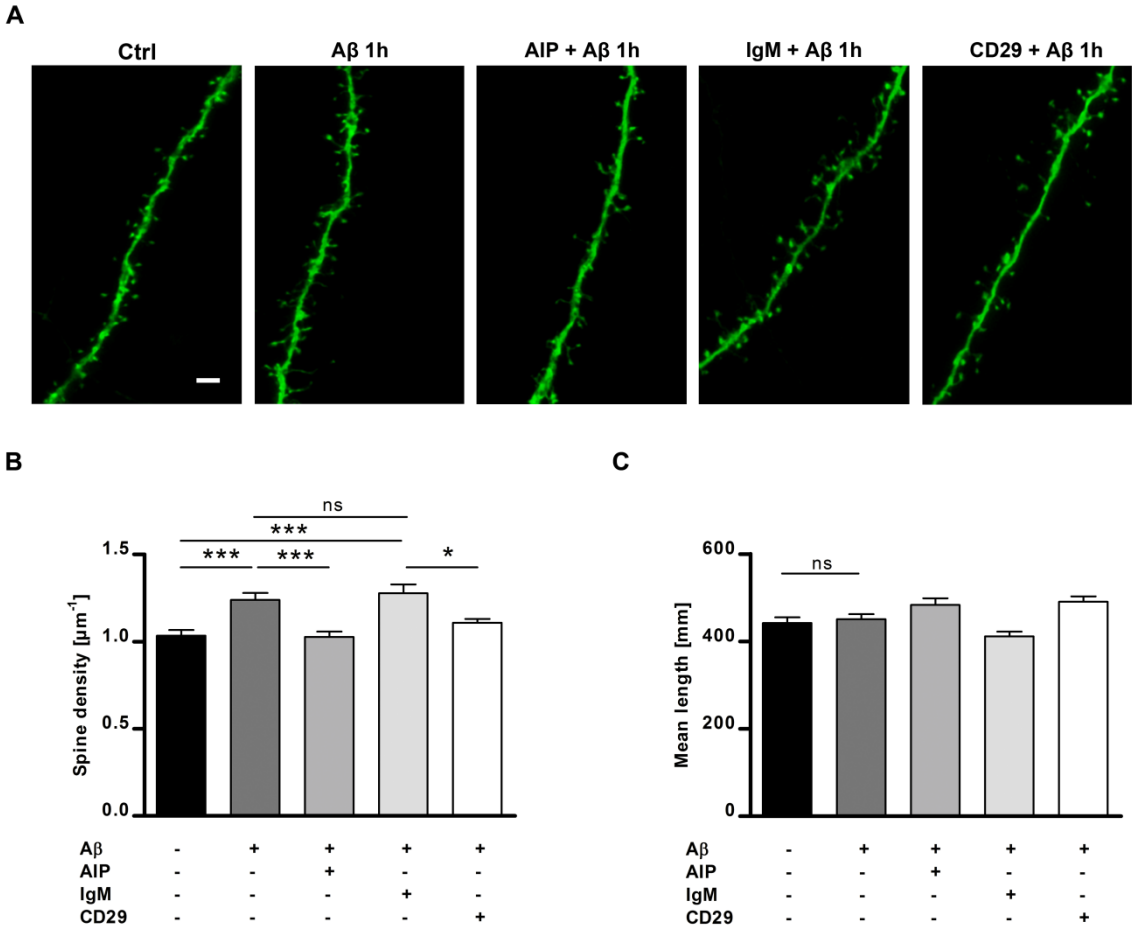

Figure R23. Hippocampal slices treated with Aβ oligomers show an increase in the total dendritic spine density, which is reverted with PKC and β1-integrin inhibitors. (A) Photographs show confocal images of apical dendritic segments from CA1 neurons in control condition and Aβ treatment in the presence of different inhibitors, AIP (PKC inhibitor) and CD29 (β1-integrin inhibitor). Scale bar, 2 μM. **(B)** Bar graph represents quantification of spine density in different cultures. **(C)** Quantitative bar graphs representing spine mean length. *p<0.05, ***p<0.001 compared to non-treated cells; paired one-way ANOVA.

Previous data indicated that spines are highly dynamic structures and that the relationship between structure and function is a positive correlation between spine size and synaptic strength. Three major classes based on the relative size of the spine head and neck can be distinguished: stubby, thin and mushroom (Tackenberg *et al.*, 2009 and Ebrahimi *et al.*, 2014). Therefore, a more in depth analysis was performed attending to spine morphological diversity in organotypic slices.

Figure R24A (bars 1 and 2) showed that the increase in spine density induced by Aβ was specific of stubby spines, as no significant changes were observed between control and Aβ treatment condition of thin and mushroom spines (**Figure R24B,** bars 1 and 2 and Figure **R24C**, bars 1 and 2). Moreover, PKC and β1-integrin inhibitors caused a strong reduction in stubby spine density (**Figure R24A**, bars 3, 4 and 5) while no effect of these molecules were observed in thin and mushroom spines type density (**Figures R24B**, bars 3, 4 and 5 and Figure **R24C**, bars 3, 4 and 5).

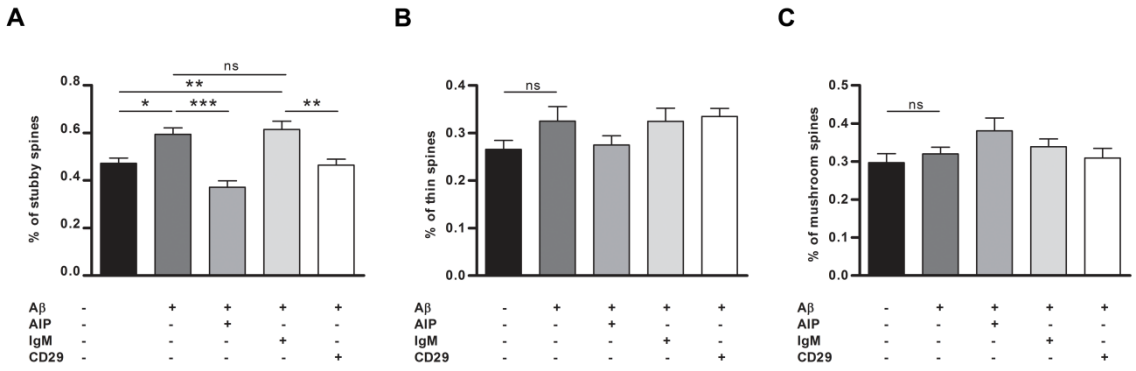

Figure R24. Aβ oligomers specifically increase the number of stubby spines, which is reverted blocking PKCs and/or β1-integrin pathways. (A-C) Bar graphs show quantification of stubby, mushroom and thin spine density after Aβ treatments. *p<0.05, **p<0.01, ***p<0.001 compared to non-treated cells; paired one-way ANOVA.

Altogether, these results suggest that an acute Aβ treatment produces an increase in stubby spine density in CA1 hippocampal neurons, which is mediated by both PKC and β1-integrin activities.

8.2. Aβ oligomers produce morphological changes promoting dendritic complexity in CA1 hippocampal neurons.

Alteration in dendritic arbor is a key feature of the neurodegenerative triad of AD. Therefore, in order to confirm the changes in the spine morphology, we investigated whether Aβ oligomers also affected dendritic arborization. To do this, we infected the organotypic hippocampal slice cultures with Sindbis virus-mediated

expressing EGFP and cultures were treated with 1 μM Aβ oligomers for 1h. Now, in order to obtain a quantitative assessment of Aβ-induced changes in total path length and number of branching points, an algorithm-based 3D reconstruction of whole CA1 neuron morphology was applied. As shown in **Figure R25A** Aβ treatment increased dendritic complexity in apical CA1 neurons compared to untreated cells.

Quantitative analysis of dendritic complexity in presence or absence of Aβ oligomers clearly showed a significant increase in both total path length (**Figure R25B**, from 2.35 mm ± 0.14 to 2.96 mm ± 0.29) and number of branching points (**Figure R25C**, from 21.33 mm ± 1.4 28.33 mm ± 3.5). However, no changes were observed in total path length or number of branching points in the basal part of CA1 neurons (**Figures R25D** and **E**).

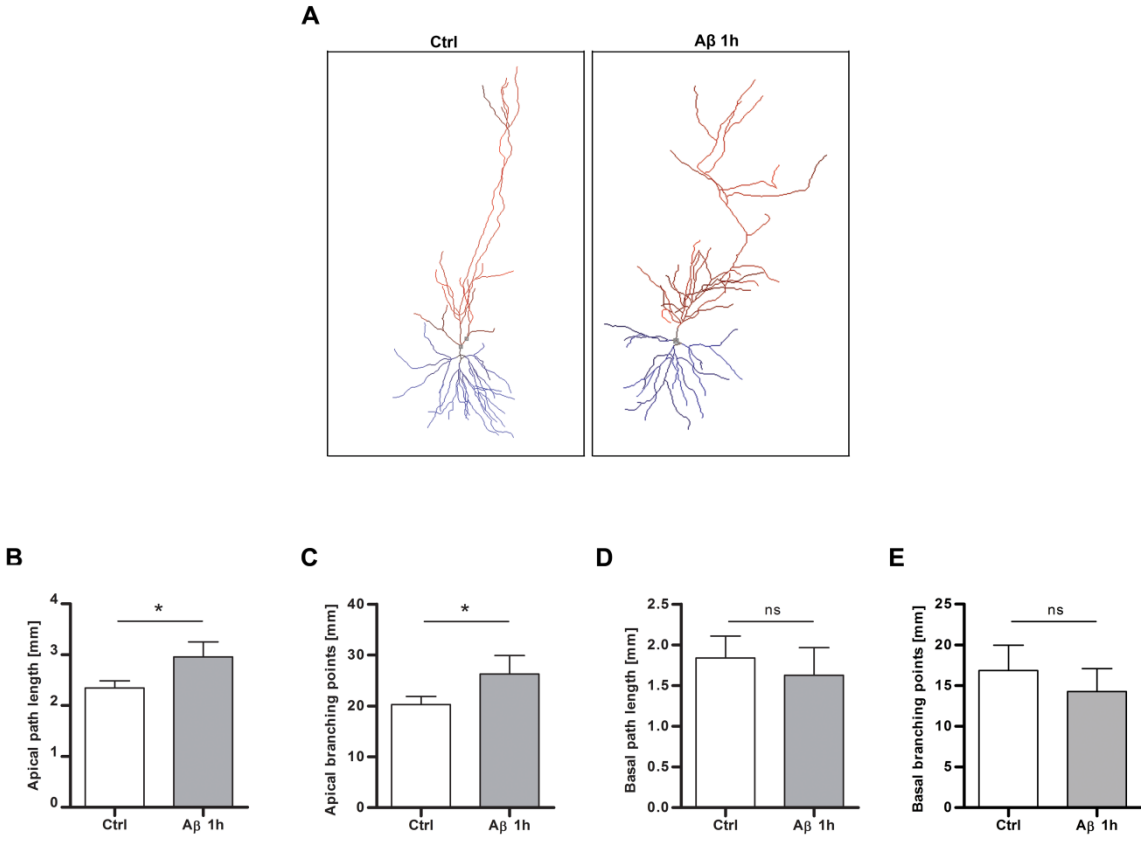

Figure R25. Effect of Aβ oligomers on dendrites of hippocampal neurons. (A) 3D reconstructions of representative CA1 neurons in untreated- and Aβ-treated cells. **(B-E)** Quantitative analysis of dendritic complexity as determined from apical path length **(B)**, apical branching points **(C)**, basal path length **(D)** and basal branching points **(E)** is shown. *p<0.05, compared to non-treated cells; paired Student`s t test.

Finally, since CA1 pyramidal neurons receive different inputs in specific subregions of the dendritic tree, we examined the subregional differences in the induction of dendritic complexity mediated by Aβ. For that, 3D Sholl analysis was performed on basal and apical branches to quantify changes in the intersection frequency of dendrites as a function of the distance from the cell body. We observed that, in the apical part, dendritic complexity was induced specifically in one segment of the tree which was localized at 15-25% of the total apical length, correlating with regions where most input from Schaffer collateral occurs (**Figure R26A**). In contrast, no changes in dendritic intersections localized in the basal part were found (**Figure R26B**).

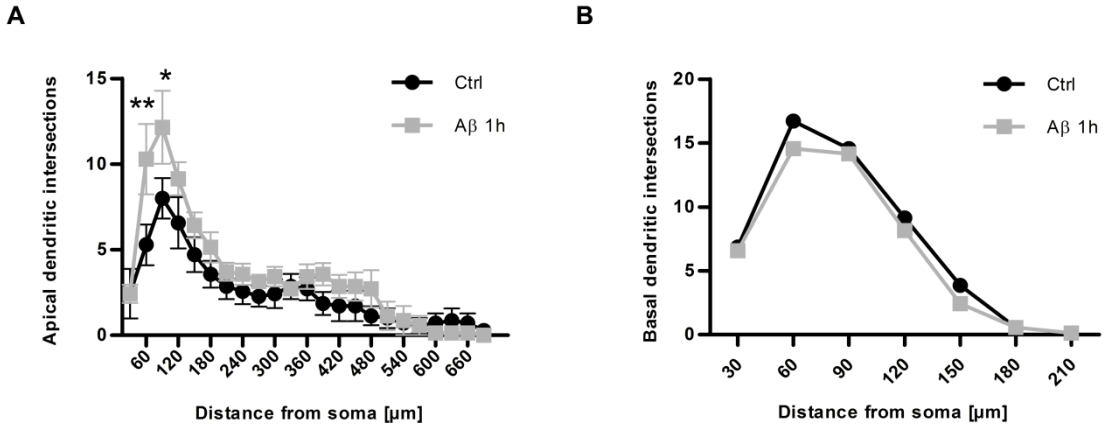

Figure R26. (A-B) Aβ oligomers induced dendritic complexity at sites of Schaffer collateral input. Sholl analysis of apical (A) and basal (B) parts of the dendritic tree in CA1 neurons after Aβ treatment is shown. *p<0.05, **p<0.01, compared to non-treated cells; paired two-way ANOVA.

Therefore, analysis of dendritic complexity based on a 3D reconstruction of the whole CA1 neuron morphology indicates an increase in the apical dendrite length and branching points, at sites of Schaffer collateral input.

Discussion

Alzheimer's disease is a progressive cognitive decline in mental function including memory, thinking, judgment, and the ability to learn. Several studies have demonstrated that amyloid β oligomers have a causal role in its pathogenesis promoting disturbances in glutamatergic neurotransmission and synapses. In the present study, we showed that soluble oligomeric Aβ differentially regulates NMDA receptor distribution and function, and promotes dendritic and spine complexity.

Specifically, we found that integrin β1 and classical PKCs were pivotal to the molecular pathways underlying this modulation. Interestingly, acute Aβ treatment differentially increased NR2B-containing NMDARs and postsynaptic PSD-95 in isolated synaptic terminals. In addition, Aβ oligomers increased NR2B subunit phosphorylation by mechanisms involving integrin β1 and classical PKCs and consequently caused an enhancement of Ca^{2+} permeability through extrasynaptic and synaptic NMDARs.

Moreover, analysis of isolated synaptic fractions purified from hippocampus of 3xTg-AD showed a synaptic protein deficit with a concomitant increase in NR2B, PSD-95 and synaptophysin protein expression levels at 6 months old. In humans, pre- and post-synaptosomal fractions purified from prefrontal cortex of control and AD patients exclusively exhibited an increase in NR2B and synaptic markers expression at early stages of AD (Braak II), but not at late stages (Braak III-IV). These findings suggested that synaptic changes governed by integrin β1 and classical PKCs could occur at early stages of the disease and contribute to pathogenesis of synaptic degeneration in AD.

Finally, we have developed and characterized a novel fusion protein composed of integrin β1 signal peptide and the glutathione S-transferase which interferes, both *in vitro* and *in vivo*, in the Aβ oligomers/Integrin β1 signaling program and reduces astrocyte stress and astrogliosis.

1. Aβ affects synaptic functions by modifying NR2A/NR2B subunit ratio.

Synaptic dysfunction is a critical pathological mechanism in AD that highly correlates with cognitive decline. NMDA receptor is a prime target for cognitive enhancement since it is centrally involved in synaptic plasticity, learning and memory,

and several studies indicate that NMDARs are critically involved in the Aβ-mediated disruption of neuronal function (Danysz & Parsons, 2012; Zhang *et al*., 2016). Classically, AD studies have been focused on understanding neuron death and synaptic loss. In this regard, it is well established that the overall expression level of NMDA receptors and synaptic proteins in AD is reduced (Gezen *et al*., 2018; Jang *et al*., 2014; Liu *et al*., 2010). Moreover, Müller and collaborators described that NR1, NR2A and NR2B subunits contribute to the Aβ-mediated decrease in the number of functional synapses (Müller *et al*., 2018). In agreement with these reports, our results show that a chronic treatment of Aβ oligomers decrease surface expression of NR2A and NR2B-containing receptors in cortical neurons, with the consequent decrease in Ca^{+2} influx through NMDA receptors. Therefore, Aβ oligomers have been characterized as a negative regulator of NMDAR expression. The loss of synaptic NMDARs and the decrease in intracellular Ca^{2+} influx may inhibit NMDAR-dependent LTP (Liang *et al*., 2017; Tu *et al*., 2014), contributing to the depression of glutamatergic transmission and reductions in memory formation. The important role of Aβ oligomers in synaptic dysfunction and neuronal loss in AD is indisputable.

However, our data support the notion of differential effects of Aβ oligomers on NMDARs over time. In relation to this, it has been described that Aβ oligomers increased the mRNA expression of NR2A and NR2B subunits of NMDARs (Karthick *et al*., 2018). Additionally, acute Aβ treatment produces an increase in the NR2B subunit located in the dendrites, suggesting that these structures, which are close to the soma, are in particular functionally sensitive to Aβ (Chang *et al*., 2016). Similarly, our results show that acute Aβ exposure mediates an increase in NR2B subunit density in the neuron membrane and in isolated synaptosomal fractions.

This observation leads us to propose that increased NR2B- over NR2A-subunits may implies increased Ca^{2+} influx modifications. Moreover, NR2 subunit composition of NMDARs determines their key properties, such as glutamate affinity, open probability and desensitization rate (Cull-Candy & Leszkiewicz, 2004; Paoletti *et al*., 2013), which makes the ratio of NR2A to NR2B an important factor in the Ca^{2+} response and synaptic plasticity (Foster *et al*., 2010). Accordingly, we observed that a

biological consequence of the Aβ-induced NR2B increase is a higher Ca^{2+} permeability through NMDARs.

2. Early modulation of NR2B subunit is related to survival and death pathways.

In relation to NMDAR location, these receptors play an important role in both synaptic function and excitotoxicity in the CNS (Wang *et al*., 2013). It is described that, in physiological conditions, synaptic NMDA receptors mediate Ca^{2+} influx. The increase in the intracellular Ca^{2+} concentration promotes the activation of CaMKIV, a kinase that phosphorylates nuclear CREB at Ser^{133} residue (Toth *et al*., 2016). This activation induces the expression of pro-survival genes such as BDNF, a main regulator of synaptic plasticity that regulates LTP (Leal *et al*., 2015) and protects neurons against apoptotic insults (Yan *et al*., 2016). In contrast, extrasynaptic NMDARs are associated with pro-death signaling pathways. Ca^{2+} ions that enter through the NMDA receptors located in the extrasynapsis mediate CREB and ERK inactivation by dephopshorylation, inhibiting the induction of BDNF expression. As a consequence, a loss of mitochondrial membrane potential and the expression of genes related to cell death occur (Wu *et al*., 2018). Since NR2A- containing NMDAR are mainly located in synaptic sites and receptors that contain NR2B are located in extraynaptic sites, numerous evidences indicate that NR2A mediates protective pathways while NR2B contributes to excytotoxic pathways. Given this, mechanisms of activation and inhibition of subunits have been proposed as a therapeutic strategy for AD (Huang *et al*., 2016). Here, we observed an enhanced Ca^{2+} permeability after a short treatment with Aβ in cultured neurons mainly produced at synaptic, but also at extrasynaptic locations. Therefore, Aβ-induced Ca^{2+} deregulation could be a consequence of higher availability of both synaptic and extrasynaptic NMDA receptors in the cell membrane, which may be related to activation of survival mechanisms together with neuronal death pathways. However, there are some evidences showing that activation of synaptic or extrasynaptic NMDAR alone is not neurotoxic, and that the degree of excitotoxicity depends on the magnitude and duration of synaptic- and extrasynaptic-NMDAR co-activation (Zhou *et al*., 2013). Further experiments should be performed to define the

contribution of synaptic and extrasynaptic NMDARs to excitotoxicity and survival pathways in neurons after oligomeric Aβ treatment.

Moreover, Ca^{2+} fluxes are known to mediate CaMKII translocation to the post-synaptic density, where it binds to NR2B subunit by high affinity and phosphorylates it at $Serine^{1303}$ residue (Tavalin & Colbran, 2017). In relation to this, we have found that Aβ leads to NR2B phosphorylation at $Serine^{1303}$ residue, suggesting that Aβ could regulate the NMDAR expression on membrane and activity by phosphorylation-mediated mechanisms. These results indicate that the increased cell surface expression of NR2B subunit could be caused by phosphorylation-induced trafficking deregulation.

3. Deregulated NMDAR subunits trafficking as a mechanism that contributes to Aβ-induced synaptic alteration.

The regulation system for the expression and maturation of NMDAR subunits is highly complex (Horak *et al*., 2014). It is well described that NR2A replaces NR2B as the primary NR2 subunit at synaptic sites during the second postnatal week in cortex and hippocampus. The timing for the switch varies for each region, but remarkably it is coincident with an increase in associative learning abilities, suggesting that this process is important for the refinement and fine tuning of neuronal circuits (McKay *et al*., 2018; Sun *et al*., 2018). In our data, we have observed that Aβ affects NR2B subunit density (typical of immature synapses) without affecting the density of the NR2A subunit (characteristic of mature synapses). Therefore, the Aβ-induced imbalance between the NR2A/NR2B ratio could reflect a tendency towards the creation of immature synapses. We postulate that this phenomenon could be an alteration induced by Aβ in the regulation of the trafficking and recycling system of the neuron, mechanisms that are severely affected in AD (Rajendran & Annaert, 2012).

Moreover, it is known that the decrease in the availability of membrane NMDA receptors, characteristic of AD, is related to an increase in the receptor

internalization. At molecular level, Aβ leads PP2B/ STEP signaling pathway activation and, as a consequence, NR2B is dephosphorylated at residue Tyr^{1472}. This dephosphorylation drives to the dissociation of the NR2B subunit with PSD-95 and protein clathrin adapter protein AP-2, producing receptor endocytosis (Snyder *et al*., 2005). In fact, a genetic reduction or pharmacological inhibition of STEP prevents the loss of NMDA receptors in synaptic membranes (Xu *et al*., 2018). In summary, Aβ involves phosphatases that cause a decrease of the receptor's availability in the membrane. According to these results, we have observed that Src protein tyrosine kinase family is dephospholyted on $Tyrosine^{416}$ after a short Aβ treatment indicating that Src kinase activity is decreased in this condition.

In contrast, we have observed that, under similar treatment of Aβ, PKCs are activated and phosphorylate NR2B subunit, so it could be a compensatory mechanism to avoid NR2B subunit dephosphorylation and NMDAR internalization from neuronal plasma membrane. PKC is an important component in signal transduction, and maintains an optimal balance between survival and apoptosis in Aβ-treated cortical neurons (Manterola *et al*., 2013). Therefore, PKC could be involved in the neurotoxicity induced by Aβ and in the neuronal degeneration of AD. In fact, a phosphoprotein study with *post-mortem* brains has identified the phosphorylation of PKC substrates as a primary early event in AD (Tagawa *et al*., 2015). In addition, it is known that several isozymes of PKC are involved in AD (Choi *et al*., 2011). In particular, an increase in the activity of the PKCα isoform contributes to AD, possibly through the action of the Aβ at synapses. Thus, it has been proposed that inhibition of PKCα can be considered as a therapy early in AD, and PKCα mutations could serve as a diagnosis for disease susceptibility (Alfonso *et al*., 2016)

Additionally, in parallel to NR2B subunit increase, we have also observed an increase on PSD-95 density in isolated synaptic terminals after a short Aβ treatment in neurons. The C-terminal of NR2 subunits has amino acid residues that recognize PDZ domains. Proteins that present these PDZ domains not only facilitate the association of NMDARs in clusters on the cell surface, but as with NR1, they can contribute to their

stability by masking the internalization domains (Kaniakova *et al*., 2012). An imbalance in the density of both proteins, NR2B subunits and the associated proteins, in our case PSD-95, could contribute to mask the internalization signal region of the NR2B subunit and that could justify the presence of these subunits in the cellular membrane.

Taken together, these results suggest that Aβ exerts complex and distinct regulatory effects on the trafficking of NR2A and NR2B, as well as on their synaptic localization.

4. Oligomeric Aβ promotes synaptic changes and gliosis by activation of β1-integrin receptor.

Several studies postulate various possible receptors involved in the toxicity of Aβ oligomers. Such receptors are rather localized at neuronal synapses and should have a high affinity for Aβ and the ability to transduce extracellular triggering factors into certain intracellular changes (Mroczko *et al*., 2018). For example, it has been described that Aβ directly activates the NMDA receptor, altering its physiological function (Texidó *et al*., 2011). Among more than 20 postulated receptors, it has been reported that the interaction between integrins and Aβ promotes neurotoxicity and inhibition of LTP (Wang *et al*., 2008). Recently, Donner *et al*. have described that synthetic Aβ monomer binds to the α2bβ3 integrin through the amino acid sequence RHDS, being directly related to cerebral amyloid angiopathy (CAA) which contribute to dementia and AD (Donner *et al*., 2016, 2018).

In agreement with these reports, we have observed using a pharmacological approach that Aβ oligomers lead NR2B subunit upregulation on neuronal membranes through PKC signaling pathway. This connection between Aβ oligomers, PKC and NR2B subunit is established by integrin β1. On other words, integrin β1 transduces the message that Aβ oligomers brings, in order to mediate a cellular response which manifests itself in a higher permeability for calcium ions and to finally alter the cellular homeostasis. These results corroborate the previous findings that, we and others, have described showing a key molecular relationship between integrin β1 and Aβ peptides

required to modulate neuronal and glial physiology (Wang *et al*., 2008,Wyssenbach *et al*., 2016). Specifically in astrocytes, Aβ oligomers via integrin β1 causes and exacerbates ROS-dependent astroglial reactivity (Wyssenbach *et al*., 2016). Going further, we planned to identify the integrin β1 extracellular region responsible to bind Aβ oligomers. We constructed and expressed a series of recombinant integrin β1 fused to the glutathione S-transferase and we realized that the minimal region of this interaction is comprising from aa 1 to aa 20, corresponding to the signal peptide (Rs). Moreover, this peptide had a functional activity not only *in vitro*, since it was able to block Aβ oligomer-induced small GTPase Rac 1 activation, ROS generation, and reduced astrogliosis in primary cultures of astrocytes. But also when we directly injected this Rs peptide in the mice brain, the astrogliosis induced by Aβ oligomers was also efficiently reduced. We postulate that the molecular mechanism by which this recombinant Rs peptide works to block the Aβ oligomer message is because the presence of this recombinant peptide in the extracellular medium interfers in the natural binding between Aβ oligomers and its receptor integrin β1. This point is very important since, in this situation, the integrin β1 presented in the cell membrane is accessible to physiological activators, this means that the Rs peptide protects the functional receptorial properties of the integrin β1.

At this time, there are not much advances in the field of therapy against AD, and this peptide opens a new avenue in the pharmacology focused on the AD. The novelty of this peptide is that it allows to attack the Aβ oligomer problem from outside the cell, preventing the toxic peptide modifies cellular signaling. In any case, and before arriving at the therapeutic area, we have developed a tool that it will allow us to understand both *in vitro* an *in vivo* the molecular mechanisms that the Aβ oligomers requires to implement its action.

Integrins are involved in signaling pathways in which molecules such as the tyrosine kinases FAK, ILK and Src or small GTPases of the Rho family play important roles. Under physiological conditions, these proteins participate actively in proliferation, survival or cell migration mediated by the activation of integrins (Fourel *et al*., 2016). In addition, PKCs may also be involved in the integrin-mediated signaling

(Fogh *et al*., 2014). In fact, we have observed that the phosphorylation of PKC induced by Aβ is mediated by the β1-integrin. Therefore, this membrane receptor mediates the Aβ-induced abnormal NR2B density in the membrane.

5. Aβ/Integrin β1 /PKC signaling regulates spine density in hippocampal neurons.

In relation to Aβ and PKC activation in neurons, Manterola and collaborators have shown that the connection between both molecules is established through PDK1. In addition, once activated the PKC, it mediates the activation of Rho, a small GTPase of the Rac1 family, activating the neuronal death program. Rho family GTPases play an essential role in the control of the reorganization of the actin cytoskeleton in response to extracellular signals, among other functions (Manterola *et al*., 2013). On the other hand, it is known that PSD-95 colocalizes with F-actin, serving as an anchor for NMDA receptors in the cell membrane, and a decrease in the levels of both proteins produces an impairment in the actin polymerization in postsynaptic sites, with pathological consequences in the state of dendritic spines (Mota *et al*., 2014). Loss of dendritic spines and changes in its shape and size are common abnormalities found in human AD brain (Baloyannis *et al*., 2011). Currently, most data suggest that increased levels of soluble oligomeric Aβ are the major factor in spine alterations (Tackenberg *et al*., 2009), and other results indicate that a chronic Aβ exposure causes a gradual change in the spine morphology from mushroom to stubby (Golovyashkina *et al*., 2015).

Accordingly, our results suggest that Aβ mediates an increase in the ability to form spines, which could explain the neuron capacity to host a greater number of NMDA receptors. This effect could be a consequence of an abnormal process in the actin polymerization. In relation to this, we have observed that an acute Aβ treatment produces an increase in the density of stubby dendritic spines. Spines with this morphology are present in numerous brain regions and are abundant during the development of the CNS, when the spines have a filopodium-like morphology with few

organelles and without a differentiated neck. This type of morphology is highly dynamic and can be retracted or extended in minutes after a chemical stimulation. Stubby spines are considered as immature synapses spines, so they are not directly related to learning and memory functions, unlike thin and mushroom spine types. According to this, the increase in stubby spine density that we observe could be related to a synaptic deregulation produced by Aβ and modulated by molecular mechanisms downstream integrin β1 and PKC activation involving actin polymerization.

In addition to spine changes, AD is accompanied by a dendritic simplification related to a brain dysfunction. In fact, it has been observed a reduction of total dendritic path length by about 40% in principal neurons of the CA1 region. This dendritic simplification is induced by Aβ and mediated by tau through NMDA receptor activation (Golovyashkina *et al*., 2015). It has also been shown that RhoA signaling pathway regulates the formation of Golgi outposts that contributes to dendritic growth and branch dynamics (Quassollo *et al*., 2015). In the case of a short treatment with Aβ, we observed a greater dendritic arborization in neurons of the CA1 region, possibly induced by a regulation of cytoskeletal dynamics. Interestingly, the zone where more dendritic complexity is produced corresponds to the sites of collateral Schaffer inputs, where LTP occurs.

Increased understanding of these early events in Aβ-induced synaptic dysfunction is likely to be important for the development of timely preventive and therapeutic interventions.

6. Synaptic alteration in young 3xTg- AD mouse model.

Several transgenic animal models, genetically predisposed to develop Alzheimer's disease-like pathology, have been engineered to facilitate the study of disease pathophysiology. The triple transgenic mouse model of AD (3xTg-AD) harbors three AD-related genetic loci: human PS1M146V, human APPswe, and human tauP301L.

These mice develop both amyloid plaques and neurofibrillary tangle-like pathology in a progressive and age-dependent manner, while these pathological hallmarks are predominantly restricted to the hippocampus, amygdala, and the cerebral cortex, the main areas of AD neuropathology in humans. This model represents, at present, one of the most advanced preclinical tools available and is being employed ever increasingly in the study of mechanisms underlying AD.

Aβ deposition is progressive, with intracellular immunoreactivity detected in some brain regions as early as three to four months of age. Extracellular Aβ deposits appear by six months in the frontal cortex and become more extensive by twelve months. Changes in tau occur later; by 12 to 15 months, aggregates of conformationally-altered and hyperphosphorylated tau are detected in the hippocampus. Synaptic dysfunction, including LTP deficits, manifests in an age-related manner, but before plaque and tangle pathology (Billings *et al*., 2005; Oddo *et al*., 2003, 2006).

We compared 1- and 6-month-old 3xTg-AD mice to determine if there was an age-related alteration in synaptic markers and NR2B subunit expression in the hippocampal region. Basal synaptic transmission and LTP was severely impaired in 3xTg-AD mice by 6 months of age. One-month-old 3xTg-AD mice did not exhibit deficits in total protein concentration of pre- and post-synaptic fractions. Likewise, no differences in NR2B subunit, PSD-95 or synaptophysin were observed in 3xTg-AD mice at 1 month of age. At 6 months of age, total protein concentration was significantly decreased in comparison with wild-type mice, which correlates with the synaptic dysfunction and LTP deficits already apparent at this age. However, NR2B, PSD-95 and synaptophysin proteins were selectively upregulated in isolated pre- and post-synaptic fractions of hippocampus. Further studies will be necessary to understand the contribution of enhanced expression of pre and postsynaptic proteins in remaining active synapses in 3xTg-AD mice.

Importantly, we propose that this synaptic alteration is an early change that precedes the accumulation of the hallmark pathological lesions. Although this remains speculative at the moment, we hope that these observations will encourage further

studies in order to test whether synaptic activity is modified at early stages of the disease.

7. Alzheimer's disease patients present an increment of NR2B subunit, PSD-95 and synaptophysin levels in prefrontal cortex at early stages of disease (Braak II).

Human biological samples are increasingly important resources for biomedical research. In AD, the study with *post-mortem* brain tissue of AD patients and controls has revealed that NMDA receptors are negatively affected by aging and by AD (Geddes *et al*., 1986; Thorns *et al*., 1997), and most reports suggest that there is a decrease in protein and mRNA levels of these receptors (Hynd *et al*., 2004; Mishizen-Eberz *et al*., 2004) and synaptic markers (Keleshian *et al*., 2013) at least in later stages of the disease.

In agreement with our previous *in vitro* data, we focused our study on analyzing NR2B and synaptic markers in prefrontal cortex (one of the main affected areas in AD brains) of control subjects and AD patients at different stages of the pathology. We have found that, at early stages of AD (Braak II), NR2B expression levels are elevated without a significant change in the total synaptic protein levels. These results are consistent with some studies that describe an increase in synaptic activity in individuals with mild cognitive impairment (Hynd *et al*., 2004; Sze *et al*., 2001). In addition, a study performed with *post-mortem* samples of patients with AD describes that the NMDA receptor subunits are differently affected during the progression of the disease. Specifically, the authors have observed that both the mRNA and protein levels of the NR1 and NR2B subunits are increased at the early stages of the disease, mainly in the granular cells of the dentate gyrus. However, NR2A levels remain constant (Mishizen-Eberz *et al*., 2004)

The increase of the NR2B subunit can occur as a response mechanism to an imbalance in extracellular Aβ levels in the first stages of the disease. With the progression of AD, the concentration of Aβ increases disproportionately and ends up

producing deterioration in the glutamatergic system and in the synapse. Therefore, the determination of these parameters at different stages of the disease, as we have done in this work, is fundamental to characterize the protein expression pattern. Otherwise, the results obtained from the analysis of samples from *post-mortem* patients show a lot of variability. Therefore, it is important to separate the samples based on the different stages of the disease according to the Braak classification.

In the present work we also study the expression of synaptic markers (synaptophysin and PSD-95) in the frontal cortex of controls and patients with AD. We observed that both synaptophysin (pre-synaptic marker) and PSD-95 (post-synaptic marker) expression levels were increased at Braak II stage of the disease, and decreased throughout progression of AD. Similarly, a significant increase in the number of neuronal profiles stained for PSD-95 and NR1 in AD patients was described. These changes in neuronal profiles appear more prominently in the middle 3 to 5 layers, while little changes were observed for the intensity of puncta (Leuba *et al*., 2014).

8. Exploring biomarkers for Alzheimer's disease.

NMDARs have sustained high interest as CNS therapeutic targets because these receptors significantly contribute to acute and chronic neuropathologies. In AD, the gradual decrease in NR2B subunit expression during the disease underlies the cognitive decline that is often observed in aging individuals. Nevertheless, therapies presumably would be most effective in the early stages of the disease and, therefore, we have focused our interest in the Aβ- induced increase of NR2B subunit density in synaptosomes as a therapeutic target at early stages of AD.

On the other hand, increased levels of PSD-95 at early stages of AD could have a beneficial effect to protect synapses or enhance synaptic formation. However, PSD-95 accumulation might rapidly become a marker of learning impairment (Nyffeler *et al*., 2007) and later of pathological events. Therefore, the altered distribution of PSD-95 could also be considered as pathological marker in AD.

Indeed, NR2B and PSD-95 proteins represent an early therapeutic target, and could be considered as pathological markers in the diagnostic of AD. Identification of individuals in the preclinical stages of AD is essential for the timely administration of disease modifying therapies. Therefore, a more profound and detailed study of these postsynaptic markers may remain as an actively investigated strategy to attenuate AD.

Conclusions

1. Short-term treatment with Aβ oligomers promotes specifically the incorporation of NR2B-containing NMDA receptors to synaptic terminals together with PSD-95 scaffolding protein and, moreover, enhances NMDA-mediated Ca^{2+} influx.

2. Changes in synaptic NR2B-containing NMDA receptors location and function require intracellular mechanisms involving integrin β1 and PKC activities.

3. Activation of integrin β1 and classical PKC isoforms by Aβ oligomers targets the NMDA receptor subunit NR2B on $Serine^{1303}$, which is a critical residue that stabilizes NMDAR on membrane surface.

4. 6-month-old 3xTg-AD mice show synaptic protein deficits concomitant with enhanced expression of NR2B subunit, PSD-95 and synaptophysin proteins in isolated synaptic terminals of hippocampus.

5. The prefrontal cortex of AD human samples reveals an abnormal increase of NR2B and synaptic proteins in both pre- and post-synaptic sites at early stages (Braak II stage) of the disease.

6. Evaluation of spine morphology in an ex vivo model of organotypic hippocampal slice cultures reveals an Aβ-mediated rapid increase in the dendritic spine density, specifically the stubby structures, in an integrin β1/classical PKC signalling pathway dependent manner.

7. 3D reconstruction of the dendritic arborization of the whole CA1 neuron morphology after a short-term treatment with Aβ oligomers establishes an increase in the apical dendrite length and branching points. Dendritic arborization occurs mostly at Schaffer collateral synapses.

8. A recombinant integrin β1 signal peptide fused to the glutathione S-transferase (GST-Rs) prevents astroglial stress and astrogliosis in Aβ-injected hippocampal dentate gyrus area of adult mouse brain.

Altogether, these results revealed that acute Aβ oligomers treatment alters the NMDA receptor subunit composition and consequently their functions in neurons. These modifications are facilitated by the active participation of the Integrin β1 and classical PKCs. This molecular program governed by Aβ oligomers promotes an increase in spine density and dendritic complexity of hippocampal neurons. Similarly, synaptic changes have been observed at early stages of AD brains. The abnormal presence of both NR2B and PSD95 in AD patients at early stages could be taken as potential new biomarkers for this pathology. The relevance of these findings to AD initiation warrants further investigation.

Bibliography

Ahmedah, H. T., Patterson, L. H., Shnyder, S. D., & Sheldrake, H. M. (2017). RGD-binding integrins in head and neck cancers. *Cancers*, *9*(6), 1–17.

Alberdi, E., Sánchez-Gómez, M. V., Cavaliere, F., Pérez-Samartín, A., Zugaza, J. L., Trullas, R., … Matute, C. (2010). Amyloid β oligomers induce Ca2+ dysregulation and neuronal death through activation of ionotropic glutamate receptors. *Cell Calcium*, *47*(3), 264–272.

Alfonso, S. I., Callender, J. A., Hooli, B., Antal, C. E., Mullin, K., Sherman, M. A., … Malinow, R. (2016). promote synaptic defects in Alzheimer ' s disease, *9*(427), 1–18.

Ali, D. W., & Salter, M. W. (n.d.). Ali_NMDAR regulation by Src_2001, 336–342.

Antal, C. E., & Newton, A. C. (2014). Tuning the signalling output of protein kinase C. *Biochemical Society Transactions*.

Antonio Sanz-Clemente, Roger A. Nicoll, & Katherine W. Roche. (2013). Diversity in NMDA receptor composition: many regulators, many consequences. *Neuroscientist*, *19*(1), 62–75.

Bading, H. (2017). Therapeutic targeting of the pathological triad of extrasynaptic NMDA receptor signaling in neurodegenerations. *The Journal of Experimental Medicine*, jem.20161673.

Baez, M. V., Cercato, M. C., & Jerusalinsky, D. A. (2018). NMDA receptor subunits change after synaptic plasticity induction and learning and memory acquisition. *Neural Plasticity*, *2018*.

Baloyannis, S. J., Manolides, S. L., & Manolides, L. S. (2011). Dendritic and spinal pathology in the acoustic cortex in Alzheimer's disease: Morphological estimation in Golgi technique and electron microscopy. *Acta Oto-Laryngologica*, *131*(6), 610–612.

Bao, F., Wicklund, L., Lacor, P. N., Klein, W. L., Nordberg, A., & Marutle, A. (2012). Different β-amyloid oligomer assemblies in Alzheimer brains correlate with age of disease onset and impaired cholinergic activity. *Neurobiology of Aging*, *33*(4), 825.e1-825.e13.

Bard, L., Sainlos, M., Bouchet, D., Cousins, S., Mikasova, L., Breillat, C., … Groc, L. (2010). Dynamic and specific interaction between synaptic NR2-NMDA receptor and PDZ proteins. *Proceedings of the National Academy of Sciences*, *107*(45), 19561–19566.

Bard, L., & Groc, L. (2011). Glutamate receptor dynamics and protein interaction: Lessons from the NMDA receptor. *Molecular and Cellular Neuroscience*, *48*(4), 298–307.

Bernard-Trifilo, J. A., Kramár, E. A., Torp, R., Lin, C. Y., Pineda, E. A., Lynch, G., & Gall, C. M. (2005). Integrin signaling cascades are operational in adult hippocampal synapses and modulate NMDA receptor physiology. *Journal of Neurochemistry*,

93(4), 834–849.

Billings, L. M., Oddo, S., Green, K. N., McGaugh, J. L., & LaFerla, F. M. (2005). Intraneuronal Aβ causes the onset of early Alzheimer's disease-related cognitive deficits in transgenic mice. *Neuron*, *45*(5), 675–688.

Bourne, J. N., Harris, K. M., Andre, J. S., Albanos, K., & Reilly, S. (2008). NIH Public Access. *Brain*, *1135*(May 2006), 47–67.

Bu, G. (2009). Apolipoprotein E and its receptors in Alzheimer's disease: pathways, pathogenesis and therapy. *Nature Reviews Neuroscience*, *10*(5), 333–344.

Burgess, A., Shah, K., Hough, O., & Hynynen, K. (2016). HHS Public Access, *15*(5), 477–491.

Carroll, R. C., & Zukin, R. S. (2002). NMDA-receptor trafficking and targeting: Implications for synaptic transmission and plasticity. *Trends in Neurosciences*, *25*(11), 571–577.

Chan, C., Weeber, E. J., Zong, L., Fuchs, E., Sweatt, J. D., & Davis, L. (2008). β1-Integrins Are Required for Hippocampal AMPA Receptor synaptic transmission.pdf, *26*(1), 223–232.

Chang, L., Zhang, Y., Liu, J., Song, Y., Lv, A., Li, Y., … Wu, Y. (2016). Differential Regulation of N-Methyl-D-Aspartate Receptor Subunits is An Early Event in the Actions of Soluble Amyloid-β1-40Oligomers on Hippocampal Neurons. *Journal of Alzheimer's Disease*, *51*(1), 197–212.

Chanpimol, S., Seamon, B., Hernandez, H., Harris-love, M., & Blackman, M. R. (2017). HHS Public Access, 45–52.

Cheah, M., & Andrews, M. (2018). Integrin Activation: Implications for Axon Regeneration. *Cells*, *7*(3), 20.

Cheignon, C., Tomas, M., Bonnefont-Rousselot, D., Faller, P., Hureau, C., & Collin, F. (2018). Oxidative stress and the amyloid beta peptide in Alzheimer's disease. *Redox Biology*, *14*(October 2017), 450–464.

Chen, B. S., & Roche, K. W. (2007). Regulation of NMDA receptors by phosphorylation. *Neuropharmacology*, *53*(3), 362–368.

Chico, L. K., Van Eldik, L. J., & Watterson, D. M. (2009). Targeting protein kinases in central nervous system disorders. *Nature Reviews Drug Discovery*, *8*(11), 892–909.

Choi, D. S., Kim, T., & Hinton, D. J. (2011). Protein kinase C-regulated Aβ production and clearance. *International Journal of Alzheimer's Disease*, *2011*.

Chung, H. J. (2004). Regulation of the NMDA Receptor Complex and Trafficking by Activity-Dependent Phosphorylation of the NR2B Subunit PDZ Ligand. *Journal of Neuroscience*, *24*(45), 10248–10259.

Ciechanover, A., & Iwai, K. (2004). The ubiquitin system: From basic mechanisms to the

patient bed. *IUBMB Life*, *56*(4), 193–201.

Cingolani, L. A., Thalhammer, A., Yu, L. M. Y., Catalano, M., Colicos, M. A., & Goda, Y. (2009). NIH Public Access. *Receptor*, *58*(5), 749–762.

Cruts, M., Hendriks, L., & Van Broeckhoven, C. (1996). The presenilin genes: a new gene family involved in Alzheimer disease pathology. *Human Molecular Genetics*, *5 Spec No*, 1449–1455.

Cull-Candy, S. B. and M. F. (2001). NMDA receptor subunits : diversity , development and disease Stuart Cull-Candy * , Stephen Brickley and Mark Farrant. *Current Opinion in Neurobiology*, *11*, 327–335.

Cull-Candy, S. G., & Leszkiewicz, D. N. (2004). Role of Distinct NMDA Receptor Subtypes at Central Synapses. *Science Signaling*, *2004*(255), re16-re16.

Danysz, W., & Parsons, C. G. (2012). Alzheimer's disease, β-amyloid, glutamate, NMDA receptors and memantine - Searching for the connections. *British Journal of Pharmacology*, *167*(2), 324–352.

Demuro, A., Mina, E., Kayed, R., Milton, S. C., Parker, I., & Glabe, C. G. (2005). Calcium Dysregulation and Membrane Disruption as a Ubiquitous Neurotoxic Mechanism of Soluble Amyloid Oligomers. *Journal of Biological Chemistry*, *280*(17), 17294–17300.

Donner, L., Fälker, K., Gremer, L., Klinker, S., Pagani, G., Ljungberg, L. U., … Elvers, M. (2016). Platelets contribute to amyloid-b aggregation in cerebral vessels through integrin αIIbβ3-induced outside-in signaling and clusterin release. *Science Signaling*, *9*(429), 1–17.

Donner, L., Gremer, L., Ziehm, T., Gertzen, C. G. W., Gohlke, H., Willbold, D., & Elvers, M. (2018). Relevance of N-terminal residues for amyloid-β binding to platelet integrin αIIbβ3, integrin outside-in signaling and amyloid-β fibril formation. *Cellular Signalling*, *50*, 121–130.

Duguid, I. C. (2013). Presynaptic NMDA receptors: Are they dendritic receptors in disguise? *Brain Research Bulletin*, *93*, 4–9.

Ehlers, M. D. (2003). Activity level controls postsynaptic composition and signaling via the ubiquitin-proteasome system. *Nature Neuroscience*, *6*(3), 231–242.

Fan, X., Jin, W. Y., & Wang, Y. T. (2014). The NMDA receptor complex: a multifunctional machine at the glutamatergic synapse. *Frontiers in Cellular Neuroscience*, *8*(June), 1–9.

Ferreira, J. S., Papouin, T., Ladépêche, L., Yao, A., Langlais, V. C., Bouchet, D., … Groc, L. (2017). Co-agonists differentially tune GluN2B-NMDA receptor trafficking at hippocampal synapses. *ELife*, *6*, 1–22.

Ferreira, S. T., Lourenco, M. V., Oliveira, M. M., & De Felice, F. G. (2015). Soluble amyloid-Î^2 oligomers as synaptotoxins leading to cognitive impairment in Alzheimerâ€^{TM}s disease. *Frontiers in Cellular Neuroscience*, *9*(May), 1–17.

Fetterolf, F., & Foster, K. A. (2011). Regulation of long-term plasticity induction by the channel and C-terminal domains of GluN2 subunits. *Molecular Neurobiology*, *44*(1), 71–82.

Fogh, B. S., Multhaupt, H. A. B., & Couchman, J. R. (2014). Protein Kinase C, Focal Adhesions and the Regulation of Cell Migration. *Journal of Histochemistry and Cytochemistry*, *62*(3), 172–184.

Fong, D. K., Rao, A., Crump, F. T., & Craig, A. M. (2002). Rapid synaptic remodeling by protein kinase C: reciprocal translocation of NMDA receptors and calcium/calmodulin-dependent kinase II. *Journal of Neuroscience*, *22*(6), 2153–2164.

Foster, K. A., Mclaughlin, N., Edbauer, D., Phillips, M., Constantine-paton, M., & Sheng, M. (2010). NIH Public Access. *J. Neurosci.*, *30*(7), 2676–2685.

Fourel, L., Valat, A., Faurobert, E., Guillot, R., Bourrin-Reynard, I., Ren, K., … Albiges-Rizo, C. (2016). β3 integrin-mediated spreading induced by matrix-bound BMP-2 controls Smad signaling in a stiffness-independent manner. *Journal of Cell Biology*, *212*(6), 693–706.

Fu, M., Yu, X., Lu, J., & Zuo, Y. (2012). Repetitive motor learning induces coordinated formation of clustered dendritic spines in vivo. *Nature*.

Galais, C., & Lorenzini, J. (2017). Half a Loaf Is (Not) Better Than None: How Austerity-Related Grievances and Emotions Triggered Protests in Spain. *Mobilization: An International Quarterly*, *22*(1), 77–95.

Geddes, J. W., Chang-Chui, H., Cooper, S. M., Lott, I. T., & Cotman, C. W. (1986). Density and distribution of NMDA receptors in the human hippocampus in Alzheimer's disease. *Brain Research*, *399*(1), 156–161.

Gezen-Ak, D., Atasoy, İ. L., Candaş, E., Alaylıoğlu, M., & Dursun, E. (2018). The Transcriptional Regulatory Properties of Amyloid Beta 1–42 may Include Regulation of Genes Related to Neurodegeneration. *NeuroMolecular Medicine*, *20*(3), 363–375.

Gianni, D., Zambrano, N., Bimonte, M., Minopoli, G., Mercken, L., Talamo, F., … Russo, T. (2003). Platelet-derived growth factor induces the β-γ-secretase-mediated cleavage of Alzheimer's amyloid precursor protein through a Src-Rac-dependent pathway. *Journal of Biological Chemistry*, *278*(11), 9290–9297.

Gibb, A. J., Ogden, K. K., McDaniel, M. J., Vance, K. M., Kell, S. A., Butch, C., … Traynelis, S. F. (2018). A structurally derived model of subunit-dependent NMDA receptor function. *Journal of Physiology*, *596*(17), 4057–4089.

Gipson, C. D., & Olive, M. F. (2017). Structural and functional plasticity of dendritic spines – root or result of behavior? *Genes, Brain and Behavior*, *16*(1), 101–117.

Glabe, C. C. (2005). Amyloid accumulation and pathogensis of Alzheimer's disease: significance of monomeric, oligomeric and fibrillar Abeta. *Sub-Cellular*

Biochemistry, *38*, 167–177.

Glasgow, N. G., Siegler Retchless, B., & Johnson, J. W. (2015). Molecular bases of NMDA receptor subtype-dependent properties. *Journal of Physiology*, *593*(1), 83–95.

Glenner, G. G., & Wong, C. W. (1984a). Alzheimer's disease: initial report of the purification and characterization of a novel cerebrovascular amyloid protein. *Biochemical and Biophysical Research Communications*, *120*(3), 885–890.

Glenner, G. G., & Wong, C. W. (1984b). Alzheimer's disease and Down's syndrome: sharing of a unique cerebrovascular amyloid fibril protein. *Biochemical and Biophysical Research Communications*, *122*(3), 1131–1135.

Gmel, G. (2010). NIH Public Access. *Europe*, *104*(9), 1487–1500.

Goate, A., Chartier-Harlin, M.-C., Mullan, M., Brown, J., Crawford, F., Fidani, L., … Hardy, J. (1991). Segregation of a missense mutation in the amyloid precursor protein gene with familial Alzheimer's disease. *Nature*, *349*(6311), 704–706.

Goebel-Goody, S. M., Davies, K. D., Alvestad Linger, R. M., Freund, R. K., & Browning, M. D. (2009). Phospho-regulation of synaptic and extrasynaptic N-methyl-d-aspartate receptors in adult hippocampal slices. *Neuroscience*, *158*(4), 1446–1459.

Golovyashkina, N., Penazzi, L., Ballatore, C., Smith, A. B., Bakota, L., & Brandt, R. (2015). Region-specific dendritic simplification induced by Aβ, mediated by tau via dysregulation of microtubule dynamics: A mechanistic distinct event from other neurodegenerative processes. *Molecular Neurodegeneration*, *10*(1).

Grant, S. G. N., & O'Dell, T. J. (2001). Multiprotein complex signaling and the plasticity problem. *Current Opinion in Neurobiology*, *11*(3), 363–368.

Grifoni, F., Tozzi, F., & Boncinelli, S. (2002). STRUCTUREAND FUNCTIONOF DENDRITIC SPINES. *Minerva Anestesiologica*.

Groc, L., Heine, M., Cousins, S. L., Stephenson, F. A., Lounis, B., Cognet, L., & Choquet, D. (2006). NMDA receptor surface mobility depends on NR2A-2B subunits. *Proceedings of the National Academy of Sciences*, *103*(49), 18769–18774.

Hansen, K. B., Yi, F., Perszyk, R. E., Furukawa, H., Wollmuth, L. P., Gibb, A. J., & Traynelis, S. F. (2018). Structure, function, and allosteric modulation of NMDA receptors. *J. Gen. Physiol*, *150*(8), 1081–1105.

Horak, M., Petralia, R. S., Kaniakova, M., & Sans, N. (2014). ER to synapse trafficking of NMDA receptors. *Frontiers in Cellular Neuroscience*, *8*(November), 1–18.

Hardingham, G. E., & Bading, H. (2010). Synaptic versus extrasynaptic NMDA receptor signalling: Implications for neurodegenerative disorders. *Nature Reviews Neuroscience*.

Hardingham, G. E., Fukunaga, Y., & Bading, H. (2002). Extrasynaptic NMDARs oppose

synaptic NMDARs by triggering CREB shut-off and cell death pathways. *Nature Neuroscience*, *5*(5), 405–414.

Hardy, J. A., & Higgins, G. A. (1992). Alzheimer's disease: the amyloid cascade hypothesis. *Science (New York, N.Y.)*, *256*(5054), 184–185.

Hardy, J., & Allsop, D. (1991). Amyloid deposition as the central event in the aetiology of Alzheimer's disease. *Trends in Pharmacological Sciences*, *12*(10), 383–388.

Hardy, J., & Selkoe, D. J. (2002). The Amyloid Hypothesis of Alzheimer's Disease: Progress and Problems on the Road to Therapeutics. *Science*, *297*(5580), 353–356.

Harris, A. Z., & Pettit, D. L. (2008). Recruiting Extrasynaptic NMDA Receptors Augments Synaptic Signaling. *Journal of Neurophysiology*, *99*(2), 524–533.

Henson, M. A., Roberts, A. C., Salimi, K., Vadlamudi, S., Hamer, R. M., Gilmore, J. H., … Philpot, B. D. (2008). Developmental regulation of the NMDA receptor subunits, NR3A and NR1, in human prefrontal cortex. *Cerebral Cortex*, *18*(11), 2560–2573.

Herms, J., Anliker, B., Heber, S., Ring, S., Fuhrmann, M., Kretzschmar, H., … Müller, U. (2004). Cortical dysplasia resembling human type 2 lissencephaly in mice lacking all three APP family members. *The EMBO Journal*, *23*(20), 4106–4115.

Herring, A., Donath, A., Steiner, K. M., Widera, M. P., Hamzehian, S., Kanakis, D., … Keyvani, K. (2012). Reelin depletion is an early phenomenon of alzheimer's pathology. *Journal of Alzheimer's Disease*, *30*(4), 963–979.

Hicke, L., & Dunn, R. (2003). Regulation of Membrane Protein Transport by Ubiquitin and Ubiquitin-Binding Proteins. *Annual Review of Cell and Developmental Biology*, *19*(1), 141–172.

Hoque, M., Rentero, C., Cairns, R., Tebar, F., Enrich, C., & Grewal, T. (2014). Annexins - Scaffolds modulating PKC localization and signaling. *Cellular Signalling*, *26*(6), 1213–1225.

Huang, Y. (2006). Apolipoprotein E and Alzheimer disease. *Neurology*, *66*(Issue 1, Supplement 1), S79–S85.

Husi, H., Ward, M. A., Choudhary, J. S., Blackstock, W. P., & Grant, S. G. N. (2000). Nn0700_661, 661–669.

Hynd, M. R., Scott, H. L., & Dodd, P. R. (2004). Differential expression of N-methyl-D-aspartate receptor NR2 isoforms in Alzheimer's disease. *Journal of Neurochemistry*, *90*(4), 913–919.

Iacobucci, G. J., & Popescu, G. K. (2017). NMDA receptors: Linking physiological output to biophysical operation. *Nature Reviews Neuroscience*.

Ivanov, A., Pellegrino, C., Rama, S., Dumalska, I., Salyha, Y., Ben-Ari, Y., & Medina, I. (2006). Opposing role of synaptic and extrasynaptic NMDA receptors in regulation of the extracellular signal-regulated kinases (ERK) activity in cultured rat hippocampal neurons. *Journal of Physiology*, *572*(3), 789–798.

Jacobs, S., Wei, W., Wang, D., & Tsien, J. Z. (2015). Importance of the GluN2B carboxy-terminal domain for enhancement of social memories. *Learning and Memory*, *22*(8), 401–410.

Jang, B. G., In, S., Choi, B., & Kim, M. J. (2014). Beta-amyloid oligomers induce early loss of presynaptic proteins in primary neurons by caspase-dependent and proteasome-dependent mechanisms. *NeuroReport*, *25*(16), 1281–1288.

Kaniakova, M., Krausova, B., Vyklicky, V., Korinek, M., Lichnerova, K., Vyklicky, L., & Horak, M. (2012). Key amino acid residues within the third membrane domains of NR1 and NR2 subunits contribute to the regulation of the surface delivery of N-methyl-D-aspartate receptors. *Journal of Biological Chemistry*, *287*(31), 26423–26434.

Karthick, C., Nithiyanandan, S., Essa, M. M., Guillemin, G. J., Jayachandran, S. K., & Anusuyadevi, M. (2018). Time-dependent effect of oligomeric amyloid-β (1–42)-induced hippocampal neurodegeneration in rat model of Alzheimer's disease. *Neurological Research*, *00*(00), 1–12.

Kaufman, A. M., Milnerwood, A. J., Sepers, M. D., Coquinco, A., She, K., Wang, L., … Raymond, L. A. (2012). Opposing Roles of Synaptic and Extrasynaptic NMDA Receptor Signaling in Cocultured Striatal and Cortical Neurons. *Journal of Neuroscience*, *32*(12), 3992–4003.

Keleshian, V. L., Modi, H. R., Rapoport, S. I., & Rao, J. S. (2013). Aging is associated with altered inflammatory, arachidonic acid cascade, and synaptic markers, influenced by epigenetic modifications, in the human frontal cortex. *Journal of Neurochemistry*, *125*(1), 63–73.

Kimberly, W. T., Zheng, J. B., Guénette, S. Y., & Selkoe, D. J. (2001). The Intracellular Domain of the β-Amyloid Precursor Protein Is Stabilized by Fe65 and Translocates to the Nucleus in a Notch-like Manner. *Journal of Biological Chemistry*, *276*(43), 40288–40292.

Kishimoto, A., Takai, Y., Mori, T., Kikkawa, U., & Nishizuka, Y. (1980). Activation of calcium and phospholipid-dependent protein kinase by diacylglycerol, its possible relation to phosphatidylinositol turnover. *Journal of Biological Chemistry*.

Klein, W. L. (2002). Abeta toxicity in Alzheimer's disease: globular oligomers (ADDLs) as new vaccine and drug targets. *Neurochemistry International*, *41*(5), 345–352.

Kono, M., Kakegawa, W., Yoshida, K., & Yuzaki, M. (2018). Interneuronal NMDA receptors regulate long-term depression and motor learning in the cerebellum. *The Journal of Physiology*, 1–36.

Kumar, G., Olley, J., Steckler, T., & Talpos, J. (2015). Dissociable effects of NR2A and NR2B NMDA receptor antagonism on cognitive flexibility but not pattern separation. *Psychopharmacology*, *232*(21–22), 3991–4003.

Kurup, P., Zhang, Y., Venkitaramani, D. V., Xu, J., & Lombroso, P. J. (2010). The role of STEP in Alzheimer's disease. *Channels (Austin, Tex.)*, *4*(5), 347–350.

Labrie, V., & Roder, J. C. (2010). The involvement of the NMDA receptor d-serine/glycine site in the pathophysiology and treatment of schizophrenia. *Neuroscience and Biobehavioral Reviews*, *34*(3), 351–372.

Lai, T. W., Shyu, W. C., & Wang, Y. T. (2011). Stroke intervention pathways: NMDA receptors and beyond. *Trends in Molecular Medicine*, *17*(5), 266–275.

Lambert, M. P., Barlow, A. K., Chromy, B. A., Edwards, C., Freed, R., Liosatos, M., … Klein, W. L. (1998). Diffusible, nonfibrillar ligands derived from Abeta1-42 are potent central nervous system neurotoxins. *Proceedings of the National Academy of Sciences of the United States of America*, *95*(11), 6448–6453.

Lan, J. Y., Skeberdis, V. A., Jover, T., Grooms, S. Y., Lin, Y., Araneda, R. C., … Zukin, R. S. (2001). Protein kinase C modulates NMDA receptor trafficking and gating. *Nature Neuroscience*.

Lau, C. G., & Zukin, R. S. (2007). NMDA receptor trafficking in synaptic plasticity and neuropsychiatric disorders. *Nature Reviews Neuroscience*, *8*(6), 413–426.

Lee, H. K. (2006). Synaptic plasticity and phosphorylation. *Pharmacology and Therapeutics*.

Leuba, G., Vernay, A., Kraftsik, R., Tardif, E., Riederer, B., & Savioz, A. (2014). Pathological Reorganization of NMDA Receptors Subunits and Postsynaptic Protein PSD-95 Distribution in Alzheimer's Disease. *Current Alzheimer Research*, *11*(1), 86–96.

Leveille, F., El gaamouch, F., Gouix, E., Lecocq, M., Lobner, D., Nicole, O., & Buisson, A. (2008). Neuronal viability is controlled by a functional relation between synaptic and extrasynaptic NMDA receptors. *The FASEB Journal*, *22*(12), 4258–4271.

Liang, J., Kulasiri, D., & Samarasinghe, S. (2017). Computational investigation of Amyloid-β-induced location-and subunit-specific disturbances of NMDAR at hippocampal dendritic spine in Alzheimer's disease. *PLoS ONE*, *12*(8), 1–22.

Liao, G. Y., Wagner, D. A., Hsu, M. H., & Leonard, J. P. (2001). Evidence for direct protein kinase-C mediated modulation of N-methyl-D-aspartate receptor current. *Molecular Pharmacology*, *59*(5), 960–964.

Liu, J., Chang, L., Roselli, F., Almeida, O. F. X., Gao, X., Wang, X., … Wu, Y. (2010). Amyloid-β induces caspase-dependent loss of PSD-95 and synaptophysin through NMDA receptors. *Journal of Alzheimer's Disease*, *22*(2), 541–556.

Lopez de Armentia, M., & Sah, P. (2003). Development and subunit composition of synaptic NMDA receptors in the amygdala: NR2B synapses in the adult central amygdala. *The Journal of Neuroscience : The Official Journal of the Society for Neuroscience*, *23*(17), 6876–6883.

Lu, J., & Zuo, Y. (2017). HHS Public Access. *Brain Res Bull*, *129*(11), 18–22. https://doi.org/10.1016/S2214-109X(16)30265-0.Cost-effectiveness

Manterola, L., Hernando-Rodríguez, M., Ruiz, A., Apraiz, A., Arrizabalaga, O., Vellón, L., … Zugaza, J. L. (2013). 1-42 β-amyloid peptide requires PDK1/nPKC/Rac 1 pathway to induce neuronal death. *Translational Psychiatry*, *3*(November 2012), 1–11.

McKay, S., Ryan, T. J., McQueen, J., Indersmitten, T., Marwick, K. F. M., Hasel, P., … Komiyama, N. H. (2018). The Developmental Shift of NMDA Receptor Composition Proceeds Independently of GluN2 Subunit-Specific GluN2 C-Terminal Sequences. *Cell Reports*, *25*(4), 841–851.e4.

Martin, K. P., & Wellman, C. L. (2011). NMDA receptor blockade alters stress-induced dendritic remodeling in medial prefrontal cortex. *Cerebral Cortex*, *21*(10), 2366–2373.

McKay, S., Ryan, T. J., McQueen, J., Indersmitten, T., Marwick, K. F. M., Hasel, P., … Komiyama, N. H. (2018). The Developmental Shift of NMDA Receptor Composition Proceeds Independently of GluN2 Subunit-Specific GluN2 C-Terminal Sequences. *Cell Reports*, *25*(4), 841–851.e4.

Mishizen-Eberz, A. J., Rissman, R. A., Carter, T. L., Ikonomovic, M. D., Wolfe, B. B., & Armstrong, D. M. (2004). Biochemical and molecular studies of NMDA receptor subunits NR1/2A/2B in hippocampal subregions throughout progression of Alzheimer's disease pathology. *Neurobiology of Disease*, *15*(1), 80–92.

Mohamad, O., Song, M., Wei, L., & Yu, S. P. (2013). Regulatory roles of the NMDA receptor GluN3A subunit in locomotion, Pain perception and cognitive functions in adult mice. *Journal of Physiology*, *591*(1), 149–168.

Morini, R., & Becchetti, A. (2010). Integrin receptors and ligand-gated channels. *Advances in Experimental Medicine and Biology*.

Moser, M., Legate, K. R., Zent, R., & Fässler, R. (2009). The tail of integrins, talin, and kindlins. *Science*.

Mota, S. I., Ferreira, I. L., Valero, J., Ferreiro, E., Carvalho, A. L., Oliveira, C. R., & Rego, A. C. (2014). Impaired Src signaling and post-synaptic actin polymerization in Alzheimer's disease mice hippocampus — Linking NMDA receptors and the reelin pathway. *Experimental Neurology*.

Mroczko, B., Groblewska, M., Litman-Zawadzka, A., Kornhuber, J., & Lewczuk, P. (2018). Cellular receptors of amyloid β oligomers (AβOs) in Alzheimer's disease. *International Journal of Molecular Sciences*, *19*(7).

Müller, M. K., Jacobi, E., Sakimura, K., Malinow, R., & von Engelhardt, J. (2018). NMDA receptors mediate synaptic depression, but not spine loss in the dentate gyrus of adult amyloid Beta (Aβ) overexpressing mice. *Acta Neuropathologica Communications*, *6*(1), 110.

Müller, U. C., Deller, T., & Korte, M. (2017). Not just amyloid: physiological functions of the amyloid precursor protein family. *Nature Reviews Neuroscience*, *18*(5), 281–298.

Newpher, T. M., & Ehlers, M. D. (2009). Spine microdomains for postsynaptic signaling and plasticity. *Trends in Cell Biology*, *19*(5), 218–227.

Nieuwenhuis, B., Haenzi, B., Andrews, M. R., Verhaagen, J., & Fawcett, J. W. (2018). Integrins promote axonal regeneration after injury of the nervous system. *Biological Reviews*, *93*(3), 1339–1362.

Nyffeler, M., Zhang, W. N., Feldon, J., & Knuesel, I. (2007). Differential expression of PSD proteins in age-related spatial learning impairments. *Neurobiology of Aging*, *28*(1), 143–155.

Oddo, S., Caccamo, A., Shepherd, J. D., Murphy, M. P., Golde, T. E., Kayed, R., … Laferla, F. M. (2003). 3xTg-AD model of Alzheimer's disease with plaques and tangles_intracellular Aβ and synaptic dysfunction.pdf, *39*, 409–421.

Oddo, S., Caccamo, A., Tran, L., Lambert, M. P., Glabe, C. G., Klein, W. L., & LaFerla, F. M. (2006). Temporal profile of amyloid-β (Aβ) oligomerization in an in vivo model of Alzheimer disease: A link between Aβ and tau pathology. *Journal of Biological Chemistry*, *281*(3), 1599–1604.

Omkumar, R. V., Kiely, M. J., Rosenstein, A. J., Min, K. T., & Kennedy, M. B. (1996). Identification of a phosphorylation site for calcium/calmodulin- dependent protein kinase II in the NR2B subunit of the N-methyl-D-aspartate receptor. *Journal of Biological Chemistry*, *271*(49), 31670–31678.

Omote, H., Miyaji, T., Juge, N., & Moriyama, Y. (2011). Vesicular Neurotransmitter Transporter : Bioenergetics and. *Biochemistry*, 5558–5565.

Pagani, G., & Gohlke, H. (2018). On the contributing role of the transmembrane domain for subunit-specific sensitivity of integrin activation. *Scientific Reports*, *8*(1), 1–14.

Paoletti, P., Bellone, C., & Zhou, Q. (2013). NMDA receptor subunit diversity: Impact on receptor properties, synaptic plasticity and disease. *Nature Reviews Neuroscience*, *14*(6), 383–400.

Paoletti, P., & Neyton, J. (2007). NMDA receptor subunits: function and pharmacology. *Current Opinion in Pharmacology*, *7*(1), 39–47.

Parajuli, L. K., Tanaka, S., & Okabe, S. (2017). Insights into age-old questions of new dendritic spines: From form to function. *Brain Research Bulletin*, *129*, 3–11.

Park, Y. K., & Goda, Y. (2016). Integrins in synapse regulation. *Nature Reviews Neuroscience*.

Parameshwaran, K., Dhanasekaran, M., & Suppiramaniam, V. (2008). Amyloid beta peptides and glutamatergic synaptic dysregulation. *Experimental Neurology*, *210*(1), 7–13.

Parsons, M. P., & Raymond, L. A. (2014). Extrasynaptic NMDA receptor involvement in central nervous system disorders. *Neuron*, *82*(2), 279–293.

Paulin, J. J. W., Haslehurst, P., Fellows, A. D., Liu, W., Jackson, J. D., Joel, Z., … Edwards, F. A. (2016). Large and small dendritic spines serve different interacting functions in hippocampal synaptic plasticity and homeostasis. *Neural Plasticity*, *2016*.

Pérez-Otaño, I., & Ehlers, M. D. (2005). Homeostatic plasticity and NMDA receptor trafficking. *Trends in Neurosciences*, *28*(5), 229–238.

Petralia, R. S., Wang, Y. X., Hua, F., Yi, Z., Zhou, A., Ge, L., … Wenthold, R. J. (2010). Organization of NMDA receptors at extrasynaptic locations. *Neuroscience*.

Quassollo, G., Wojnacki, J., Salas, D., Gastaldi, L., Marzolo, M. P., Conde, C., … Cáceres, A. (2015). A RhoA Signaling Pathway Regulates Dendritic Golgi Outpost Formation. *Current Biology : CB*.

Raab-Westphal, S., Marshall, J. F., & Goodman, S. L. (2017). Integrins as therapeutic targets: Successes and cancers. *Cancers*, *9*(9), 1–28.

Rajendran, L., & Annaert, W. (2012). Membrane Trafficking Pathways in Alzheimer's Disease. *Traffic*, *13*(6), 759–770.

Raychaudhuri, M., & Mukhopadhyay, D. (2007). AICD and its adaptors - in search of new players. *Journal of Alzheimer's Disease : JAD*, *11*(3), 343–358.

Sala, C., & Segal, M. (2014). Dendritic Spines: The Locus of Structural and Functional Plasticity. *Physiological Reviews*, *94*(1), 141–188

Santos, A. N., Ewers, M., Minthon, L., Simm, A., Silber, R.-E., Blennow, K., … Hampel, H. (2012). Amyloid-β oligomers in cerebrospinal fluid are associated with cognitive decline in patients with Alzheimer's disease. *Journal of Alzheimer's Disease : JAD*, *29*(1), 171–176.

Scannevin, R. H., & Huganir, R. L. (2000). Postsynaptic organisation and regulation of excitatory synapses. *Nature Reviews Neuroscience*.

Scheff, S. W., Price, D. A., Schmitt, F. A., & Mufson, E. J. (2006). Hippocampal synaptic loss in early Alzheimer's disease and mild cognitive impairment. *Neurobiology of Aging*, *27*(10), 1372–1384.

Scott, D. B., Blanpied, T. A., Swanson, G. T., Zhang, C., & Ehlers, M. D. (2001). An NMDA receptor ER retention signal regulated by phosphorylation and alternative splicing. *J Neuroscience*, *21*(9), 3063–3072.

Segal, M. (2017). Dendritic spines: Morphological building blocks of memory. *Neurobiology of Learning and Memory*, *138*, 3–9.

Selkoe, D. J. (1991). The molecular pathology of Alzheimer's disease. *Neuron*, *6*(4), 487–498.

Sheng, L., Leshchyns'Ka, I., & Sytnyk, V. (2013). Cell adhesion and intracellular calcium signaling in neurons. *Cell Communication and Signaling*, *11*(1).

Sheng, M., & Hoogenraad, C. C. (2007). The Postsynaptic Architecture of Excitatory

Synapses: A More Quantitative View. *Annual Review of Biochemistry*, *76*(1), 823–847.

Sheng, M., & Kim, E. (2011). The postsynaptic organization of synapses. *Cold Spring Harbor Perspectives in Biology*, *3*(12), 1–20.

Sinai, L., Duffy, S., & Roder, J. C. (2010). Src inhibition reduces NR2B surface expression and synaptic plasticity in the amygdala. *Learning and Memory*, *17*(8), 364–371.

Skeberdis, V. A., Lan, J. Y., Opitz, T., Zheng, X., Bennett, M. V. L., & Suzanne Zukin, R. (2001). mGluR1-mediated potentiation of NMDA receptors involves a rise in intracellular calcium and activation of protein kinase C. *Neuropharmacology*, *40*(7), 856–865.

Snyder, E. M., Nong, Y., Almeida, C. G., Paul, S., Moran, T., Choi, E. Y., … Greengard, P. (2005). Regulation of NMDA receptor trafficking by amyloid-β. *Nature Neuroscience*, *8*(8), 1051–1058.

Standley, S., Petralia, R. S., Gravell, M., Hamilton, R., Wang, Y. X., Schubert, M., & Wenthold, R. J. (2012). Trafficking of the NMDAR2B receptor subunit distal cytoplasmic tail from endoplasmic reticulum to the synapse. *PLoS ONE*, *7*(6).

Steigerwald, F., Schulz, T. W., Schenker, L. T., Kennedy, M. B., Seeburg, P. H., & Köhr, G. (2000). C-Terminal truncation of NR2A subunits impairs synaptic but not extrasynaptic localization of NMDA receptors. *The Journal of Neuroscience : The Official Journal of the Society for Neuroscience*, *20*(12), 4573–4581.

Strack, S., McNeill, R. B., & Colbran, R. J. (2000). Mechanism and regulation of calcium/calmodulin-dependent protein kinase II targeting to the NR2B subunit of the N-methyl-D-aspartate receptor. *Journal of Biological Chemistry*, *275*(31), 23798–23806.

Stuart Cull-Candy, S. B. and M. F. (2001). NMDA receptor subunits : diversity , development and disease Stuart Cull-Candy * , Stephen Brickley and Mark Farrant. *Current Opinion in Neurobiology*, *11*, 327–335.

Sun, W., Hansen, K. B., Jahr, C. E., & Health, O. (2018). the Developmental Shift in Channel Properties, *94*(1), 58–64.

Sze, S. C. W., Wong, C. K. C., & Yung, K. K. L. (2001). Modulation of the gene expression of N-methyl-D-aspartate receptor NR2B subunit in the rat neostriatum by a single dose of specific antisense oligodeoxynucleotide. *Neurochemistry International*, *39*(4), 319–327.

Tackenberg, C., Ghori, A., & Brandt, R. (2009). Thin, Stubby or Mushroom: Spine Pathology in Alzheimers Disease. *Current Alzheimer Research*.

Tagawa, K., Homma, H., Saito, A., Fujita, K., Chen, X., Imoto, S., … Okazawa, H. (2015). Comprehensive phosphoproteome analysis unravels the core signaling network that initiates the earliest synapse pathology in preclinical Alzheimer's disease brain. *Human Molecular Genetics*, *24*(2), 540–558.

Takai, Y., Kishimoto, A., Iwasa, Y., Kawahara, Y., Mori, T., & Nishizuka, Y. (1979). Calcium-dependent activation of a multifunctional protein kinase by membrane phospholipids. *Journal of Biological Chemistry*.

Takami, M., Nagashima, Y., Sano, Y., Ishihara, S., Morishima-Kawashima, M., Funamoto, S., & Ihara, Y. (2009). -Secretase: Successive Tripeptide and Tetrapeptide Release from the Transmembrane Domain of -Carboxyl Terminal Fragment. *Journal of Neuroscience*, *29*(41), 13042–13052.

Talantova, M., Sanz-Blasco, S., Zhang, X., Xia, P., Akhtar, M. W., Okamoto, S. -i., … Lipton, S. A. (2013). A induces astrocytic glutamate release, extrasynaptic NMDA receptor activation, and synaptic loss. *Proceedings of the National Academy of Sciences*, *110*(27), E2518–E2527.

Tang, T. T. T., Badger, J. D., Roche, P. A., & Roche, K. W. (2010). Novel approach to probe subunit-specific contributions to N-Methyl-D-aspartate (NMDA) receptor trafficking reveals a dominant role for NR2B in receptor recycling. *Journal of Biological Chemistry*, *285*(27), 20975–20981.

Tavalin, S. J., & Colbran, R. J. (2017). CaMKII-mediated phosphorylation of GluN2B regulates recombinant NMDA receptor currents in a chloride-dependent manner. *Molecular and Cellular Neuroscience*.

Texidó, L., Martín-Satué, M., Alberdi, E., Solsona, C., & Matute, C. (2011). Amyloid β peptide oligomers directly activate NMDA receptors. *Cell Calcium*, *49*(3), 184–190.

Thomas, C. G. (2006). Synaptic and Extrasynaptic NMDA Receptor NR2 Subunits in Cultured Hippocampal Neurons. *Journal of Neurophysiology*.

Thorns, V., Mallory, M., Hansen, L., & Masliah, E. (1997). Alterations in glutamate receptor 2/3 subunits and amyloid precursor protein expression during the course of Alzheimer's disease and Lewy body variant. *Acta Neuropathologica*, *94*(6), 539–548.

Tomiyama, T., Matsuyama, S., Iso, H., Umeda, T., Takuma, H., Ohnishi, K., … Mori, H. (2010). A Mouse Model of Amyloid Oligomers: Their Contribution to Synaptic Alteration, Abnormal Tau Phosphorylation, Glial Activation, and Neuronal Loss In Vivo. *Journal of Neuroscience*, *30*(14), 4845–4856.

Tovar, K. R., & Westbrook, G. L. (2002). Mobile NMDA receptors at hippocampal synapses. *Neuron*, *34*(2), 255–264.

Tu, S., Okamoto, S., Lipton, S. A., & Xu, H. (2014). Oligomeric A β -induced synaptic dysfunction in Alzheimer ' s disease, 1–12.

Van Dyke, W., & Maddow, B. (2011). Integrin Structure , Activation , and Interactions, 1–15.

Vazquez-Sanchez, S., Bobeldijk, S., Dekker, M. P., Van Keimpema, L., & Van Weering, J. R. T. (2018). VPS35 depletion does not impair presynaptic structure and function. *Scientific Reports*, *8*(1), 1–12.

Verdier, Y., Zarándi, M., & Penke, B. (2004). Amyloid β-peptide interactions with neuronal and glial cell plasma membrane: Binding sites and implications for Alzheimer's disease. *Journal of Peptide Science*.

Viola, K. L., & Klein, W. L. (2015). Amyloid β oligomers in Alzheimer's disease pathogenesis, treatment, and diagnosis. *Acta Neuropathologica*, *129*(2), 183–206.

Violin, J. D., Zhang, J., Tsien, R. Y., & Newton, A. C. (2003). A genetically encoded fluorescent reporter reveals oscillatory phosphorylation by protein kinase C. *Journal of Cell Biology*, *161*(5), 899–909.

von Engelhardt, J. (2009). Synaptic NR2A- but not NR2B-containing NMDA receptors increase with blockade of ionotropic glutamate receptors. *Frontiers in Molecular Neuroscience*, *2*(October), 1–14.

von Rotz, R. C., Kohli, B. M., Bosset, J., Meier, M., Suzuki, T., Nitsch, R. M., & Konietzko, U. (2004). The APP intracellular domain forms nuclear multiprotein complexes and regulates the transcription of its own precursor. *Journal of Cell Science*, *117*(19), 4435–4448.

Wang, N. X., Lee, H.-J., & Zheng, J. J. (2008). Therapeutic use of PDZ protein-protein interaction antagonism. *Drug News & Perspectives*, *21*(3), 137–141.

Wang, Q., Klyubin, I., Wright, S., Griswold-Prenner, I., Rowan, M. J., & Anwyl, R. (2008). Av Integrins Mediate Beta-Amyloid Induced Inhibition of Long-Term Potentiation. *Neurobiology of Aging*, *29*(10), 1485–1493.

Wang, Q., Walsh, D. M., Rowan, M. J., Selkoe, D. J., & Anwyl, R. (2004). Block of Long-Term Potentiation by Naturally Secreted and Synthetic Amyloid -Peptide in Hippocampal Slices Is Mediated via Activation of the Kinases c-Jun N-Terminal Kinase, Cyclin-Dependent Kinase 5, and p38 Mitogen-Activated Protein Kinase as well as M. *Journal of Neuroscience*, *24*(13), 3370–3378.

Wang, Z. C., Zhao, J., & Li, S. (2013). Dysregulation of synaptic and extrasynaptic N-methyl-D-aspartate receptors induced by amyloid-β. *Neuroscience Bulletin*, *29*(6), 752–760.

Wehrle-Haller, B. (2012). Assembly and disassembly of cell matrix adhesions. *Current Opinion in Cell Biology*, *24*(5), 569–581.

Weidemann, A., Eggert, S., Reinhard, F. B. M., Vogel, M., Paliga, K., Baier, G., … Evin, G. (2002). A novel epsilon-cleavage within the transmembrane domain of the Alzheimer amyloid precursor protein demonstrates homology with Notch processing. *Biochemistry*, *41*(8), 2825–2835.

Williamson, R., Scales, T., Clark, B., Gibb, G., Reynolds, C., Kellie, S., … Anderton, B. (2002). Rapid tyrosine phosphorylation of neuronal proteins including tau and focal adhesion kinase in response to amyloid-beta peptide exposure: involvement of Src family protein kinases. *The Journal of Neuroscience : The Official Journal of the Society for Neuroscience*, *22*(1), 10–20.

Wu, X., & Reddy, D. S. (2012). Integrins as receptor targets for neurological disorders. *Pharmacology and Therapeutics*, *134*(1), 68–81.

Wyssenbach, A., Quintela, T., Llavero, F., Zugaza, J. L., Matute, C., & Alberdi, E. (2016). Amyloid β-induced astrogliosis is mediated by β1-integrin via NADPH oxidase 2 in Alzheimer's disease. *Aging Cell*, *15*(6), 1140–1152.

Xia, H., Hornby, Z. D., & Malenka, R. C. (2001). An ER retention signal explains differences in surface expression of NMDA and AMPA receptor subunits. *Neuropharmacology*, *41*(6), 714–723.

Xu, J., Kurup, P., Nairn, A. C., & Lombroso, P. J. (2018). Synaptic NMDA Receptor Activation Induces Ubiquitination and Degradation of STEP61. *Molecular Neurobiology*, *55*(4), 3096–3111.

Yan, X., Liu, J., Ye, Z., Huang, J., He, F., Xiao, W., … Luo, Z. (2016). CaMKII-Mediated CREB phosphorylation is involved in Ca2+-Induced BDNF mRNA transcription and neurite outgrowth promoted by electrical stimulation. *PLoS ONE*, *11*(9), 1–22.

Yan, Y. G., Zhang, J., Xu, S. J., Luo, J. H., Qiu, S., & Wang, W. (2014). Clustering of surface NMDA receptors is mainly mediated by the C-terminus of GluN2A in cultured rat hippocampal neurons. *Neuroscience Bulletin*, *30*(4), 655–666.

Yang, G., Lai, C. S. W., Cichon, J., Ma, L., Li, W., & Gan, W. B. (2014). Sleep promotes branch-specific formation of dendritic spines after learning. *Science*.

Yao, L., & Zhou, Q. (2017). Enhancing NMDA Receptor Function: Recent Progress on Allosteric Modulators. *Hindawi Neural Plasticity*, *2017*.

Ye, F., Zeng, M., & Zhang, M. (2018). Mechanisms of MAGUK-mediated cellular junctional complex organization. *Current Opinion in Structural Biology*, *48*, 6–15.

Yuste, R. (2015a). From the neuron doctrine to neural networks. *Nature Reviews Neuroscience*, *16*(8), 487–497.

Yuste, R. (2015b). The discovery of dendritic spines by Cajal. *Frontiers in Neuroanatomy*, *9*(April), 1–6.

Yuste, R., & Majewska, A. (2001). On the function of dendritic spines. *Neuroscientist*.

Zhang, Y., Li, P., Feng, J., & Wu, M. (2016). Dysfunction of NMDA receptors in Alzheimer's disease. *Neurological Sciences*, *37*(7), 1039–1047.

Zheng, H., & Koo, E. H. (2011). Biology and pathophysiology of the amyloid precursor protein. *Molecular Neurodegeneration*, *6*(1), 27.

Zhou, Q., & Sheng, M. (2013). NMDA receptors in nervous system diseases. *Neuropharmacology*, *74*, 69–75.

Zorumski, C. F., & Izumi, Y. (2012). NMDA receptors and metaplasticity: Mechanisms and possible roles in neuropsychiatric disorders. *Neuroscience and Biobehavioral Reviews*.